Iodine(III)-Catalyzed, Enantioselective 1,2-Difluorination of Cinnamamides

Iodine(III)-Catalyzed, Enantioselective 1,2-Difluorination of Cinnamamides

A dissertation presented by

Moriana Khaled Haj

to

The Department of Chemistry and Chemical Biology

in partial fulfillment of the requirements

for the degree of

Doctor of Philosophy

in the subject of

Chemistry

Harvard University

Cambridge, Massachusetts

May 2020

Dissertation Advisor: Eric N. Jacobsen *Moriana Khaled Haj*

Iodine(III)-Catalyzed, Enantioselective 1,2-Difluorination of Cinnamamides

Abstract

Iodine(III) catalysis has emerged as an effective strategy for enabling a wide range of alkene difunctionalization reactions. In Chapter 1, we describe the development of an enantioselective 1,2-difluorination of cinnamamides catalyzed by chiral aryl iodides. Using HF-pyridine as a fluoride source and *m*CPBA as a stoichiometric oxidant, the aryl iodide catalyst can be oxidized *in situ* to an iodoarene difluoride, which difluorinates cinnamamide substrates. These reactions can afford both 1,2-difluoride and rearranged 1,1-difluoride products arising from competing anchimeric assistance pathways. We identified that selectivity for the 1,2-difluorination pathway can be achieved by incorporation of an *N*-*tert*-butyl amide substituent into the substrate and by tuning the HF loading. The products of the reaction and their derivatives contain vicinal, fluoride-bearing stereocenters and may serve as building blocks for the preparation of compounds including this motif.

In Chapter 2, we describe the synthesis of chiral iodoarene difluorides via the direct oxidation of iodoarenes with XeF_2. When reacted with an alkene in biphasic HF-pyridine/dichloromethane these compounds recapitulate the catalytic reactivity described in Chapter 1, and studies in the isolated phases of the reaction mixture indicate that steps involving substrate fluorination likely take place in the HF-pyridine layer. Studies of the stoichiometric reactivity of chiral iodoarene difluorides have also revealed that HF is not required to activate them toward reaction with alkenes; the homogeneous, stoichiometric reaction between a chiral

iodoarene difluoride and a cinnamamide substrate proceeds with high chemoselectivity and enantioselectivity in hexafluoroisopropanol. In Chapter 3, we report progress toward the development of an electrocatalytic 1,2-difluorination of alkenes. We found that *p*-iodotoluene catalyzes the electrochemical difluorination of a terminal alkene substrate in hexafluoroisopropanol solvent with $Et_3N•3HF$ as the fluoride source. We also examined resorcinol-derived catalysts in this transformation and identified catalyst features that impact reactivity, gaining insights that could potentially inform development of chiral catalysts compatible with electrochemical oxidation.

Table of Contents

Acknowledgments

I would like to begin by thanking my research advisor, Professor Eric Jacobsen. Eric's scientific perspective has had an enormous influence on me, and his astute observations and questions have continually challenged me to think more deeply. Eric is an excellent teacher with a remarkable ability to convey complicated information in a clear and compelling manner; although I still have a lot to learn, his guidance and advice have been instrumental in helping me develop my presentation and writing skills. By bringing together a group of students with diverse perspectives and skill sets and providing us with the resources and freedom to explore, Eric has created a uniquely invigorating environment for conducting research. Having the opportunity to work in his lab and learn from him has been a privilege.

I would also like to thank Professors Christina Woo and Ted Betley for serving on my committee. At each stage of my graduate education, they have provided thoughtful feedback and challenged me to clearly define my goals, and these efforts have undeniably improved the quality of my work. Their encouragement and support throughout have been extremely valuable to me.

I would like to express my gratitude to Professor Tom Hoye, my undergraduate research advisor at the University of Minnesota. Starting from our very first meeting, when I was so new to organic chemistry that I didn't yet know how to interpret a simple skeletal formula, Tom has unfailingly treated me with the utmost seriousness and respect and supported me in every endeavor. His thoughtfulness and integrity have influenced me on both a professional and a personal level. Tom was an extraordinarily patient and kind mentor, and I will never forget the time I spent working with him.

Thank you to all of the members of the Jacobsen lab, beginning with Nicole Minotti, our lab administrator. Nicole keeps the lab running smoothly and brings an unmatched dedication to her work. I am very grateful for her hard work on behalf of all of us.

I feel extremely lucky that I entered grad school with a cohort of wonderful classmates. In particular, I would like to thank Prithvi Vangal and Ethan Magno for their friendship over the past several years, as well as for reading and correcting portions of this thesis. Prithvi, my labmate in the Jacobsen group, is an incredibly intelligent scientist (some might even say a mechanistic genius), and he is always generous in using his talent and time to help others, including me. Many of us enjoy mocking him for his positive attitude, but Prithvi's optimistic outlook and resilience have truly influenced me for the better. I am so glad that our time in the group coincided and that Prithvi welcomed me into 202D, the quiet office. Ethan, who works down the hall in the Myers lab, is an extremely talented chemist who is always eager to hear about other people's chemistry and help work through synthetic problems. Although Prithvi and I take every opportunity to allude to his fancy private-school background, Ethan is one of the most nonjudgmental and accepting people I have ever met. His encouragement and advice have helped me navigate many challenges, and he is often even happier about my successes than I am. Prithvi's and Ethan's support has meant so much to me, and I hope the three of us will continue to spend time together and celebrate each other's achievements long after we all graduate.

Dr. Steven Banik is an exceptional researcher, and I was fortunate to have him as my first mentor in the lab. In addition to his scientific brilliance, I will always remember his sense of humor and the patience and thoughtfulness he displayed while working with me. Because of these qualities, I have no doubt that he has a remarkable career ahead of him, both as a researcher and as a teacher and advisor. I spent my PhD working on fluorination chemistry, a direction

Steven pioneered in our group, and I also wish to acknowledge several other people who worked in the same project area during my time in the group. Thank you to Dr. Katrina Mennie, Hayden Sharma, Dr. Mark Levin, and John Ovian — I have been inspired by your creative thinking and have learned so much from each of you.

I was very happy to have the opportunity to collaborate with members of the Nocera lab. I had a great time working on electrochemistry with Tom Keane. I appreciated that he generously took the time to work with me on a project in a field that was out of my area of expertise, and that he patiently and thoughtfully answered my questions without ever making me feel stupid for asking them. David Gygi's enthusiasm and encouragement were always motivational, and he kindly assisted me with several experiments and shared ideas and literature related to our projects. In addition, comparing notes during our job searches was a much-needed bright spot during a stressful time. Prior to any official collaboration, Ben Zhang helped me carry out several experiments, and I am very grateful for his willingness to do so.

Thank you to all three members of Team Oxetane: Dan Strassfeld, Dr. Zach Wickens, and Dr. Russ Algera. When I was a younger graduate student trying to acclimate to a new environment, Dan's approachability and friendliness quickly made me feel welcome. Throughout my time in graduate school, Dan has been a source of both scientific insight and moral support, and I want to thank him for always expressing confidence in my abilities and a genuine willingness to help me in any way he could. Zach helped me through some of the most challenging stages of my PhD, at times talking with me almost every day about my progress and planned next steps. His constructive attitude and willingness to spend time mentoring me during an extremely busy time in his postdoc were unforgettable. Russ's arrival in the lab coincided with my immersion in teaching CHEM 17, and as a result we almost never spoke during the first

few months of his postdoc, although we shared a bay and worked in adjacent offices. Despite this inauspicious start, Russ became a coworker I could always turn to when I needed to talk over a problem or get a new perspective. Our scientific discussions inspired me to try new things (the wide array of outlandish fluorinating reagents I've accumulated are a testament to that), and our conversations about careers helped me to identify what really matters to me and to make decisions accordingly.

The postdocs in the group have consistently enriched my experience here with their knowledgeable advice and kindness. In addition to those already named, I particularly want to thank Drs. Alison Wendlandt, Shauna Paradine, Libby Hennessy, Jan Metternich (a great officemate), Elias Picazo, and Diego Diaz (another great officemate). I also want to acknowledge some of the younger students who have enhanced my graduate school experience. Qiuhan Li is a fantastic chemist and a wonderfully kind and empathetic person; our conversations always put a smile on my face, and I'm so glad I got to share an office with him for the last three years. Dennis Kutateladze's intelligence, work ethic, and gentle enthusiasm make him an excellent coworker, and I have enjoyed having him in lab immensely. John Ovian is a very talented chemist and a conscientious lab member, and I have always been impressed by the respect for others and quiet leadership he demonstrates. I have enjoyed getting to know David Graff, a bright and thoughtful individual whose independent mindset I admire.

My family has been incredibly supportive throughout my education and especially during my PhD. I'm glad that I had the chance to go through grad school at the same time as my sister Amelia, who will be completing her PhD during the same week that I finish mine. Her understanding and sense of humor throughout have made this experience a much happier one. My parents have always encouraged me to persevere and do my best, and this guidance from

them has been just as valuable to me in completing graduate school as all of the scientific advice I've received from others. Their confidence and support have been immensely reassuring. I can't thank them enough for everything.

List of Abbreviations

$[\alpha]_D^T$	specific rotation at T (˚C) and 589 nm
Å	Angstrom
A	ampere
Ac	acetyl
anti	on opposite sides
aq.	aqueous
Ar	aryl
Bn	benzyl
Bu	butyl
˚C	degree Celsius
c	centi
cal	calorie
Cbz	benzyloxycarbonyl
cis	on the same side
CV	cyclic voltammetry
δ	chemical shift in parts per million
d	day(s); doublet (spectral)
DAST	diethylaminosulfur trifluoride
DCE	dichloroethane
DFT	density functional theory
DOSY	diffusion ordered spectroscopy
d.r.	diastereomeric ratio

E	*Ger.*, entgegen; applied potential (electrochemistry)
e.e.	enantiomeric excess
erythro	on the same side, in a Fischer projection
ESI	electrospray ionization
Et	ethyl
equiv	equivalent
Fc	ferrocene
FT	Fourier transform
g	gram
GABA	γ-aminobutyric acid
GC	gas chromatography
gem	geminal
h	hour(s)
HFIP	1,1,1,3,3,3-hexafluoro-2-propanol
HPLC	high-performance liquid chromatography
HRMS	high resolution mass spectrometry
Hz	Hertz
i	*iso*
IR	infrared
j	current density
J	coupling constant
k	rate constant
k	kilo

L	ligand; liter(s)
log*P*	logarithm of the partition coefficient
μ	micro
m	*meta*
m	meter(s); milli; multiplet (spectral)
M	molar; metal
*m*CPBA	*meta*-chloroperbenzoic acid
Me	methyl
Mes	2,4,6-trimethylphenyl
min	minute
mol	mole
MS	mass spectrometry
NBS	*N*-bromosuccinimide
n.d.	not determined
NIS	*N*-iodosuccinimide
NMR	nuclear magnetic resonance
NOE	nuclear Overhauser effect
p	*para*
Ph	phenyl
PIDA	phenyliodine(III) diacetate
Pr	propyl
prot	protein
psi	pound(s) per square inch

pyr	pyridine
q	quartet (spectral)
R	rectus
rt	room temperature
S	sinister
s	singlet (spectral)
syn	on the same side
t	*tert*, tertiary
t	triplet (spectral)
t_R	retention time
TBA	tetrabutylammonium
Tf	trifluoromethanesulfonate
TFA	trifluoroacetic acid
TFE	2,2,2-trifluoroethanol
THF	tetrahydrofuran
TMA	tetramethylammonium
threo	on opposite sides, in a Fischer projection
TMS	trimethylsilyl
trans	on the opposite side
Ts	tosyl, *p*-toluenesulfonyl
UV	ultraviolet
V	volt(s)
wt	weight

Z	*Ger.*, zusammen

Chapter 1

Catalytic, Enantioselective 1,2-Difluorination of Cinnamamides

1.1 Introduction[1]

The stereocontrolled introduction of fluorine atoms into organic molecules is a long-standing challenge in synthetic chemistry driven, to a significant extent, by the beneficial properties fluorination can impart to the physical and biological properties of compounds.[2] In

[1] Portions of this chapter have been reproduced or adapted from: Haj, M. K.; Banik, S. M.; Jacobsen, E. N. *Org. Lett.* **2019**, *21*, 4919–4923, https://doi.org/10.1021/acs.orglett.9b00938

[2] (a) Zhou, Y.; Wang, J.; Zhanni, G.; Wang, S.; Zhu, W.; Aceña, J. L.; Soloshonok, V. A.; Izawa, K.; Liu, H. *Chem. Rev.* **2016**, *116*, 422–518. (b) Gillis, E. P.; Eastman, K. J.; Hill, M. D.; Donnelly, D. J.; Meanwell, N. A. *J. Med. Chem.* **2015***, 58*, 8315–8359. (c) Wang, J.; Sanchez-Rosello, M.; Aceña, J. L.; del Pozo, C.; Sorochinsky, A. E.; Fustero, S.; Soloshonok, V. A.; Liu, H. *Chem. Rev.* **2014**, *114*, 2432–2506. (d) Purser, S.; Moore, P. R.; Swallow, S.; Gouverneur, V. *Chem. Soc. Rev.* **2008**, *37*, 320–330. (e) Hagmann, W. K. *J. Med. Chem.* **2008**, *51*, 4359–4369.

medicinal chemistry, selective fluorination of organic compounds serves as a broadly effective strategy for influencing characteristics such as solubility, lipophilicity, and metabolic stability. Modulation of biological properties via selective fluorination has also proven to be a valuable tool for development of new agrochemicals.[3] Because of their hydrophobicity and high chemical and thermal stability, fluorinated materials have found widespread use in a variety of applications, including surfaces and coatings, sensors, biomedical devices, microelectronics, and fluorous phase separations.[4]

The diverse applications of fluorinated compounds stem from fluorine's unique electronic properties. Fluorine is the most electronegative element in the periodic table. As a result, it forms highly polarized bonds to carbon that possess a substantial degree of ionic character. Due to this partial ionic character, the C–F bond is remarkably strong, with a bond dissociation energy of 105.5 kcal mol^{-1}. The C–F dipole can engage in electrostatic interactions with charges or with other dipoles, and the σ^* antibonding orbital can participate in hyperconjugative interactions that influence molecular conformation.[5]

Vicinal difluorides represent a particularly interesting and underexplored class of fluorinated compounds. This chapter describes the development of a method for preparing enantioenriched vicinal difluorides via the 1,2-difluorination of cinnamamides catalyzed by chiral aryl iodides. Section 1.2 introduces the properties of vicinal difluorides and describes traditional methods for their preparation. Section 1.3 outlines precedent for alkene 1,2-difluorination promoted by hypervalent aryl iodide difluorides, and places this work in the

[3] Jeschke, P. *ChemBioChem* **2004**, *5*, 570–589.

[4] (a) Pagliaro, M.; Ciriminna, R. *J. Mater. Chem.* **2005**, *15*, 4981–4991. (b) Okazoe, T. *Proc. Jpn. Acad. Ser. B Phys. Biol. Sci.* **2009**, *85*, 276–289. (c) Dams, R.; Hintzer, K. In *Fluorinated Polymers: Volume 2: Applications*; The Royal Society of Chemistry; Cambridge, **2016**; pp 1–31.

[5] O'Hagan, D. *Chem. Soc. Rev.* **2008**, *37*, 308–319.

context of other hypervalent iodine-promoted alkene difunctionalization chemistry. In sections 1.4 and 1.5, we report the development of an enantioselective aryl-iodide catalyzed 1,2-difluorination of primary cinnamamides and discuss the mechanistic implications of product partitioning between the desired 1,2-difluoride product and a 1,1-difluorinated side product. Section 1.6 recounts the extension of this approach to secondary cinnamamides, resulting in a more practical approach to synthesis of enantioenriched vicinal difluoride building blocks, while section 1.7 focuses on how steric and electronic properties of the substrate influence product partitioning. Methods for derivatization of the 1,2-difluoride products are set out in section 1.8.

1.2 Properties and Synthesis of Vicinal Difluorides

An intriguing feature of the vicinal difluoride motif is its known preference for adopting gauche conformations. In the prototypical example of 1,2-difluoroethane, the conformer in which the two fluorine atoms have a gauche relationship is favored over the anti conformer (Figure 1.1).[6] Computational modeling suggests that the gauche conformer is 0.9 kcal mol^{-1} lower in energy, a preference that is attributed to a hyperconjugative effect in which C–H bonds donate into the σ^* orbitals of both C–F bonds.[7] This hyperconjugative stabilization suffices to overcome the destabilizing effect of positioning two electronegative atoms next to each other. Evidence for the existence of a fluorine gauche effect has also been found in the solid state: the X-ray crystal structures of both *syn* and *anti* 2,3-difluorosuccinic acid show the fluorine gauche effect.[8]

---

[6] For NMR studies of 1,2-difluoroethane, see: (a) Abraham, R. J.; Kemp, R. H. *J. Chem. Soc. B* **1971**, 1240–1245. (b) Pedersen, B.; Klæboe, P.; Torgrimsen, T. *Acta Chem. Scand.* **1971**, *25*, 2367–2369.

[7] For molecular modeling studies examining the gauche effect, see: (a) Wolfe, S. *Acc. Chem. Res.* **1972**, *5*, 102–11. (b) Goodman, L.; Gu, H.; Pophristic, V. *J. Phys. Chem. A* **2005**, *109*, 1223–1229. (c) Souza, F. R.; Freitas, M. P.; Rittner, R. *J. Mol. Struct. Theochem.* **2008**, *863*, 137–140.

[8] O'Hagan, D.; Rzepa, H. S.; Schüler, M.; Slawin, A. M. Z. *Beilstein J. Org. Chem.* **2006**, *2*, No. 19.

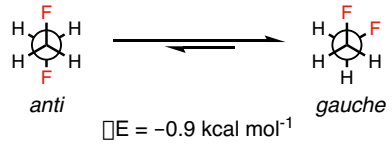

Figure 1.1 The vicinal difluoride gauche effect.

In general, compounds containing fluoride substituents adjacent to electronegative substituents other than fluoride (for example, F–C–C–O and F–C–C–N) prefer to assume gauche conformations. [9,10] However, vicinal dibromides and vicinal dichlorides do not display the gauche effect, instead preferentially adopting anti conformations.[11]

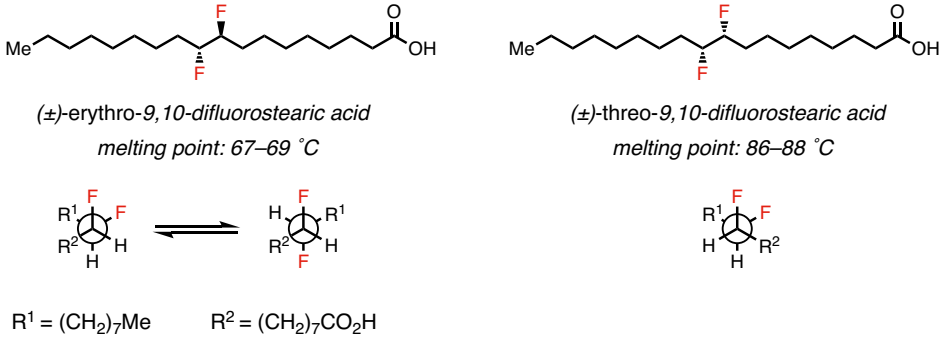

Figure 1.2 Conformational effects on the melting points of (±)-*erythro*- and (±)-*threo*-9,10-difluorostearic acids.

The conformational effects of vicinal difluorination discussed above can influence molecular structure and function in a variety of contexts. As a result, the vicinal difluoride gauche effect can be exploited as a tool for achieving conformational control and, by extension, exerting influence over various properties of interest. A study of *threo* (*syn*) and *erythro* (*anti*) 9,10-difluorostearic acid aptly demonstrates the effect that conformation can have on bulk

[9] For a review on the fluorine gauche effect, see: Thiehoff, C.; Rey, Y. P.; Gilmour, R. *Isr. J. Chem.* **2017**, *57*, 92–100.

[10] Linclau, B.; Leung, L.; Nonnenmacher, J.; Tizzard, G. *Beilstein J. Org. Chem.* **2010**, *6*, No. 62.

[11] See ref. 5.

physical properties (Figure 1.2).[12] The *anti* isomer has an appreciably lower melting point than the *syn* isomer, an observation that may reflect higher chain disorder in the *anti* isomer. This explanation is consistent with conformational analysis of the two isomers. The *anti* isomer has two viable rotamers: one that displays the fluorine gauche effect but also places two bulky alkyl groups gauche to each other, and one that adopts an extended *zig-zag* conformation but positions the two fluorine atoms anti to each other. In contrast, the *syn* isomer can adopt a single conformation that positions the fluorine atoms gauche to each other while maintaining an extended *zig-zag* conformation, resulting in greater conformational stability and thus, more efficient chain packing and a higher melting point.

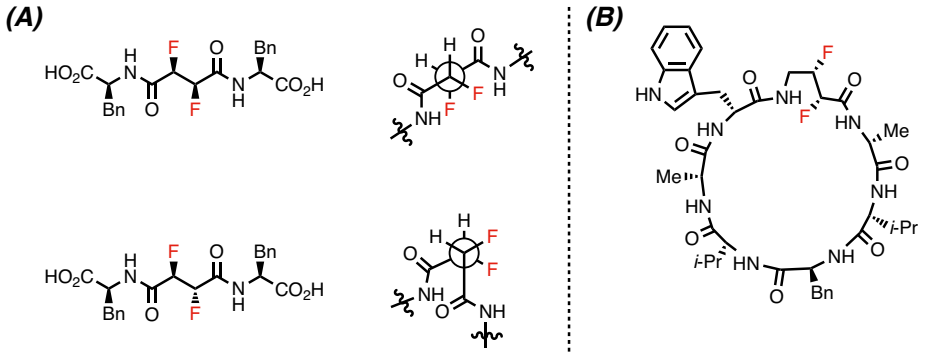

Figure 1.3 Effect of vicinal difluorination on peptide conformation. (A) Conformational preferences of the *syn* and *anti* isomers of bis(amino acid amides) of 2,3-difluorosuccinic acid. (B) A fluorinated analog of unguisin A.

Some studies have explored the impact of vicinal difluorination on peptide conformation.[13] According to X-ray crystal structure and solution state NMR data, the fluorine atoms assume a gauche conformation in both the *syn* and *anti* diastereomers of bis(amino acid

[12] Tavasli, M.; O'Hagan, D.; Pearson, C.; Petty, M. C. *Chem. Commun.* **2002**, 1226–1227.

[13] Selective monofluorination is also known to influence peptide conformation. For a pioneering example demonstrating that incorporation of 4(*R*)-fluoroproline residues increases the stability of collagen, see: Holmgren, S. K.; Taylor, K. M.; Bretscher, L. E.; Raines, R. T. *Nature* **1998**, *392*, 666–667.

amides) of 2,3-difluorosuccinic acid (Figure 1.3A).[14] The vicinal difluoride also influences the conformation of the bis(amides), due to an α-fluoroamide dipole minimization effect in which C–F bonds preferentially orient antiparallel to adjacent amide carbonyl bonds. Hunter and coworkers have demonstrated that incorporation of a vicinal difluoride motif alters the conformation of the naturally occurring cyclic peptide unguisin A (Figure 1.3B).[15]

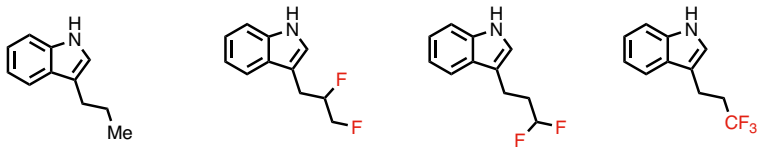

log *P*	3.3	2.5	2.9	3.1
solubility$_{aq\ pH=6.5}$ (μmol/L)	200	>1720	n.d.	30
human clearance rate [min^{-1}/(mg/μL)$_{prot}$]	513	212	372	410

Figure 1.4 Pharmacological properties of a series of fluorinated 3-substituted indoles.

While the pharmacological properties of vicinal difluorides have not been widely studied, Carreira, Müller, and coworkers have investigated how different fluorination patterns affect the pharmacological properties of a series of fluorinated 3-substituted indoles.[16] Of the compounds tested, the 1,2-difluorinated derivative possessed the lowest lipophilicity, the highest aqueous solubility, and the slowest clearance rate in humans (Figure 1.4). Notably, the vicinally difluorinated compound is less lipophilic than its geminally difluorinated counterpart. The authors attribute this observation to an increase in dipole moment resulting from a vicinal gauche arrangement of the fluoride substituents. These promising data motivate further exploration of the potential use of vicinal difluorination to modulate the biological properties of molecules.

---

[14] Schüler, M.; O'Hagan, D.; Slawin, A. M. Z. *Chem. Commun.* **2005**, 4324–4326.

[15] Hu, X.-G.; Thomas, D. S.; Griffith, R.; Hunter, L. *Angew. Chem., Int. Ed.* **2014**, *53*, 6176–6179.

[16] Huchet, Q. A.; Kuhn, B.; Wagner, B.; Kratochwil, N. A.; Fischer, H.; Kansy, M.; Zimmerli, D.; Carreira, E. M.; Müller, K. *J. Med. Chem.* **2015**, *58*, 9041–9060.

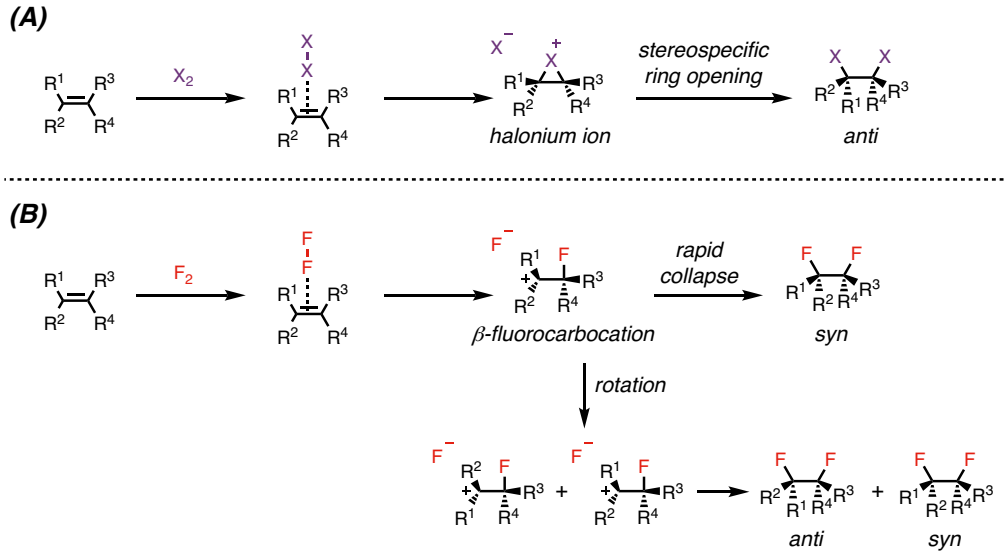

Scheme 1.1 (A) Alkene dihalogenation via stereospecific opening of a halonium ion. (B) Alkene difluorination proceeding through a β-fluorocarbocation intermediate.

The conceptually simplest approach to preparation of vicinal difluorides is through direct alkene difluorination with fluorine gas (F_2). Although examples of alkene difluorination with F_2 have been reported, this method is much less commonly employed than the analogous uses of bromine and chlorine to dihalogenate alkenes.[17] The scarcity of these transformations may be attributed in part to the extreme toxicity of F_2 and the specialized apparatuses required to handle it. Another barrier to widespread use of F_2 is its high reactivity, which results in limited functional group tolerance. When F_2 has been used to fluorinate alkenes, diastereoselectivity has presented a significant challenge. Unlike dibromination and dichlorination with molecular halogens, which generally proceed through stereospecific opening of halonium ion intermediates, difluorination with F_2 is proposed to involve the intermediacy of β-fluorocarbocations (Scheme 1.1). In some cases, high diastereoselectivity has been achieved, an outcome that is proposed to arise through the fast collapse of tight ion pairs. However, diastereoselectivity is highly

[17] For examples of racemic alkene fluorination with F_2, see: (a) Merritt, R. F.; Johnson, F. A. *J. Org. Chem.* **1966**, *31*, 1859–1863. (b) Barton, D. H. R.; Lister-James, J.; Hesse, R. H.; Pechet, M. M.; Rozen, S. *J. Chem. Soc., Perkin Trans. 1* **1982**, *1*, 1105–1110. (c) Purrington, S. T.; Kagen, B. S.; Patrick, T. B. *Chem. Rev.* **1986**, *86*, 997–1018.

substrate-dependent and controlling it has required extensive optimization of reaction conditions. Most successful examples take place at cryogenic temperatures and involve F_2 dilution with N_2 gas.[18]

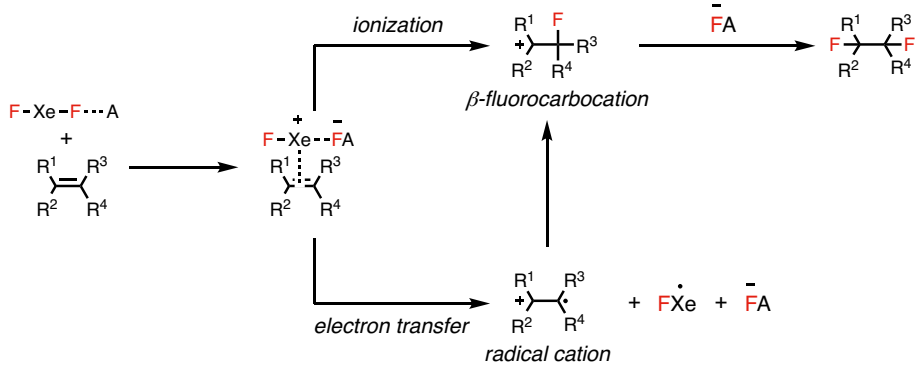

Scheme 1.2 Mechanistic pathways for alkene fluorination with XeF_2.

Xenon difluoride (XeF_2) can also be used to difluorinate alkenes.[19] Because it exists as a crystalline solid, it offers a practical advantage over fluorine gas on laboratory scale, although it still presents serious safety concerns. Alkene difluorination with XeF_2 typically requires the addition of an acid catalyst such as HF, trifluoroacetic acid, boron trifluoride etherate, or silicon tetrafluoride. The acid catalyst activates XeF_2, enabling the formation of an alkene-XeF_2 complex. The reaction is proposed to involve the intermediacy of a β-fluorocarbocation, which may be generated directly from the alkene-XeF_2 complex by fluoride attack, or via a radical cation intermediate formed by electron transfer within the alkene-XeF_2 complex (Scheme 1.2). Because of the cationic intermediates involved in the reaction, diastereocontrol is typically poor.

[18] For reports of diastereoselective 1,2-difluorination using dilute F_2 at low temperature, see: (a) Rozen, S.; Brand, M. *J. Org. Chem.* **1986**, *51*, 3607–3611. (b) Vints, I.; Rozen, S. *J. Org. Chem.* **2014**, *79*, 7261–7265. (c) Vints, I.; Rozen, S. *Tetrahedron* **2016**, *72*, 632–636.

[19] For examples of racemic alkene fluorination with XeF_2, see: (a) Šket, B.; Zupan, M. *J. Chem. Soc., Perkin Trans. 1*, **1977**, *1*, 2169–2172. (b) Shellhamer, D. F.; Conner, R. J.; Richardson, R. E.; Heasley, V. L.; Heasley, G. E. *J. Org. Chem.* **1984**, *49*, 5015–5018. (c) Stavber, S.; Sotler, T.; Zupan, M. Popovic, A. *J. Org. Chem.* **1994**, *59*, 5891–5894. (d) Shellhamer, D. F.; Chiaco, M. C.; Gallego, K. M.; Low, W. S. C.; Carter, B.; Heasley, V. L.; Chapman, R. D. *J. Fluorine Chem.* **1995**, *72*, 83–87. (e) Tius, M. A. *Tetrahedron* **1995**, *51*, 6605–6634. (f) Tamura, M.; Takagi, T.; Quan, H.-d.; Sekiya, A. *J. Fluorine Chem.* **1999**, *98*, 163–166.

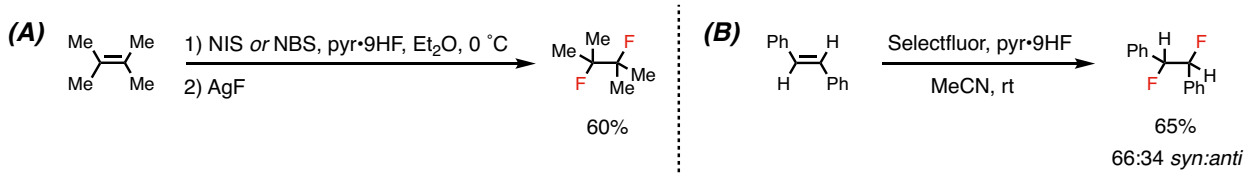

Scheme 1.3 (A) Alkene difluorination with *N*-halosuccinimide/HF-pyridine. (B) Alkene difluorination with Selectfluor/HF-pyridine.

An alternative approach to alkene difluorination involves the combination of an electrophilic fluorinating reagent and a nucleophilic fluorinating reagent. Olah and coworkers pioneered a two-step version of this approach in which 1,2-halofluorination of alkenes with an *N*-halosuccinimide and HF-pyridine was followed by treatment with silver fluoride (Scheme 1.3A).[20] Lal employed a related strategy to difluorinate styrenes, with Selectfluor serving as the electrophilic fluorinating reagent and HF-pyridine serving as the nucleophilic fluoride source (Scheme 1.3B).[21] Although this method generated difluorinated products in moderate yields, it exhibited poor diastereoselectivity.

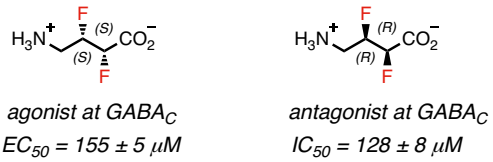

Figure 1.5 Enantiomers of *syn*-2,3-difluoro-4-aminobutyric acid exhibit opposite activities at the $GABA_C$ receptor.

All of the difluorination methods discussed above suffer from poor diastereocontrol due to the involvement of cationic intermediates. An additional limitation of these methods is that

[20] (a) Olah, G. A.; Welch, J. T.; Vankar, Y. D.; Nojima, M.; Kerekes, I.; Olah, J. A. *J. Org. Chem.* **1979**, *44*, 3872–3881. For another example of vicinal difluoride synthesis via alkene halofluorination followed by halide displacement with a nucleophilic fluoride source, see: (b) O'Hagan, D.; Rzepa, H. S.; Schüler, M.; Slawin, A. M. Z. *Beilstein J. Org. Chem.* **2006**, *2*, 19.

[21] Lal, G. S. *J. Org. Chem.* **1993**, *58*, 2791–2796.

they do not present the opportunity for extension to enantioselective difluorination; however, control of absolute stereochemistry may be essential for certain applications. A study of the bioactivity of fluorinated γ-aminobutyric acid derivatives elegantly supports this point. The mammalian central nervous system relies on γ-aminobutyric acid (GABA) to serve as a neurotransmitter by interacting with multiple GABA receptors. Conformationally restricted GABA analogues can be used to study the bioactive conformations of GABA at its receptors, an endeavor ultimately aimed toward development of selective GABA receptor ligands for therapeutic applications. Hunter and coworkers synthesized stereoisomers of 2,3-difluoro-4-aminobutyric acid from chiral diol starting materials and determined that the *syn* enantiomers exhibit opposite activities at the $GABA_C$ receptor, with the *(S,S)* enantiomer acting as an agonist while the *(R,R)* enantiomer serves as an antagonist (Figure 1.5).[22] This finding emphasizes that the ability to control the absolute stereochemistry of vicinal difluorides may be critical for their potential future application in the design of conformationally defined bioactive molecules.

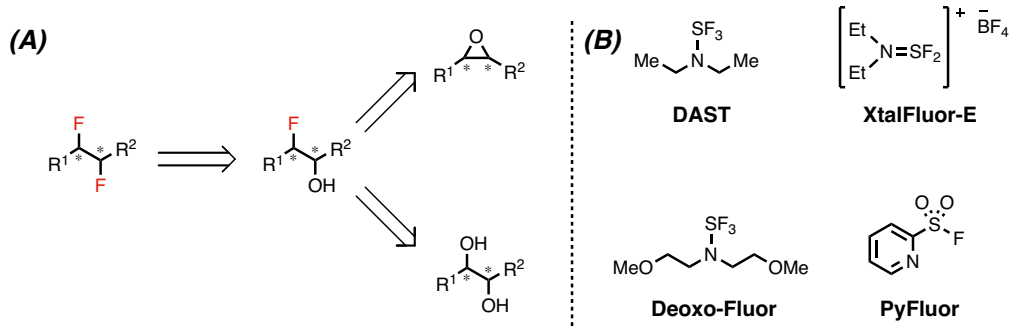

Scheme 1.4 Enantiocontrolled synthesis of 1,2-difluorides. (A) Retrosynthesis involving deoxyfluorination of stereodefined 1,2-fluoroalcohols. (B) Representative deoxyfluorination reagents.

The direct, enantioselective, 1-2 difluorination of alkenes represents a most appealing approach to synthesis of vicinal difluorides, but no general methods have yet been identified for

[22] Yamamoto, I.; Jordan, M. J. T.; Gavande, N.; Doddareddy, M. R.; Chebib, M.; Hunter, L. *Chem. Commun.* **2012**, *48*, 829–831.

accomplishing such a transformation. Reported examples of enantiocontrolled synthesis of vicinal difluorides most often involve deoxyfluorination of 1,2-fluoroalcohols derived from stereodefined epoxides or diols (Scheme 1.4A).[23] Deoxyfluorination is typically achieved using aminosulfurane reagents such as diethylaminosulfur trifluoride (DAST) or its analogue bis(2-methoxyethyl)aminosulfur trifluoride (Deoxo-Fluor) (Scheme 1.4B).[24] However, these reactions are prone to competitive elimination pathways and are often low-yielding (Scheme 1.5).[25]The aminodifluorosulfinium tetrafluoroborate salt XtalFluor-E has been developed as a solid, more thermally stable alternative to the aminosulfurane reagents.[26] The recently developed sulfonyl fluoride reagent PyFluor demonstrates high selectivity for substitution over elimination in some substrate classes.[27] While progress has been made in the development of new deoxyfluorination reagents, none of these reagents have found widespread application in the synthesis of vicinal difluorides. New methods for direct, enantioselective alkene difluorination could enable a more thorough exploration of the effect that the vicinal difluoride motif has on molecular structure and function.

---

[23] For syntheses of enantioenriched vicinal difluorides via deoxyfluorination of stereodefined epoxides and diols, see: (a) Bell, H. M.; Hudlicky, M. *J. Fluorine Chem.* **1980**, *15*, 191–200. (b) Burmakov, A. I.; Motnyak, L. A.; Kunshenko, B. V.; Alexeeva, L. A.; Yagupolskii, L. M. *J. Fluorine Chem.* **1981**, *19*, 151–161. (c) Hamatani, T.; Matsubara, S.; Matsuda, H.; Schlosser, M. *Tetrahedron* **1988**, *44*, 2875–2881. (d) Marson, C. M.; Melling, R. C. *Chem. Commun.* **1998**, 1223–1224. (e) O'Hagan, D.; Rzepa, H. S.; Schüler, M.; Slawin, A. M. Z. *Beilstein J. Org. Chem.* **2006**, *2*, 19. (f) Hunter, L.; Jolliffe, K. A.; Jordan, M. J. T.; Jensen, P.; Macquart, R. B. *Chem. –Eur. J.* **2011**, *17*, 2340–2343.

[24] Lal, G. S.; Pez, G. P.; Pesaresi, R. J.; Prozonic, F. M.; Cheng, H. *J. Org. Chem.* **1999**, *64*, 7048–7054.

[25] (a) Clark, J. L.; Hollecker, L.; Mason, J. C.; Stuyver, L. J.; Tharnish, P. M.; Lostia, S.; McBrayer, T. R.; Schinazi, R. F.; Watanabe, K. A.; Otto, M. J.; Furman, P. A.; Stec, W. J. Patterson, S. E.; Pankiewicz, K. W. *J. Med. Chem.* **2005**, *48*, 5504–5508. (b) Tavasli, M.; O'Hagan, D.; Pearson, C.; Petty, M. C. *Chem. Commun.* **2002**, 1226–1227.

[26] Beaulieu, F.; Beauregard, L.-P.; Courchesne, G.; Couturier, M.; LaFlamme, F.; L'Heureux, A. *Org. Lett.* **2009**, *11*, 5050–5053.

[27] Nielsen, M. K.; Ugaz, C. R.; Li, W.; Doyle, A. G. *J. Am. Chem. Soc.* **2015**, *137*, 9571–9574.

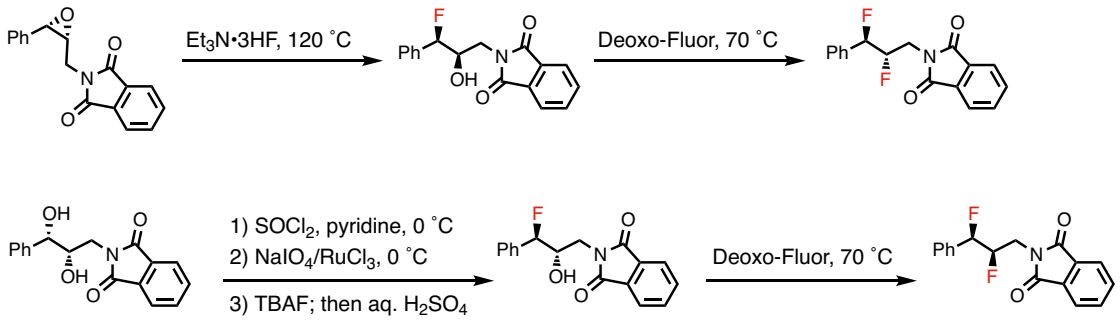

Scheme 1.5 Representative syntheses of stereodefined 1,2-difluorides from stereodefined epoxides and diols.

1.3 Alkene Difunctionalization Reactions Promoted by Hypervalent Iodine Compounds

In 1886, Willgerodt synthesized iodobenzene dichloride, the first reported preparation of a hypervalent iodine compound.[28] Hypervalent iodine compounds have since emerged as an effective and versatile class of reagents for promoting a diverse range of alkene difunctionalization reactions.[29] Aryl-λ^3-iodanes ($ArIL_2$), the most common hypervalent iodine compounds, adopt a pseudotrigonal bipyramidal geometry containing a three-center four-electron L–I–L bond (Figure 1.6A).[30] Their synthetic utility results from their high leaving group ability. Aryl-λ^3-iodanes are hypernucleofuges — hypervalent leaving groups that undergo reductive elimination to restore the normal valency of the hypervalent atom and that display leaving group abilities surpassing those of super leaving groups such as triflate (Figure 1.6B).

[28] Willgerodt, C. *J. Prakt. Chem.* **1886**, *33*, 154–160.

[29] For selected recent reviews, see: (a) Romero, R. M.; Wöste, T. H.; Muñiz, K. *Chem. – Asian J.* **2014**, *9*, 972–983. (b) Yoshimura, A.; Zhdankin, V.V. *Chem. Rev.* **2016**, *116*, 3328–3435. (c) Kohlhepp, S. V.; Gulder, T. *Chem. Soc. Rev.* **2016**, *45*, 6270–6288. (d) Claraz, A.; Masson, G. *Org. Biomol. Chem.* **2018**, *16*, 5386–5402. (e) Flores, A.; Cots, E.; Berges, J.; Muñiz, K. *Adv. Synth. Catal.* **2019**, *361*, 2–25.

[30] Ochiai, M. In *Hypervalent Iodine Chemistry: Modern Developments in Organic Synthesis.* Wirth, T., Ed.; Springer-Verlag Berlin and Heidelberg GmbH & Co. KG: Berlin, **2003**; pp 8–68.

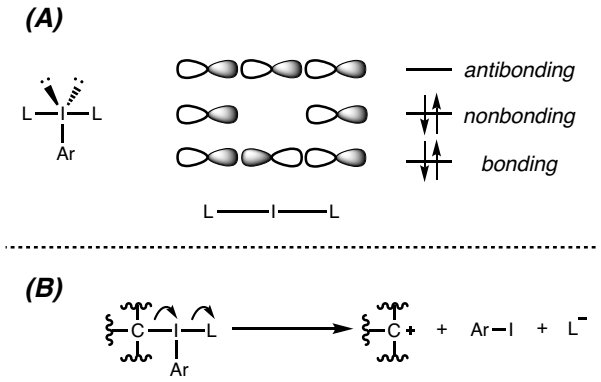

Figure 1.6 (A) $ArIL_2$ pseudotrigonal bipyramidal geometry and molecular orbital picture of the three-center-four-electron L–I–L bond. (B) Hypernucleofuge reductive elimination process.

There has been remarkable progress over the past decade in the development of enantioselective alkene difunctionalization reactions using hypervalent iodine reagents and catalysts.[31] These enantioselective methods include oxylactonization, diacetoxylation, and diamination reactions. A variety of chiral aryl iodide scaffolds have been developed over the course of these efforts (Figure 1.7).

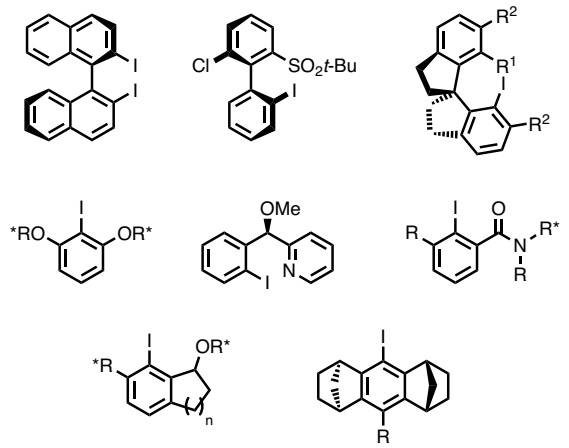

Figure 1.7 Chiral aryl iodide scaffolds.

[31] (a) Fujita, M.; Yoshida, Y.; Miyata, K.; Wakisaka, A.; Sugimura, T. *Angew. Chem. Int. Ed.* **2010**, *49*, 7068–7071. (b) Romero, R. M.; Wöste, T. H.; Muñiz, K. *Chem. – Asian J.* **2014**, *9*, 972–983. (c) Mizar, P.; Laverny, A.; El-Sherbini, M.; Farid, U.; Brown, M.; Malmedy, F.; Wirth, T. *Chem. – Eur. J.* **2014**, *20*, 9910–9913. (d) Haubenreisser, S.; Wöste, T. H.; Martínez, C.; Ishihara, K.; Muñiz, K. *Angew. Chem. Int. Ed.* **2016**, *55*, 413–417. (e) Wöste, T. H.; Muñiz, K. *Synthesis* **2016**, *48*, 816–827. (f) Muñiz, K.; Barreiro, L.; Romero, R. M.; Martínez, C. *J. Am. Chem. Soc.* **2017**, *139*, 4354–4357. (g) Gelis, C.; Dumoulin, A.; Bekkaye, M.; Neuville, L.; Masson, G. *Org. Lett.* **2017**, *19*, 278–281.

Nevado and coworkers reported the first enantioselective fluorofunctionalization reaction mediated by hypervalent iodine. They found that upon treatment with a chiral lactate-derived aryl iodide difluoride, alkene substrates bearing a pendant amine afford aminofluorinated substrates (Figure 1.8).[32] The reactions proceed via alkene activation promoted by a chiral aryl iodide difluoride, followed by amine cyclization and subsequent fluoride trapping. This report also includes several examples of intermolecular reactions between alkenes and exogenous amines promoted by an achiral aryl iodide difluoride.

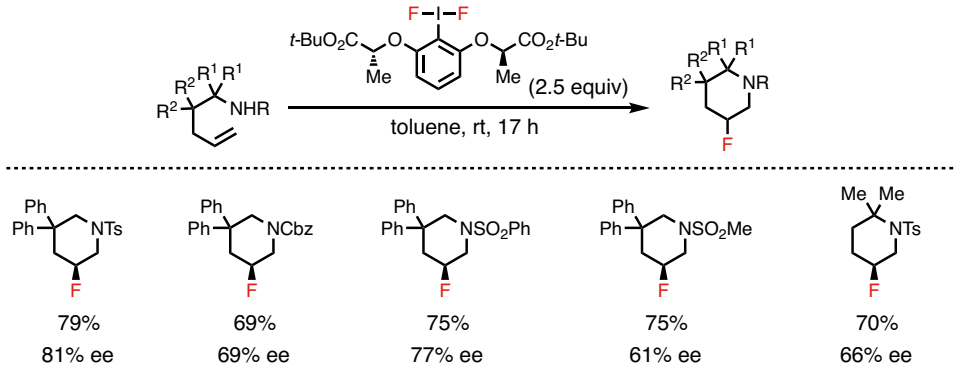

Figure 1.8 Enantioselective, intramolecular aminofluorination of alkenes.

Hara and coworkers published the seminal report of hypervalent iodine-promoted difluorination of alkenes.[33] Upon treatment with stoichiometric *p*-iodotoluene difluoride in neat triethylamine pentahydrofluoride, difluorination of a variety of terminal and cyclic alkenes proceeded in moderate to good yields (Figure 1.9). This protocol was successfully applied to substrates containing free alcohols, esters, and acetals. In addition, terminal alkenes could be selectively difluorinated in the presence of internal alkenes. Varying the HF source had a detrimental impact; no reaction took place in the presence of triethylamine trihydrofluoride, and

[32] Kong, W.; Feige, P.; de Haro, T.; Nevado, C. *Angew. Chem. Int. Ed.* **2013**, *52*, 2469–2473.

[33] Hara, S.; Nakahigashi, J.; Ishi-I, K.; Sawaguchi, M.; Sakai, H.; Fukuhara, T.; Yoneda, N. *Synlett* **1998**, 495–496.

use of HF-pyridine resulted in lower yields. A similar strategy employing polyvalent selenium and tellurium fluorinating reagents had been previously reported, but this method suffered from poor diastereoselectivity and only resulted in the vicinal difluorination of select substrates, instead affording fluorochalcogenated compounds in many cases.[34]

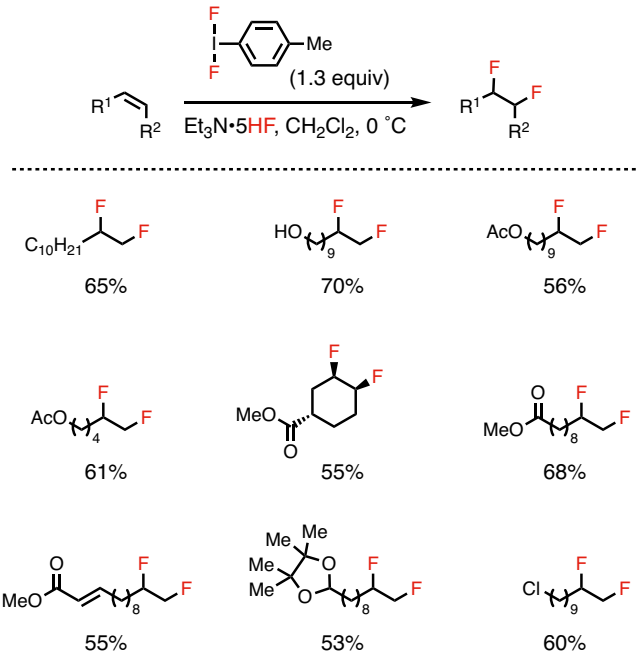

Figure 1.9 Vicinal difluorination of alkenes with stoichiometric *p*-iodotoluene difluoride.

The Gilmour lab and our group recently developed catalytic variants of the alkene 1,2-difluorination first reported by Hara. Our system engaged HF-pyridine as a nucleophilic fluoride source and *meta*-chloroperbenzoic acid (*m*CPBA) as the stoichiometric oxidant.[35] This protocol is broadly applicable to terminal alkenes, trisubstituted internal alkenes, and acrylamides, affording vicinal difluoride products with generally high diastereoselectivities (Figure 1.10). Limitations of the method include phenols and other electron-rich arenes, which are susceptible

[34] Lermontov, S. A.; Zavorin, S. I.; Bakhtin, I. V.; Pushin, A. N.; Zefirov, N. S.; Stang, P. J. *J. Fluorine Chem.* **1997**, *87*, 75–83.

[35] Banik, S. M.; Medley, J. W.; Jacobsen, E. N. *J. Am. Chem. Soc.* **2016**, *138*, 5000–5003.

to oxidation, as well as symmetrical 1,2-disubstituted alkenes, which form intractable mixtures of fluorinated and oligomeric products. The contemporaneously reported method from the Gilmour group, which can be applied to a variety of terminal alkenes, uses Selectfluor as the stoichiometric oxidant and a mixture of HF-pyridine and triethylamine trihydrofluoride as the fluoride source.[36]

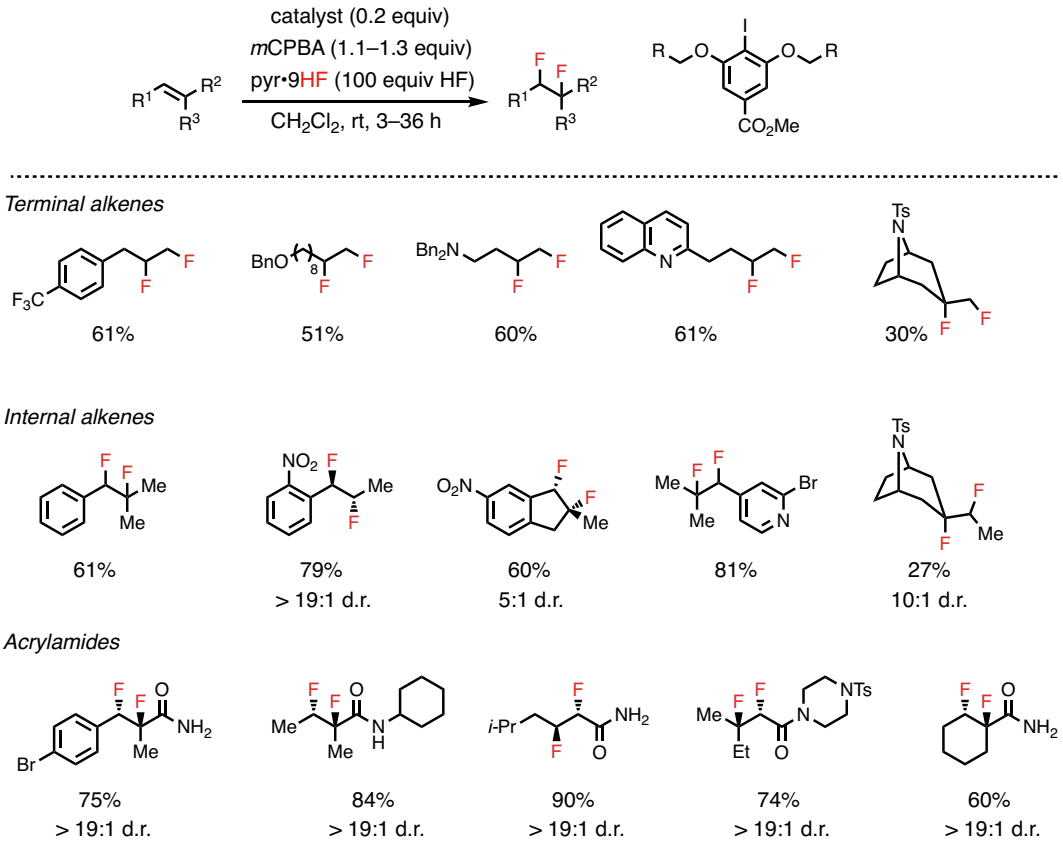

Figure 1.10 Aryl iodide-catalyzed, diastereoselective 1,2-difluorination of alkenes.

In the proposed catalytic cycle for the aryl iodide-catalyzed difluorination, *m*CPBA oxidizes the aryl iodide **I**, forming an iodosylarene **II** that undergoes deoxyfluorination with HF (Scheme 1.6). The resulting aryl iodide difluoride **III** forms an iodonium complex **IV** with the alkene substrate. Formation of an *anti*-fluoroiodinated intermediate **V** then occurs, with the

[36] Molnár, I. G.; Gilmour, R. *J. Am. Chem. Soc.* **2016**, *138*, 5004–5007.

fluoride substituent occupying the more substituted alkene carbon. Stereospecific displacement affords the vicinal difluoride product and regenerates the aryl iodide catalyst.

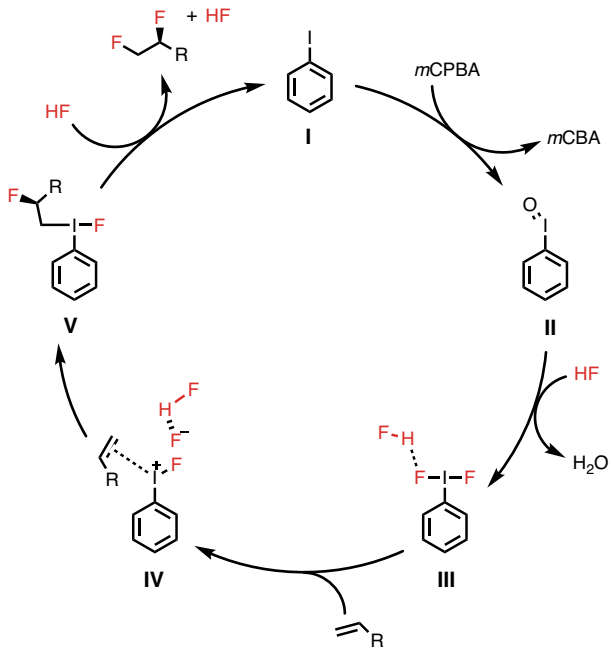

Scheme 1.6 Proposed catalytic cycle for aryl iodide-catalyzed 1,2-difluorination of alkenes.

Some styrenyl substrates are susceptible to rearrangement pathways that afford 1,1-difluorinated products.[37,38] Building on this precedent, our group developed an enantioselective 1,1-difluorination protocol that converts β-substituted styrenes to products containing difluoromethylated tertiary and quaternary stereocenters (Figure 1.11).[39] Using related chiral resorcinol-derived catalysts, our group has developed additional reactions involving neighboring

[37] (a) Dimroth, O.; Bockemüller, W. *Ber. Dtsch. Chem. Ges. B* **1931**, *64*, 516–522. (b) Bockmüller, W. *Ber. Dtsch. Chem. Ges. B* **1931**, *64*, 522–530. Both preceding references originally reported products resulting from 1,2-difluorination, but were later shown to produce 1,1-difluorinated products: (c) Bornstein, J.; Borden, M. R.; Nunes, F.; Tarlin, H. I. *J. Am. Chem. Soc.* **1963**, *85*, 1609–1615.

[38] For examples of racemic 1,1-difluorination of alkenes with hypervalent iodine reagents and catalysts, see: (a) Hara, S.; Nakahigashi, J.; Ishi-I, K.; Fukuhara, T.; Yoneda, N. *Tetrahedron Lett.* **1998**, *39*, 2589–2592. (b) Ilchenko, N. O.; Tasch, B. O.; Szabo, K. J. *Angew. Chem. Int. Ed.* **2014**, *53*, 12897–12901. (c) Kitamura, T.; Muta, K.; Oyamada, J. *J. Org. Chem.* **2015**, *80*, 10431–10436. (d) Scheidt, F.; Neufeld, J.; Schäfer, M.; Thiehoff, C.; Gilmour, R. *Org. Lett.* **2018**, *20*, 8073–8076.

[39] Banik, S. M.; Medley, J. W.; Jacobsen, E. N. *Science* **2016**, *353*, 51–54.

group participation, including a fluorolactonization of styrenyl substrates and a fluoroaziridination of allylic amines.[40]

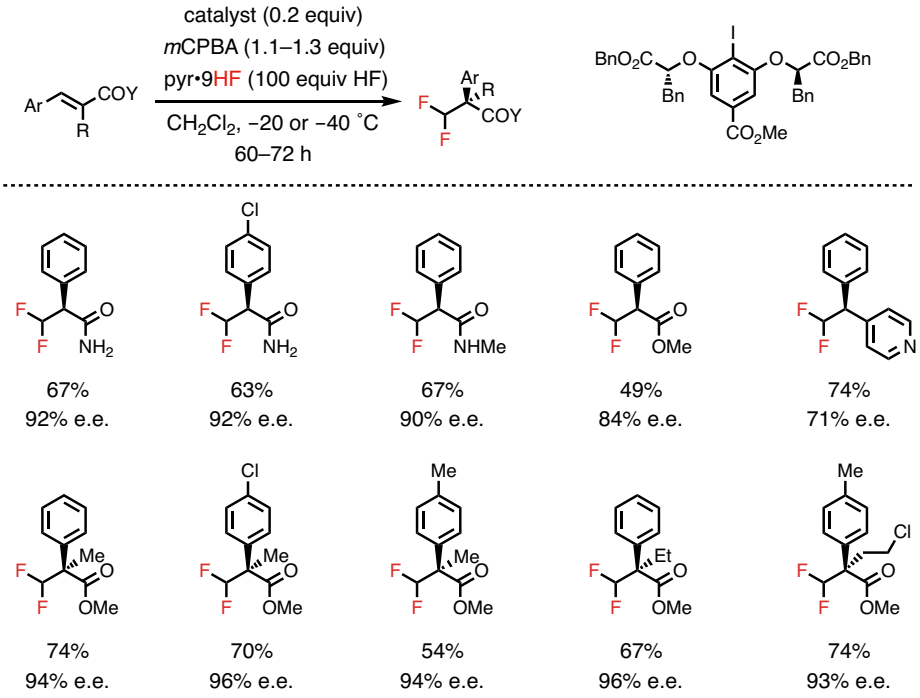

Figure 1.11 Aryl iodide-catalyzed, enantioselective 1,1-difluorination of β-substituted styrenes.

1.4 Catalytic, Enantioselective 1,2-Difluorination: Reaction Development with Primary Cinnamamides[41]

Our group's report of an alkene 1,2-difluorination protocol included a single example of an enantioselective variant in the 1,2-difluorination of trisubstituted cinnamamide **2a** catalyzed

[40] (a) Woerly, E. M.; Banik, S. M.; Jacobsen, E. N. *J. Am. Chem. Soc.* **2016**, *138*, 13858–13861. (b) Mennie, K. M.; Banik, S. M.; Reichert, E. C.; Jacobsen, E. N. *J. Am. Chem. Soc.* **2018**, *140*, 4797–4802.

[41] The work described in Sections 1.4 and 1.5 was performed in collaboration with Dr. Steven M. Banik, and portions of the data found here are also described in Dr. Banik's dissertation: Banik, S. M. I. Chiral Squaramide Catalysts for Lewis Acid Activation in Asymmetric Catalysis II. Catalytic, Stereoselective Difluorination Reactions. Ph.D. Thesis, Harvard University, **2016**.

by chiral aryl iodide **1a** (Scheme 1.7).[42] The 1,2-difluoride product **3a** is formed in 93% e.e. and displays an anti relationship between the two fluorides, a feature that is presumed to result from an amide anchimeric assistance pathway. We aimed to extend this approach to development of an aryl iodide-catalyzed 1,2-difluorination reaction that provides versatile synthetic building blocks containing contiguous secondary and tertiary fluorine-bearing stereocenters.

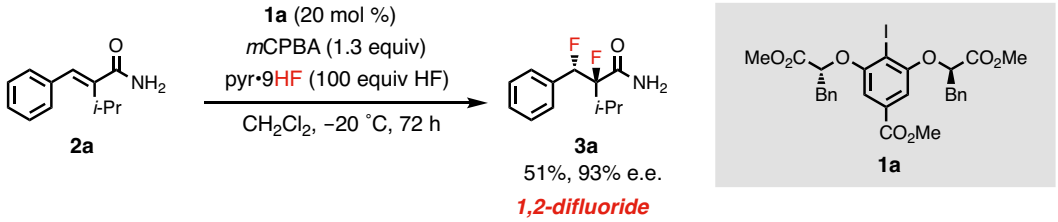

Scheme 1.7 Enantioselective 1,2-difluorination of a trisubstituted cinnamamide.

In the difluorination of trisubstituted cinnamamide **2b** catalyzed by aryl iodide **1b**, a mixture of 1,2- and 1,1-difluoride products **3b** and **4b** was obtained unselectively (Scheme 1.8). Product partitioning is proposed to arise from the initial fluoroiodination adduct **VI**, which can undergo aryl iodide displacement either by the amide carbonyl oxygen or by the aryl group (Scheme 1.9). The basis for enantioinduction is likely common to both pathways and was explored computationally in a recent collaborative study.[43]

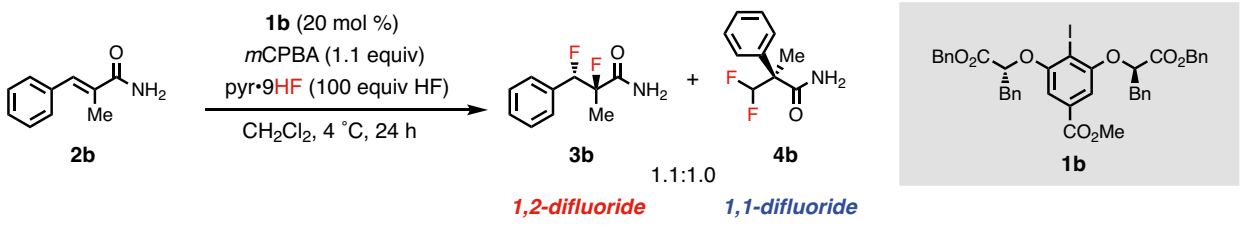

Scheme 1.8 Competition between 1,2- and migratory 1,1-difluorination.

[42] The initial report of aryl iodide-catalyzed alkene difluorination from Gilmour and coworkers also included a single enantioselective example of difluorination of a terminal alkene, in which use of a chiral resorcinol-derived aryl iodide afforded product in 22% ee (see ref. 36).

[43] Zhou, B.; Haj, M. K.; Jacobsen, E. N.; Houk, K. N.; Xue, X.-S. *J. Am. Chem. Soc.* **2018**, *140*, 15206–15218.

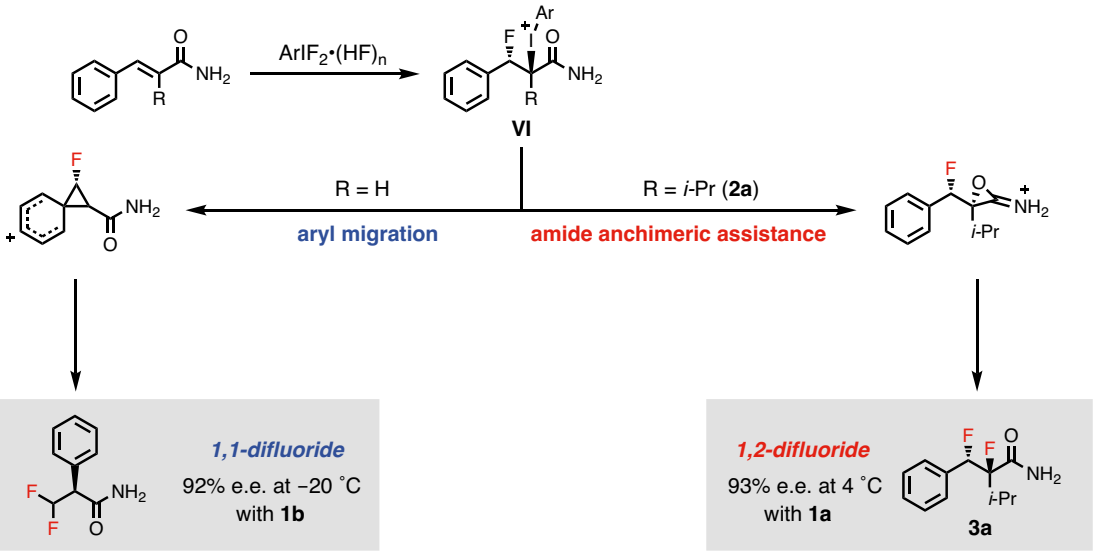

Scheme 1.9 Mechanistic rationale for 1,2- vs. 1,1-difluorination.

Investigation of primary cinnamamides bearing α-alkyl substituents revealed that **1b** catalyzes both 1,1- and 1,2-difluorination of these substrates, with the 1,2-difluoride products generated in high enantiomeric excess (Figure 1.12). Ratios of the two products depend strongly on substrate features such as aromatic substitution and the identity of the α-alkyl substituent. For substrates with more electron-rich arenes (**2f**), the 1,1-difluoride product predominates, whereas 1,2-difluorination is favored for substrates bearing electron-withdrawing substituents on the arene (**2c–d**). Chemoselectivity for 1,2- vs. 1,1-difluorination was observed to be correlated directly to the nucleophilicity of the arene, as evidenced by the positive linear correlation ($\rho^+ = 11$) between the Hammett substituent constants ρ^+ and log(**3:4**) for substrates **2b–f** (Figure 1.13).

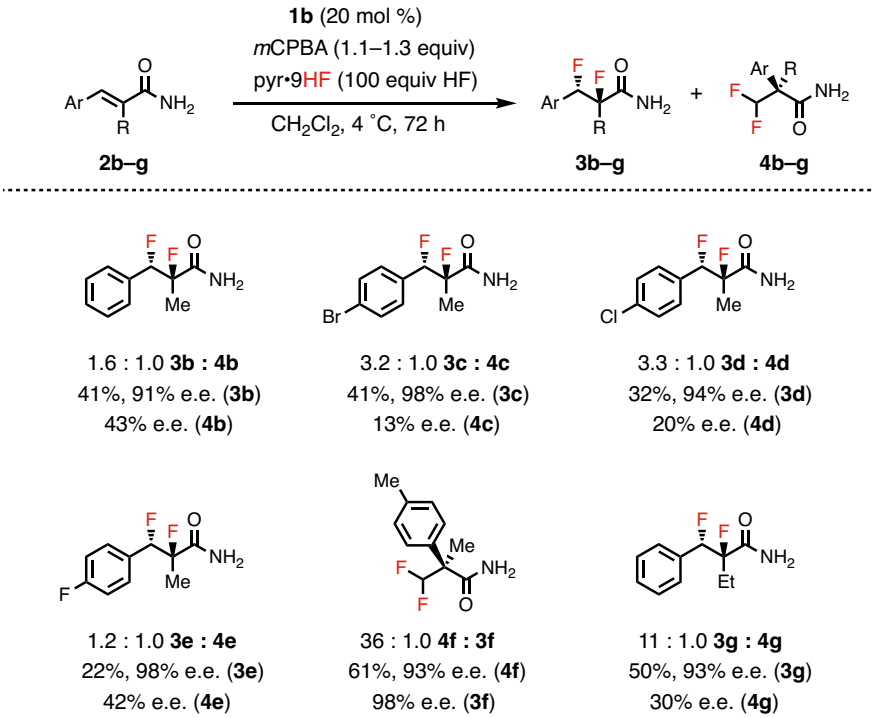

Figure 1.12 Primary cinnamamide substrate scope. Reactions were conducted on a 1.04 mmol scale with 11 equiv of HF-pyridine. Ratios of 1,2-difluoride to 1,1-difluoride were determined by ^{19}F NMR analysis of crude product mixtures. Isolated yields of diastereomerically pure compounds are reported. The relative and absolute configurations of all 1,2-difluorination products were assigned by analogy to **3a**.

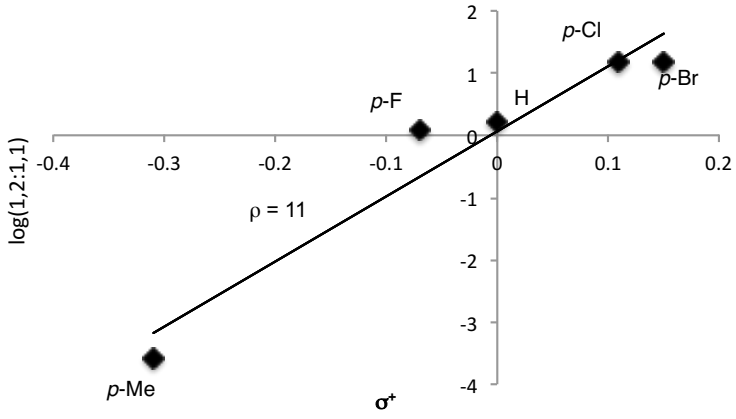

Figure 1.13 Hammett plot of σ^+ values of the aryl substituents in **2b–f** versus the product ratio (log(1,2:1,1)) obtained for each substrate.

Substrate **2g**, which bears an ethyl substituent α to the amide carbonyl, undergoes 1,2-difluorination with significantly higher product selectivity than α-methyl substrate **2b**. We prepared the α-ethyl analogues of substrates **2d** and **2f** to probe the generality of this effect (Figure 1.14). Upon replacement of the methyl group in electron-deficient *p*-chloro substrate **2d** with an ethyl group in substrate **2h**, the selectivity for 1,2-difluorination over 1,1-difluorination increased from 3.3:1.0 to greater than 60:1.0. We observed a similarly striking increase in 1,2-product selectivity when comparing the highly 1,1-selective electron-rich *p*-methyl substrate **2f** with its α-ethyl analogue **2i**. The presence of a bulky substituent α to the amide carbonyl may hinder attack by the bulkier neighboring group (aryl vs. amide), thereby leading to higher 1,2-product selectivity.

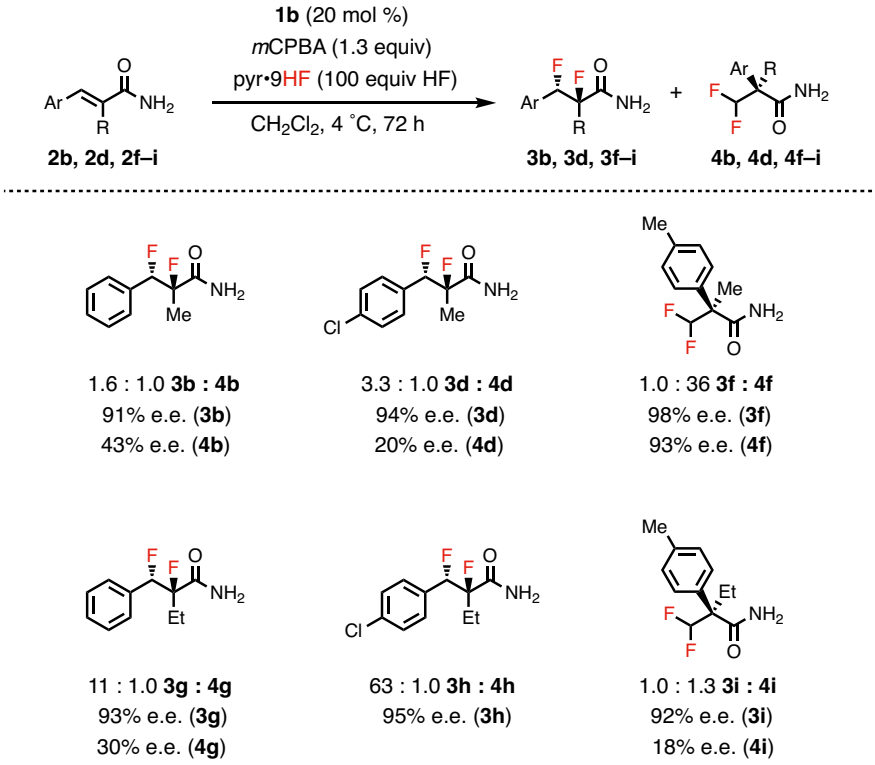

Figure 1.14 Comparison of α-methyl vs. α-ethyl substrates. Reactions were conducted on a 1.04 mmol scale with 11 equiv of HF-pyridine. Ratios of 1,2-difluoride to 1,1-difluoride were determined by ^{19}F NMR analysis of crude product mixtures. The relative and absolute configurations of all 1,2-difluorination products were assigned by analogy to **3a**.

Several catalysts were screened using the 1,2-selective substrate **2g** (Figure 1.15). Catalyst **1b** proved optimal, affording product in 60% yield and 93% e.e. after 24 h. Using analogous catalysts with more electron-withdrawing arene substituents *para* to the iodine substituent (**1c–d**) did not result in improved yields or enantioselectivities, but use of catalysts lacking an electron-withdrawing *para* substituent (**1e–h**) resulted in dramatically diminished conversions and enantioselectivities. This data suggests that the *para*-substituent does not affect the inherent enantioselectivity of 1,2-difluorination. Rather, we hypothesize that more electron-rich catalysts lacking an electron-withdrawing *para*-substituent decompose under the reaction conditions to form species that retain some catalytic activity but impart poor enantioselectivity.[44] Replacing the benzyl groups on the catalyst arms with cyclohexyl groups (**1i**) results in diminished conversion and enantioselectivity; previous studies have suggested that these benzyl groups may participate in cation-π interactions that selectively stabilize the transition state leading to the major enantiomer.[45] Replacing the ester groups on the catalyst arms with *N*-mesityl amides (**1j–k**) results in a precipitous drop in conversion and enantioselectivity.

[44] In other reactions that proceed at lower HF-pyridine loadings, aryl iodides lacking a *para*-ester substituent are efficient and highly enantioselective catalysts, presumably because catalyst decomposition pathways are slower under these reaction conditions (see ref. 40a).

[45] See ref. 39.

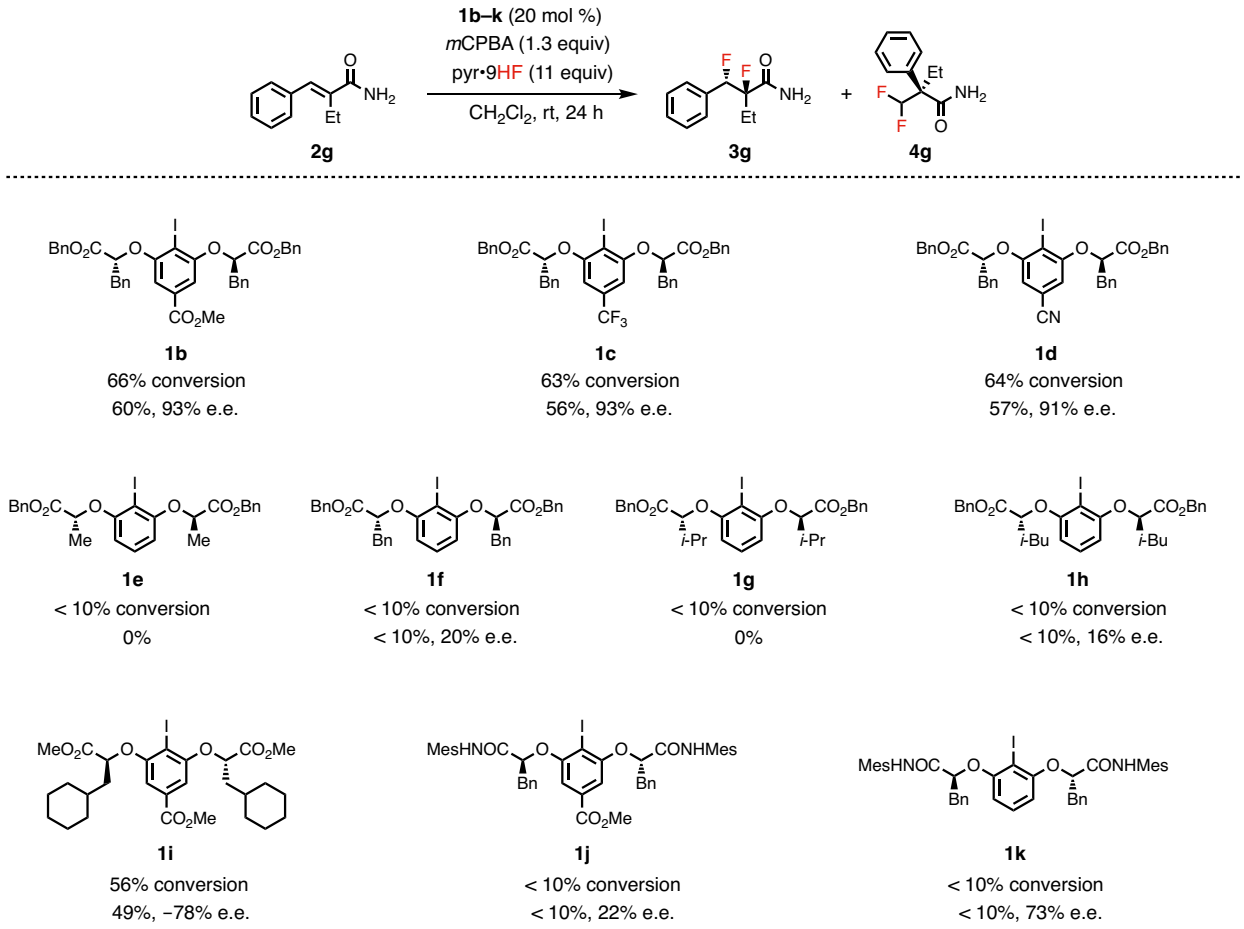

Figure 1.15 Survey of chiral catalysts for the 1,2-difluorination of primary cinnamamides. Reactions were conducted on a 0.05 mmol scale with 11 equiv of HF-pyridine. Reported yields were determined by ^{19}F NMR using trifluorotoluene as an internal standard.

1.5 Mechanistic Implications of Product Partitioning

Subtle changes to substrate structure dramatically affect product ratios and enantioselectivities in the difluorination reactions of primary cinnamamides. Specifically, (i) relatively small increases in α-alkyl substituent size have a remarkable impact on product ratio, and (ii) for the majority of reactions, the 1,2-difluoride product and the 1,1-difluoride product are generated with notably different levels of enantioselectivity, even though they presumably arise

from a common intermediate. Mechanistic proposals accounting for these observations are discussed here.

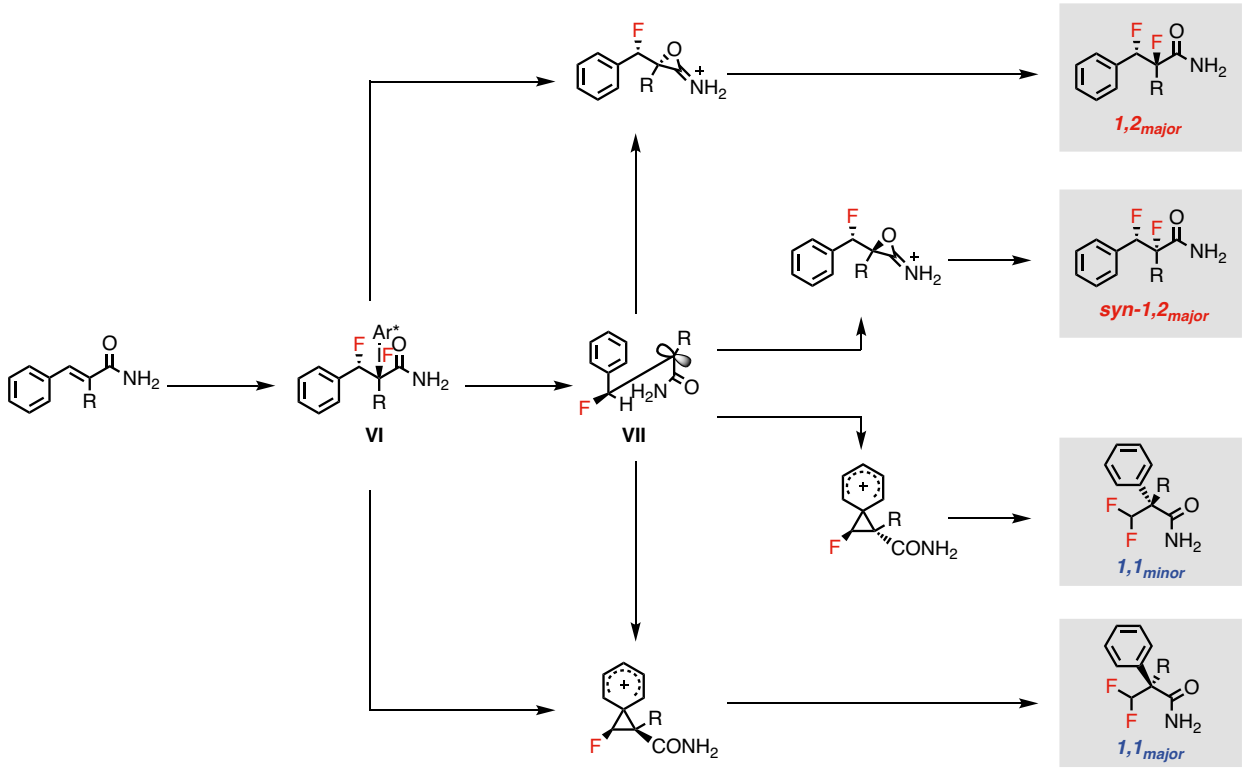

Scheme 1.10 A mechanistic proposal for divergent enantioenrichment in the 1,2- and 1,1-difluoride products involving ionization of a fluoroiodinated intermediate.

Almost every cinnamamide substrate tested afforded 1,2-difluoride product with greater than 90% e.e. and 1,1-difluoride product with substantially lower e.e. Erosion of 1,1-difluoride enantioenrichment could occur through ionization of the C–I bond in the fluoroiodinated intermediate **VI** to form a carbocation **VII**, which could participate in non-stereospecific aryl migration (Scheme 1.10). This pathway would form both enantiomers of 1,1-difluoride, eroding the enantioselectivity imparted by direct, stereospecific phenonium formation from the fluoroiodinated intermediate. However, if this pathway operates competitively, it should also lead to non-stereospecific amide oxygen attack, resulting in formation of two diastereomers of

1,2-difluoride. The experimentally observed high diastereoselectivity of 1,2-difluorination suggests that complete ionization of the fluoroiodinated intermediate to form a carbocation is unlikely.

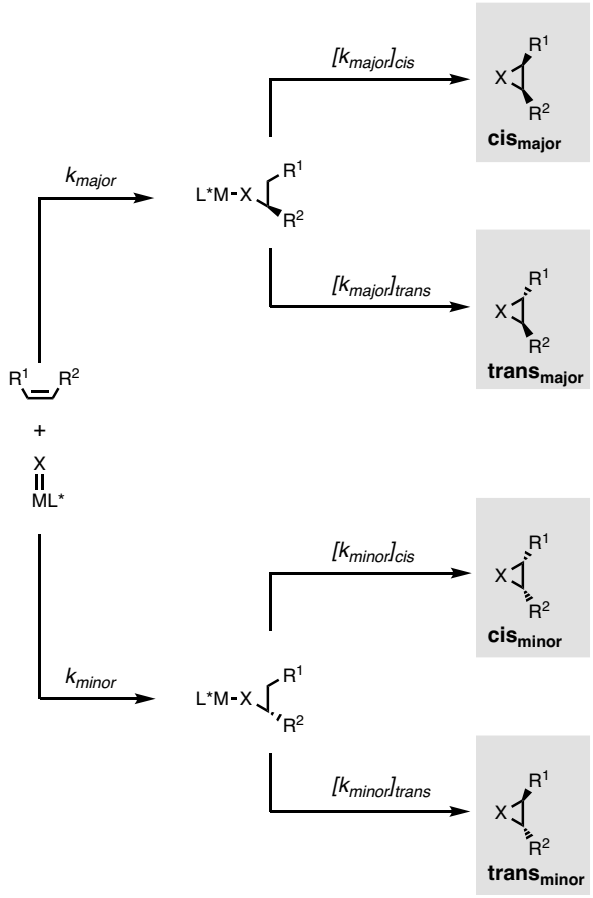

Scheme 1.11 In asymmetric additions to alkenes catalyzed by chiral metal complexes, a diastereomeric partitioning model accounts for enhancement of the enantioenrichment of the major isomeric product at the expense of the enantioenrichment of the minor isomeric product.

The enantioselectivity disparity between the 1,2-difluoride and the 1,1-difluoride could suggest a mechanism in which the two diastereomers of fluoroiodinated intermediate proceed to 1,2-difluoride and 1,1-difluoride products at different relative rates. In general, steps following the first irreversible step of a multistep asymmetric reaction do not influence the enantioselectivity of that reaction. However, an exception exists for nonstereospecific reactions

in which an irreversible step produces a pair of intermediates that may react at different rates in subsequent steps. Jacobsen and coworkers described this scenario in the context of two asymmetric additions to alkenes: (salen)Mn-catalyzed epoxidation and (bisimine)Cu-catalyzed aziridination (Scheme 1.11).[46] In both of these transformations, the first irreversible step is generation of a metal-bound radical intermediate; if a chiral metal complex is used, a pair of diastereomeric radical intermediates will result. Each of these radical intermediates has the potential to form both cis and trans products, but because diastereomers may react at different rates, the partitioning of each intermediate between cis and trans products may diverge. Enhancement of the enantiomeric excess of the major product arises as a consequence of this diastereomeric partitioning.

This line of reasoning can also be applied to the enantioselective, aryl iodide-catalyzed alkene difluorination reaction; diastereomeric partitioning of intermediates **VI** and **VIII** could potentially account for the different levels of enantioenrichment in the 1,2-difluoride versus the 1,1-difluoride products (Scheme 1.12). In this scenario, enantioselectivity depends on two factors: the facial selectivity of fluoroiodination to form intermediates **VI** and **VIII**, and the relative rates at which these intermediates partition to the 1,2- and 1,1-difluoride products. Enhancement of the enantiomeric excess of the 1,2-difluoride could take place if the preferentially formed intermediate **VI** partitions selectively to the 1,2-difluoride while the disfavored intermediate **VIII** partitions selectively to the 1,1-difluoride (Equation 1).

$$\frac{k_{1,2\ major}}{k_{1,1\ major}} > \frac{k_{1,2\ minor}}{k_{1,1\ minor}} \qquad (1)$$

[46] For a discussion of diastereomeric partitioning resulting in enantiodifferentiation after the first irreversible step, see: Zhang, W.; Lee, N. H.; Jacobsen, E. N. *J. Am. Chem. Soc.* **1994**, *116*, 425–426.

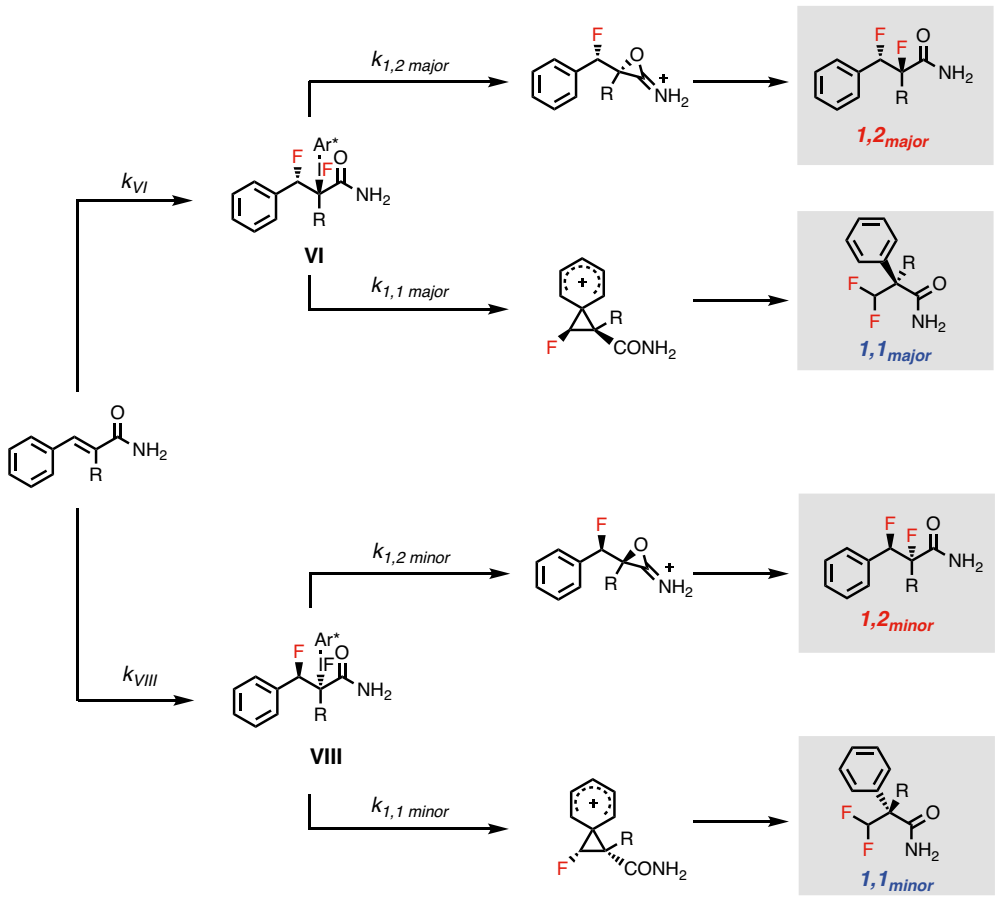

Scheme 1.12 A mechanistic proposal for divergent enantioenrichment in the 1,2- and 1,1-difluoride products involving diastereomeric partitioning of a fluoroiodinated intermediate.

The facial selectivity of fluoroiodination ($e.e._{facial}$) depends on k_{VI} and k_{VIII}, and can be calculated from the experimentally measured percentages and enantioselectivities of the 1,2-difluoride and 1,1-difluoride products (Equation 2).

$$e.e._{facial} = \frac{\mathbf{VI} - \mathbf{VIII}}{\mathbf{VI} + \mathbf{VIII}} \times 100 = \left(e.e._{1,2} \times \%1,2\right) + \left(e.e._{1,1} \times \%1,1\right) \qquad (2)$$

The partitioning of each fluoroiodinated intermediate is a function of product ratio and of the enantiomeric excess of both products. Equations 3 and 4 describe the partitionings of intermediates **VI** and **VIII** respectively.

$$\frac{k_{1,2\ major}}{k_{1,1\ major}} = \frac{1,2}{1,1} \times \frac{1 + e.e._{1,2}}{1 + e.e._{1,1}} \tag{3}$$

$$\frac{k_{1,2\ minor}}{k_{1,1\ minor}} = \frac{1,2}{1,1} \times \frac{1 - e.e._{1,2}}{1 - e.e._{1,1}} \tag{4}$$

The partitioning of intermediate **VI** relative to intermediate **VIII** (*P*) can be calculated using Equation 5.

$$P = \frac{k_{1,2\ major}/k_{1,1\ major}}{k_{1,2\ minor}/k_{1,1\ minor}} = \frac{(1 + e.e._{1,2})(1 - e.e._{1,1})}{(1 + e.e._{1,1})(1 - e.e._{1,2})} \tag{5}$$

To assess whether a diastereomeric partitioning model might account for the different levels of enantioenrichment in the 1,2-difluoride versus the 1,1-difluoride products, we calculated $e.e._{facial}$ and *P* for each substrate tested (Figure 1.16). Notably, the calculated value of $e.e._{facial}$ for α-ethyl substrate **2g** is much higher than that for α-methyl substrate **2b**. This comparison indicates that if a diastereomeric partitioning model is operative, catalyst must interact closely with the α-alkyl substituent, allowing it to distinguish between methyl and ethyl substituents. Calculated values of *P* varied widely, ranging from 0.3 for electron-rich substrate **2f** (minimal partitioning) to 76 for electron-deficient substrate **2c** (extreme partitioning), suggesting that arene electronic effects strongly influence the relative rates of amide oxygen attack and aryl migration in intermediate **VI** vs. intermediate **VIII**. However, accounting for the observed enantioselectivities solely within the framework of a diastereomeric partitioning model would require an extreme level of partitioning that far exceeds any obtained in studies of similar

scenarios.[47] While we cannot rule out the possibility that a diastereomeric partitioning pathway contributes to the mechanism to some degree, other mechanistic interpretations of the unusual differences in the enantiomeric excesses of the 1,2-difluoride and 1,1-difluoride products must be considered.

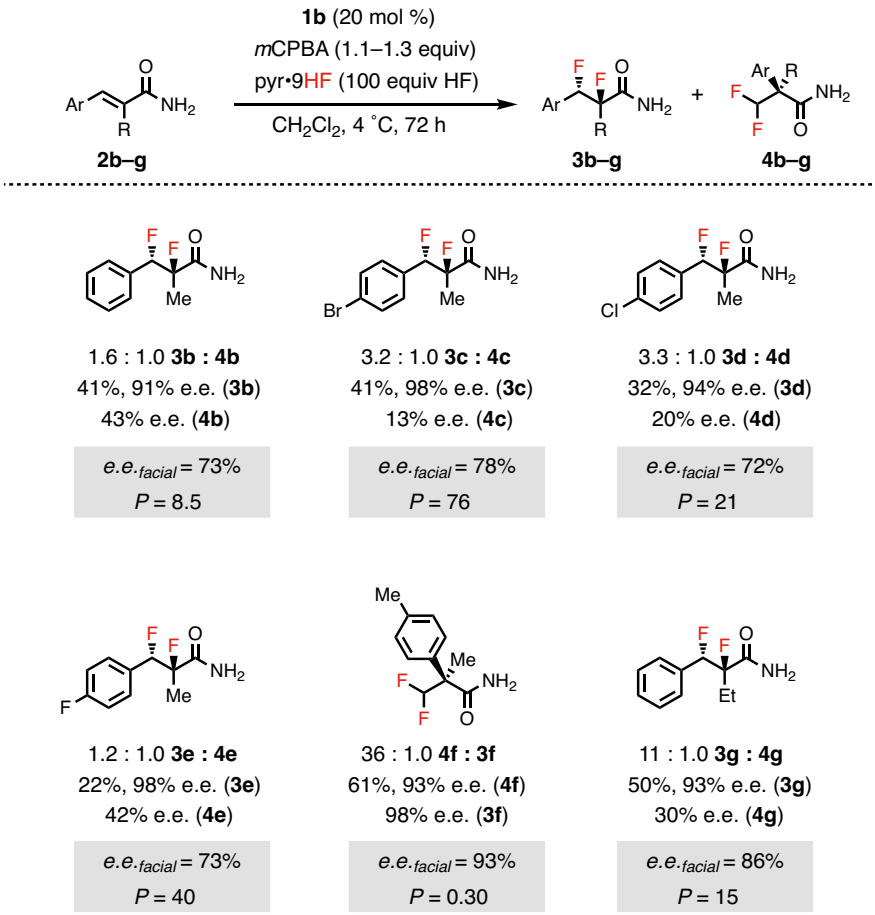

Figure 1.16 Calculated values of $e.e._{facial}$ and P for a variety of substrates.

Another explanation accounting for erosion of 1,1-difluoride enantioenrichment involves only stereospecific steps. In this pathway, after stereospecific amide oxygen attack to form the oxiraniminium intermediate **IX**, stereospecific aryl migration occurs to give a phenonium ion (Scheme 1.13). This intermediate is the diastereomer of the phenonium ion formed through

[47] See ref. 46.

direct aryl migration from the fluoroiodinated intermediate **VI**, and fluoride attack on each of these diastereomeric phenonium ions produces opposite enantiomers of 1,1-difluoride product. This model is consistent with the experimentally observed high diastereoselectivity of 1,2-difluorination. Increasing the size of the α-alkyl substituent would also hinder attack by the bulkier nucleophile (phenyl vs. fluoride), resulting in the observed trend in product ratios.

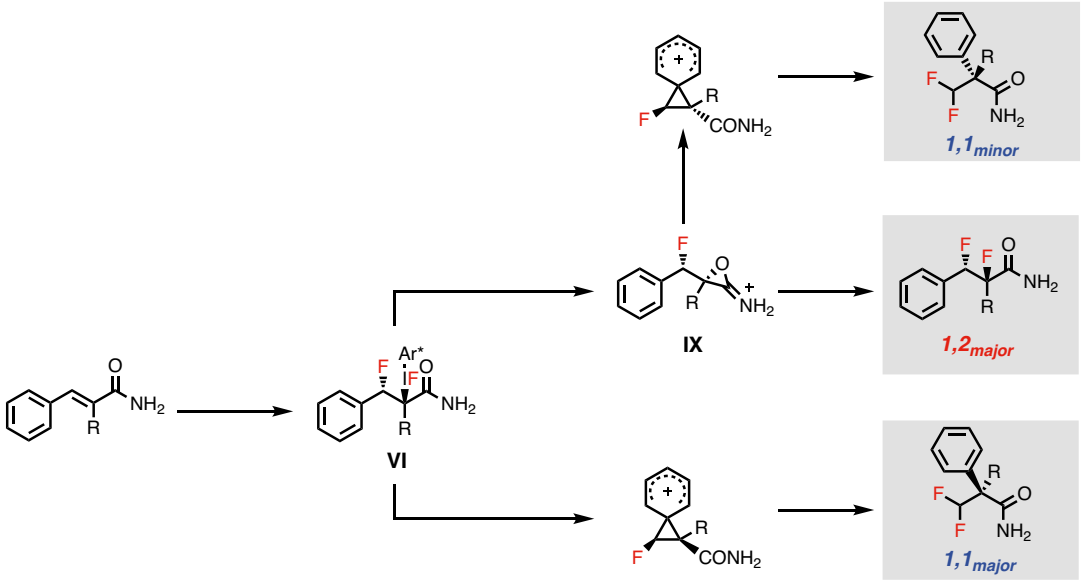

Scheme 1.13 A mechanistic proposal for divergent enantioenrichment in the 1,2- and 1,1-difluoride products involving double intramolecular displacement of a fluoroiodinated intermediate.

1.6 Catalytic, Enantioselective 1,2-Difluorination: Reaction Development with Secondary Cinnamamides

As described in the previous sections, we have found that the scope of the 1,2-difluorination of primary cinnamamides is severely limited due to competing rearrangement pathways. Here, we address that selectivity challenge through a systematic study of the factors influencing product distribution, leading to a protocol for the highly chemo- and enantioselective 1,2-difluorination of trisubstituted cinnamamide substrates. These reactions provide versatile synthetic building blocks bearing contiguous secondary and tertiary fluorinated stereocenters.

Concurrent with our efforts, Gilmour and coworkers reported a complementary method for the enantioselective 1,2-difluorination of simple, electron-deficient styrenes.[48]

Table 1.1 Survey of amide *N*-substituents in the 1,2-difluorination of cinnamamides.[a]

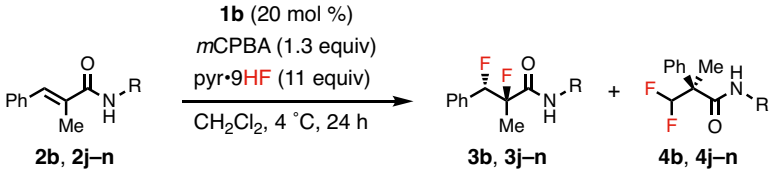

2b, **2j–n** **3b**, **3j–n** **4b**, **4j–n**

entry	substrate	R	pyr•9HF (equiv)	**3 : 4**	yield of **3** (%)	e.e. of **3** (%)
1	**2b**	H	11	1.1 : 1.0	17	91
2	**2j**	Me	11	1.1 : 1.0	38	95
3	**2k**	Et	11	1.3 : 1.0	44	95
4	**2l**	*i*-Pr	11	1.6 : 1.0	46	96
5	**2m**	*n*-Bu	11	1.7 : 1.0	48	94
6	**2n**	*t*-Bu	11	5.9 : 1.0	65	96

[a] Reactions were conducted on a 0.10 mmol scale, with yields of 1,2-difluoride determined by ^{1}H NMR using nitrobenzene as an internal standard. Reported ratios of 1,2-difluoride to 1,1-difluoride were determined by ^{19}F NMR analysis of crude product mixtures.

We hypothesized that the amide anchimeric assistance pathway leading to the 1,2-product might be enhanced through judicious introduction of *N*-substituents.[49] To test this hypothesis, we evaluated a series of *N*-substituted amides as model substrates for the enantioselective 1,2-difluorination reaction with catalyst **1b** (Table 1.1). While tertiary amide derivatives of **2b** displayed poor reactivity (Scheme 1.14), secondary amides underwent reaction more efficiently than primary amide **2b**. Thus, the difluorination of *N*-methyl amide **2j** proceeded with improved yield and enantioselectivity, although without any change in product ratio (entry 2). Increasing the size of the secondary amide *N*-substituent resulted in modest improvements in product

[48] Scheidt, F.; Schäfer, M.; Sarie, J.; Daniliuc, C.; Molloy, J.; Gilmour, R. *Angew. Chem., Int. Ed.* **2018**, *57*, 16431–16435.

[49] Substitution has been demonstrated to lower the strain energy in small rings in specific cases. See: Bach, R. D.; Dmitrenko, O. *J. Org. Chem.* **2002**, *67*, 2588–2599.

selectivity (entries 3–5). The *N*-*tert*-butyl amide **2n** afforded 1,2-difluoride product in the highest yields, but still suffered from a robust 1,1-difluorination side reaction (entry 6).

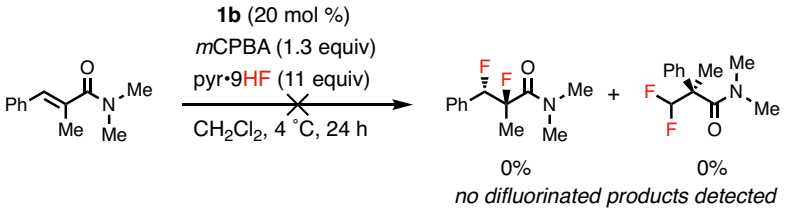

Scheme 1.14 Attempted difluorination of a tertiary amide.

Decreasing the HF-pyridine concentration led to a modest improvement in selectivity for the 1,2-difluoride product **3j**, with optimal yields obtained using 5.6 equiv (Table 1.2, entry 2).[50] The dependence of product ratio on HF-pyridine loading might be attributable to attenuation of amide nucleophilicity by hydrogen bonding between the amide and HF.[51] The 1,2- to 1,1-selectivity in the difluorination of secondary amides **2k**–**n** displayed significant sensitivity to HF-pyridine loading (entries 3–6). Under these modified conditions, increasing the size of the secondary amide *N*-substituent again resulted in increased selectivity for formation of 1,2-difluoride products. Difluorides **3j–n** were all formed in useful yields, and notably, the *N*-*tert*-butyl amide **2n** afforded the desired 1,2-difluoride **3n** almost exclusively.

[50] At an HF-pyridine loading of 2.8 equiv, a superior ratio of 1,2-difluoride to 1,1-difluoride was obtained (56:1.0). However, this reaction afforded a reduced yield of 64%. Decreasing the HF-pyridine loading further led to substantially lower yields as well as diminished enantioselectivity.

[51] However, primary amide **2b** did not display the same sensitivity to HF-pyridine loading.

Table 1.2 Survey of amide *N*-substituents in the 1,2-difluorination of cinnamamides at reduced HF-pyridine loadings.[a]

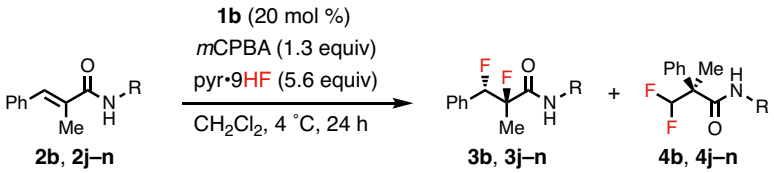

entry	substrate	R	pyr•9HF (equiv)	**3 : 4**	yield of **3** (%)	e.e. of **3** (%)
1[b]	**2b**	H	5.6	1.2 : 1.0	19	91
2	**2j**	Me	5.6	3.3 : 1.0	51	94
3	**2k**	Et	5.6	4.3 : 1.0	61	95
4	**2l**	*i*-Pr	5.6	4.8 : 1.0	56	95
5	**2m**	*n*-Bu	5.6	6.9 : 1.0	63	94
6	**2n**	*t*-Bu	5.6	39 : 1.0	81	96

[a] Unless noted otherwise, reactions were conducted on a 1.00 mmol scale and isolated yields of **3** are listed. Reported ratios of 1,2-difluoride to 1,1-difluoride were determined by ^{19}F NMR analysis of crude product mixtures. [b] Reaction conducted on a 0.10 mmol scale, with yields of 1,2-difluoride determined by ^{1}H NMR using nitrobenzene as an internal standard.

Several catalysts were screened using the optimal *N*-*tert*-butyl cinnamamide substrate **2n** (Figure 1.17). Similar catalyst structure-activity effects were observed with **2n** as with the primary amide substrate **2b**.[52] Catalysts **1b** and **1l** both afforded product in 96% e.e.; however, catalyst **1b** gave higher product selectivity and a higher yield of the 1,2-difluoride product, and therefore it was selected as the optimal catalyst for investigation of the substrate scope.

[52] Refer to Section **1.4**, Figure **1.15** for catalyst trends with the primary amide substrate **2b**.

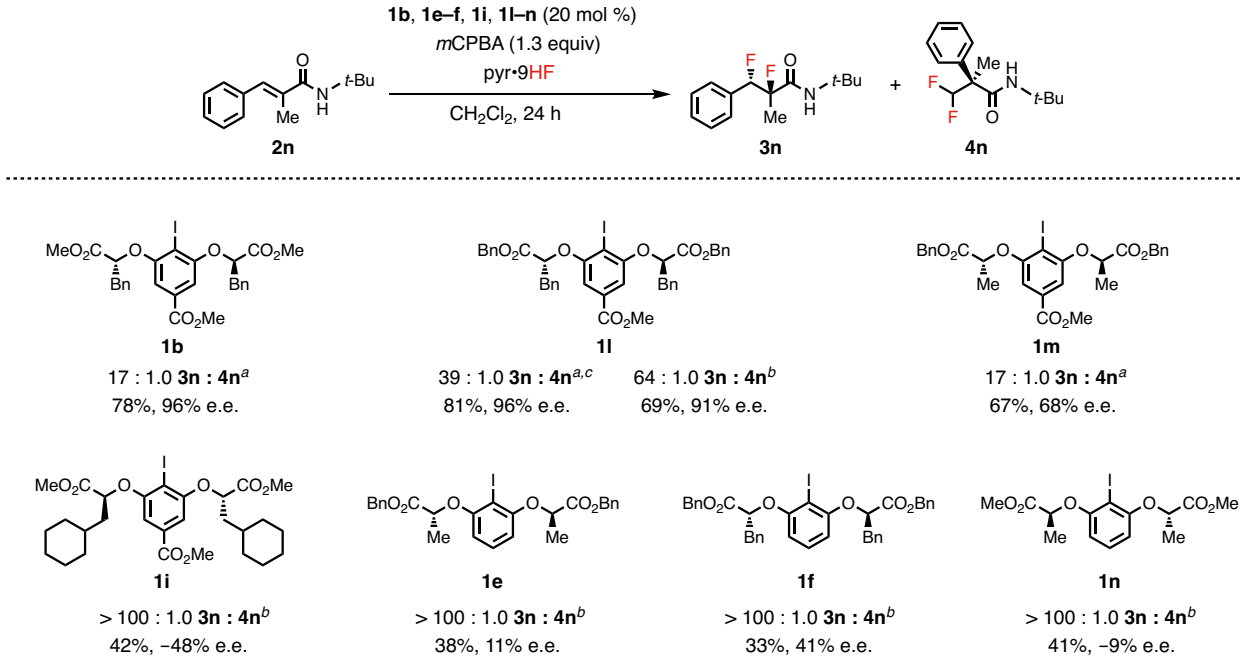

Figure 1.17 Survey of chiral catalysts for 1,2-difluorination of *N*-*tert*-butyl cinnamamides. Unless noted otherwise, reactions were conducted on a 0.10 mmol scale, and reported yields of 1,2-difluoride were determined by ^{1}H NMR using nitrobenzene as an internal standard. Reported ratios of 1,2-difluoride to 1,1-difluoride were determined by ^{19}F NMR analysis of crude product mixtures. [a]Reactions were conducted with 5.6 equiv of HF-pyridine. [b]Reactions were conducted with 3.4 equiv of HF-pyridine. [c]Reaction was conducted on a 1.00 mmol scale and the isolated yield of **3n** is listed.

Under the optimized conditions, a variety of *tert*-butyl cinnamamide derivatives were found to undergo highly diastereo- and enantioselective formation of the corresponding 1,2-difluorination products (Figure 1.18).[53] Substrates bearing electron-withdrawing and mildly electron-donating substituents were particularly effective (**2o–q**). The electron-rich cinnamamide **2r** underwent reaction with only modest chemoselectivity to generate a 2.2:1.0 ratio of the desired 1,2-difluoride to the 1,1-difluoride, with the 1,2-difluoride isolated in 40% yield and 98% e.e. This result is nonetheless notable because it overturns the overwhelming selectivity for 1,1-difluoride observed for the analogous primary amide substrate.

[53] The reactions of **2r** and **2u** yielded the 1,2-difluorides as 6.1:1.0 and 5.1:1.0 mixtures of diastereomers, respectively. For all other substrates, difluorination reactions proceeded with greater than 25:1.0 d.r. Diastereomeric ratios were determined by ^{19}F NMR analysis of the crude reaction mixtures.

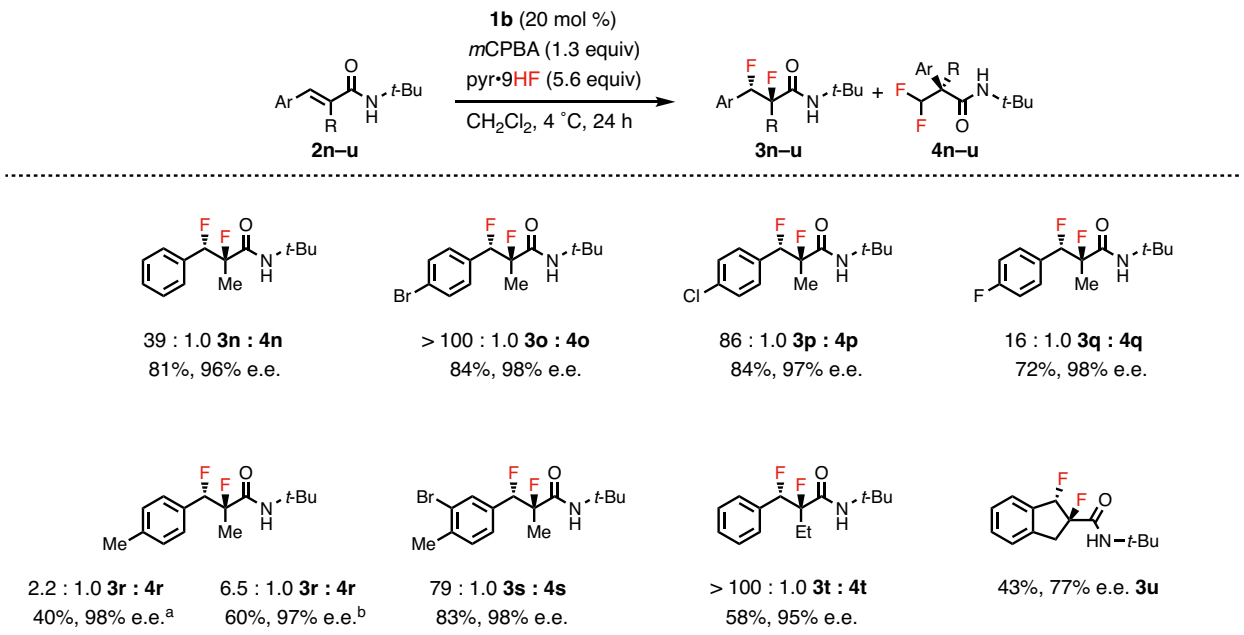

Figure 1.18 Scope of the enantioselective 1,2-difluorination of *N-tert*-butyl cinnamamides. Reactions were conducted on a 1.00 mmol scale with 5.6 equiv of HF-pyridine. Reported ratios of 1,2-difluoride to 1,1-difluoride were determined by ^{19}F NMR analysis of crude product mixtures. Isolated yields of diastereomerically pure 1,2-difluoride are reported unless otherwise noted. The relative and absolute configurations of all 1,2-difluorination products were assigned by analogy to those of **3a**. [a]Reaction conducted with 2.8 equiv of HF-pyridine. [b]Reaction conducted on a 0.20 mmol scale with 2.8 equiv of HF-pyridine and added pyridine (pyr/HF = 1:4.5). The reported yield was determined by ^{1}H NMR using nitrobenzene as an internal standard.

Additional increases in chemoselectivity for the 1,2-product **3r** were obtained by decreasing the ratio of HF to pyridine, with optimal yields achieved at a ratio of 4.5:1.0 (Table 1.3, entry 3). While product selectivity for 1,2-difluoride continued to increase as the ratio of HF to pyridine was lowered further, yield and conversion sharply declined. Although we have not performed a systematic investigation of the effect of the reaction medium on product distribution for other substrates, Gilmour and coworkers have demonstrated clearly that 1,2:1,1 product ratios are dependent on amine concentrations in difluorinations of electron-deficient styrenes.[54]

[54] See ref. 48.

Table 1.3 Effect of the HF:pyridine ratio on product ratio.[a]

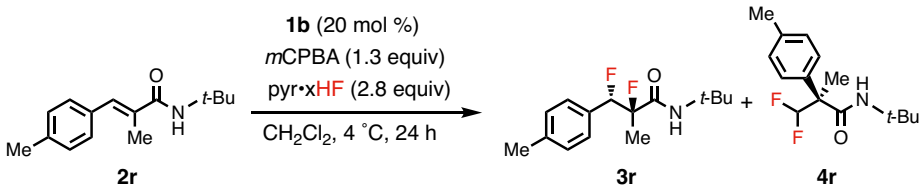

entry	HF:pyridine	**3r : 4r**	yield of **3r** (%)	e.e. of **3r** (%)
1	9.0 : 1.0	1.7 : 1.0	47	98
2	7.5 : 1.0	2.1 : 1.0	53	97
3	4.5 : 1.0	6.5 : 1.0	60	97
4	3.5 : 1.0	13 : 1.0	7	97
5	2.0 : 1.0	–	0	–

[a] Reactions were conducted on a 0.20 mmol scale with 2.8 equiv of HF-pyridine and additional pyridine to achieve the listed ratios of HF:pyridine. Reported ratios of 1,2-difluoride to 1,1-difluoride were determined by ^{19}F NMR analysis of crude product mixtures. Reported yields were determined by ^{1}H NMR using nitrobenzene as an internal standard.

Chemoselectivity for 1,2- vs. 1,1-difluorination was observed to be correlated directly to the nucleophilicity of the arene, as evidenced by the positive linear correlation ($\rho^+ = 4.34$) between the Hammett substituent constants ρ^+ and log(**3:4**) for substrates **2n** and **2p–r** (Figure 1.19). The α-alkyl substituent of the cinnamamide could also be varied (Figure 1.18). Substrate **2t**, which bears an ethyl substituent at the α-position of the cinnamamide, undergoes 1,2-difluorination exclusively. Indene **2u**, which is not susceptible to an aryl migration pathway, afforded **3u** in moderate yield and enantioselectivity. Nonstyrenyl unsaturated amides display poor reactivity under the reaction conditions.

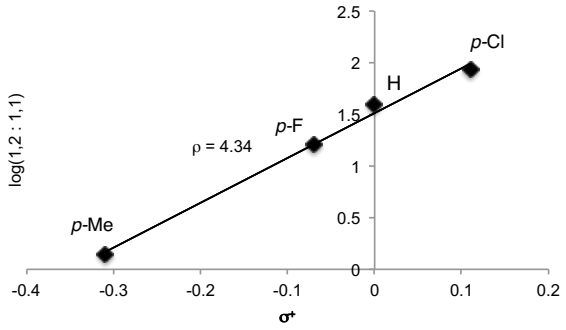

Figure 1.19 Hammett plot of σ^+ values of the aryl substituents in **2n** and **2p–r** versus the product ratio (log(1,2:1,1)) obtained for each substrate.

1.7 Steric and Electronic Effects on Product Partitioning

We sought to elucidate the basis for the significant impact of the amide *N*-substituent on product ratio. A strong linear free-energy correlation was observed between the 1,2- vs. 1,1-product ratios and the Charton values (ν) of the amide *N*-substituents for **2b and 2j–n**, indicating that the effect is primarily steric in nature (Figure 1.20).[55] Larger substituents thus appear to enhance amide anchimeric assistance relative to aryl migration, thereby favoring the 1,2-difluorination pathway.

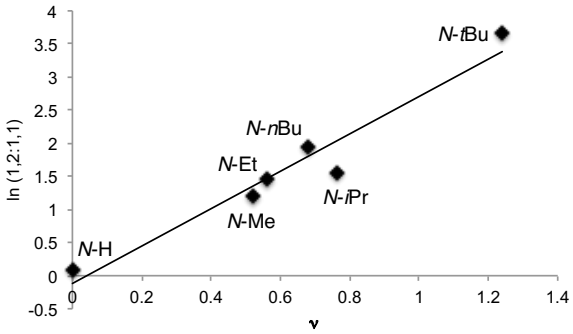

Figure 1.20 Plot of Charton values (ν) for amide *N*-substituents of **2b and 2j–n** versus the product ratio (ln(1,2:1,1)) obtained for each substrate.

[55] Charton, M. *J. Am. Chem. Soc.* **1975**, *97*, 1552–1556.

The electronic effect of the amide *N*-substituent on the competition between the aryl migration and amide trapping pathways was probed by examining substrates bearing fluorinated *N*-substituents (Figure 1.21). Substrates bearing electron-withdrawing *N*-alkyl substituents underwent difluorination with lower product selectivity for the 1,2-difluoride. The experimentally measured infrared stretching frequencies of the amide carbonyls of **2k and 2v–x** correlate to ln(**3:4**). As might be anticipated, decreased nucleophilicity of the amide oxygen disfavors anchimeric assistance relative to phenonium ion formation.

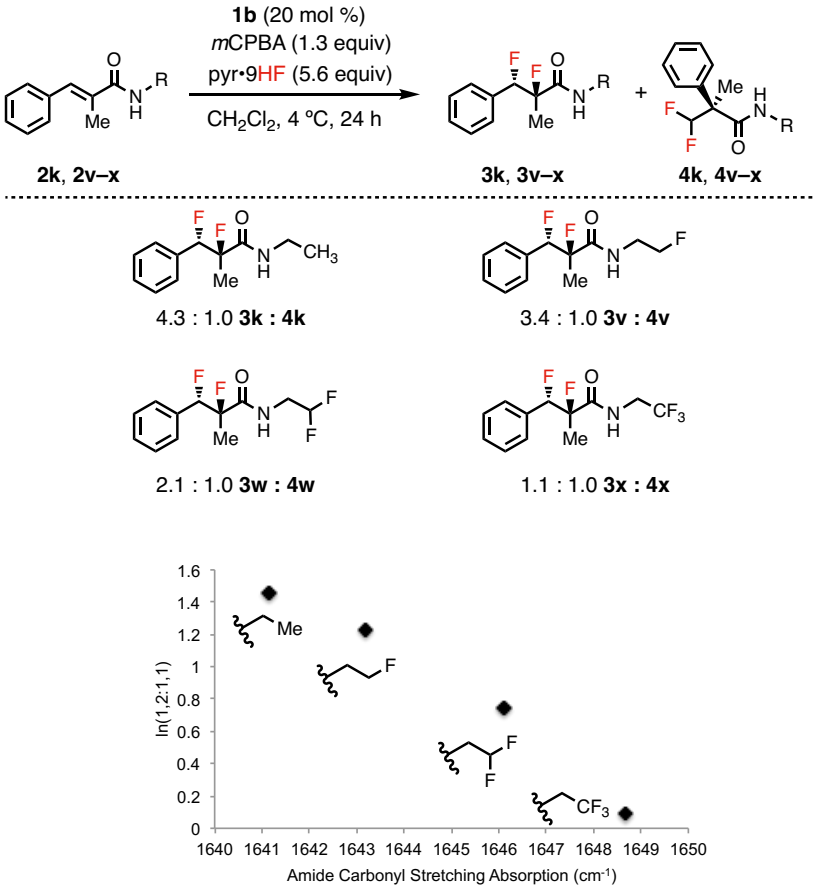

Figure 1.21 Plot of amide carbonyl stretching absorptions for **2k** and **2v–x** versus the product ratio (ln(1,2:1,1)) obtained for each substrate. Reactions were conducted on a 1.00 mmol scale. Reported ratios of 1,2-difluoride to 1,1-difluoride were determined by ^{19}F NMR analysis of the crude mixture.

1.8 Derivatization of 1,2-Difluoride Products

The products of the difluorination reaction can be derivatized to access versatile, enantioenriched vicinal difluoride building blocks. The arene of **3n** can be degraded oxidatively to give carboxylic acid **5**, thereby providing a 1,4-dicarbonyl bearing a second functional handle off the stereodefined difluoride framework (Scheme 1.15).[56] Notably, this oxidative degradation method was unsuccessful when applied to primary amide **3g**.

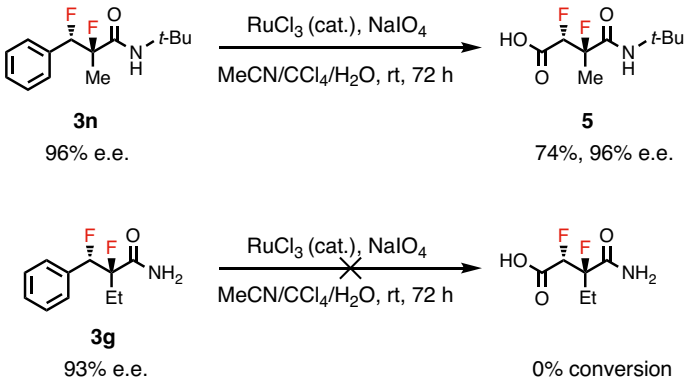

Scheme 1.15 Product derivatization via arene degradative oxidation.

Efforts to derivatize the *tert*-butyl amide portion of the difluorination products proved challenging. A variety of unsuccessful functional group transformations were attempted, including basic hydrolysis, reduction to a primary alcohol with samarium iodide, and treatment with Schwartz's reagent to access the corresponding aldehyde.[57] Cleavage of *tert*-butyl amides to their corresponding primary amides has been reported to take place under highly acidic conditions.[58] We surveyed a variety of acidic reaction conditions to gauge their effectiveness in

[56] Carlsen, H. J.; Katsuki, T.; Martin, V. S.; Sharpless, K. B. *J. Org. Chem.* **1981**, *46*, 3936–3938.

[57] For examples of amide reduction with samarium iodide, see: (a) Szostak, M.; Spain, M.; Eberhart, A. J.; Procter, D. J. *J. Am. Chem. Soc.* **2014**, *136*, 2268–2271. For the transformation of an *N-tert*-butyl amide to an aldehyde using Schwartz's reagent, see: (b) Groendyke, B. J.; AbuSalim, D. I.; Cook, S. P. *J. Am. Chem. Soc.* **2016**, *138*, 12771–12774.

[58] For examples employing trifluoroacetic acid, see: (a) Vacca, J. P.; Dorsey, B. D.; Guare, J. P.; Holloway, M. K.; Hungate, R. W.; Levin, R. B. Patent US5413999, 1995. (b) Erba, E.; La Rosa, C. *Tetrahedron* **2016**, *72*, 7975–7981.

the dealkylation of the *tert*-butyl amide of difluoride product **3n** (Table 1.4). Treatment of **3n** with TFA at room temperature or at 50 ˚C did not yield any dealkylated product; however, at more elevated temperatures, these conditions resulted in complete decomposition of starting material. Treatment with boron trifluoride complexes also resulted in decomposition of **3n**. Treatment with HF-pyridine at room temperature resulted in partial cleavage of the *tert*-butyl group, but this method suffered from the formation of epimerized byproducts. Milder triethylamine-HF complexes failed to promote the dealkylation reaction. While dealkylation using Me_2O•5HF proceeded more efficiently, epimerization remained problematic, and reproducibility when using different batches of Me_2O•5HF proved poor.[59] After screening a variety of other mineral acids, we found that treatment of **3n** with a solution of 33 wt % hydrogen bromide in acetic acid resulted in efficient cleavage of the *tert*-butyl group to afford primary amide **3b**. Complete conversion of **3n** was observed within 24 h at 40 ˚C, and dealkylated product **3b** was isolated in 89% yield with no erosion of enantiomeric excess.

For an example employing boron trifluoride diethyl etherate, see: (c) Tong, S.; Zhao, S.; He, Q.; Wang, Q.; Wang, M.-X.; Zhu, J. *Angew. Chem. Int. Ed.* **2017**, *56*, 6599–6603. For an example employing boron trifluoride acetic acid complex, see: (d) Dawidowski, M.; Herold, F.; Wilczek, M.; Turło, J.; Chodkowski, A.; Gomólka, A.; Kleps, J. *Tetrahedron* **2012**, *68*, 8222–8230. For an example employing hydrochloric acid in HFIP to remove a variety of acid-labile protecting groups, see: (e) Palladino, P.; Stetsenko, D. A. *Org. Lett.* **2012**, *14*, 6346–6349. For an example employing copper(II) triflate, see: (f) Evans, V.; Mahon, M. F.; Webster, R. L. *Tetrahedron* **2014**, *70*, 7593–7597.

[59] For the first reported preparation of Me_2O•5HF, see: Bucsi, I.; Török, B.; Marco, A. I.; Rasul, G.; Prakash, G. K. S.; Olah, G. A. *J. Am. Chem. Soc.* **2002**, *124*, 7728–7736.

Table 1.4 Development of reaction conditions for cleavage of the *N-tert*-butyl amide to the primary amide.[a]

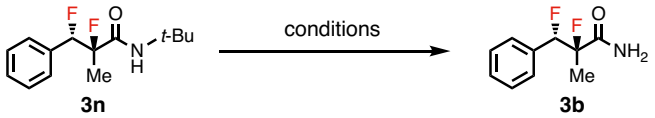

3n **3b**

entry	conditions	conversion (%)	yield of **3b** (%)	e.e. of **3b** (%)
1	TFA, rt, 18 h	0	0	–
2	TFA, 50 ˚C, 24 h	0	0	–
3	TFA, 80 ˚C, 3 h	100	0	–
4	BF_3•Et_2O, 1,2-DCE, 80 ˚C, 1 h	100	0	–
5	BF_3•2AcOH, 1,2-DCE, rt	100	0	–
6	pyr•9HF/CH_2Cl_2, rt, 48 h	58	46	n.d.
7	Et_3N•3HF/CH_2Cl_2, rt, 24 h	0	0	–
8	Et_3N•5HF/CH_2Cl_2, rt, 24 h	0	0	–
9	Me_2O•5HF/CH_2Cl_2, rt, 48 h	77	62	n.d.
10	1.0 M HCl in Et_2O, rt, 6 d	0	0	–
11	4.0 M HCl in dioxane, rt, 6 d	0	0	–
12	0.4 M HBr in benzene, rt, 3 d	0	0	–
13	33 wt. % HBr in AcOH, rt, 3d	81	79	n.d.
14	33 wt. % HBr in AcOH, 40 ˚C, 24 h	100	89[b]	96

[a] Unless otherwise noted, reported yields were determined by ^{1}H NMR using nitrobenzene as an internal standard. [b] The isolated yield of **3b** is reported.

This derivatization method was used to determine the absolute configuration of the 1,2-difluoride products (Scheme 1.16). The *N-tert*-butyl derivative of cinnamamide **2a**, **2y**, was prepared and subjected to the difluorination reaction conditions to afford the corresponding 1,2-difluoride as the exclusive product in 97% e.e. This product was treated with 33 wt % hydrobromic acid in acetic acid at 40 ˚C to afford the primary amide product **3a**. The sign of the measured optical rotation of **3a** prepared by this method matched that previously reported for **3a** prepared directly by difluorination of **2a**. The relative and absolute configurations of **3a** have been previously assigned by X-ray diffraction of a single crystal.[60] In addition, chiral GC

[60] See ref. 35.

analysis of **3a** prepared by both methods verified that the major and minor enantiomers eluted in the same order, confirming the assignment of absolute stereochemistry by analogy.

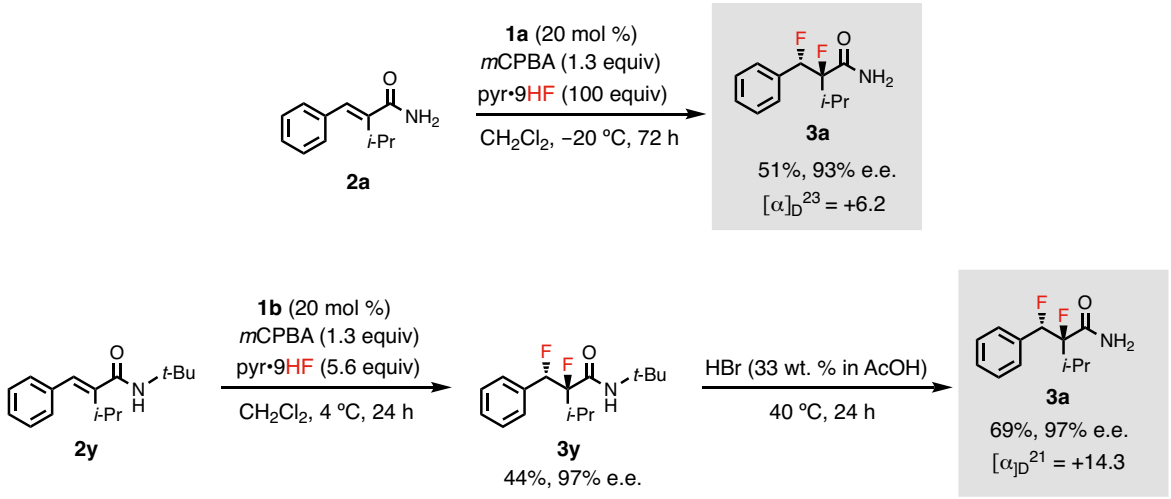

Scheme 1.16 Assignment of 1,2-difluoride absolute stereochemistry by analogy to previously reported **3a** (see ref. 35).

1.9 Conclusions and Outlook

We have developed a catalytic, enantioselective 1,2-difluorination of cinnamamides. The competing 1,1-difluorination resulting from phenonium rearrangement was suppressed through enhancement of anchimeric assistance by a proximal *tert*-butyl amide. The reaction medium was observed to influence product partitioning dramatically, with selectivity for 1,2-difluorination increasing at lower HF-pyridine loadings and at lower ratios of HF to amine. The products of this reaction and their derivatives may serve as versatile building blocks for the preparation of 1,2-difluoride-containing compounds, enabling further study of this interesting motif. The insights gained in this study may be leveraged in efforts to extend the scope of this methodology to other enantioselective fluorofunctionalization reactions.

1.10 Experimental Information

1.10.1 General Experimental Procedures and Note of Caution

General Experimental Procedures

All reactions for the preparation of substrates and catalysts were performed in standard, dry glassware fitted with rubber septa under an inert atmosphere of nitrogen unless otherwise described. All difluorination reactions were performed in polyethylene tubes sealed with a high density polyethylene cap under an atmosphere of air. Stainless steel gas-tight syringes or cannulae were used to transfer air- and moisture-sensitive liquids. Reported concentrations refer to solution volumes at room temperature. Concentration of organic solutions under reduced pressure was performed using house vacuum (ca. 40 mm Hg) at 30 ºC. Column chromatography was performed with SiliaFlash® P60 (40-63μm, 60 Å) silica gel from Silicycle. Thin layer chromatography (TLC) was used for reaction monitoring, and product detection was performed using pre-coated glass plates covered with 0.20 mm silica gel with fluorescent indicator; plates were visualized by exposure to UV light (λ = 254 nm) or by staining with potassium permanganate or ninhydrin.

Note of Caution

Pyridine•9HF is a corrosive and toxic substance that will corrode glassware. Safe handling can be conducted with plastic syringes and metal needles, with $NaHCO_3$ (aq.) or NaOH (aq.) employed to quench excess HF. Though reactions should not be conducted in glassware when employing pyridine•9HF, glassware may be used to quench reactions provided sufficient quantities of base are present. Always handle pyridine•9HF while wearing gloves and in a fume

hood. As a precautionary measure, have calcium gluconate gel nearby and apply immediately and liberally on skin exposed to pyridine•9HF.

1.10.2 Materials and Instrumentation

Materials

Reagents were purchased in reagent grade from commercial suppliers and used as received, unless otherwise described. Anhydrous solvents (benzene, dichloromethane, diethyl ether, *N, N*-dimethylformamide, tetrahydrofuran, and toluene) were prepared by passing the solvent through an activated alumina column. Triethylamine and diisopropylethylamine were distilled over calcium hydride at atmospheric pressure.

Instrumentation

Proton nuclear magnetic resonance (^{1}H NMR) spectra were recorded on an Inova-500 spectrometer, are reported in parts per million downfield from tetramethylsilane, and are referenced to the residual protium resonances of the NMR solvent ($CDCl_3$: 7.26 [$CHCl_3$], acetone-d6: 2.05 [acetone-d5], DMSO-d6: 2.50 [DMSO-d5]). Proton-decoupled carbon-13 nuclear magnetic resonance (13C {1 H} NMR) spectra were recorded on an Inova-500 spectrometer, are reported in parts per million downfield from tetramethylsilane, and are referenced to the carbon resonances of the NMR solvent (CDCl3: 77.23, acetone-d6: 29.92, DMSO-d6: 39.61). Chemical shifts for fluorine-19 nuclear magnetic resonance (19F NMR) were recorded on an Inova-500 spectrometer, are reported in parts per million downfield from chlorotrifluoromethane, and are referenced to the fluorine resonance of chlorotrifluoromethane (δ = 0). Data are represented as follows: chemical shift, multiplicity (br = broad, s = singlet, d = doublet, t = triplet, q = quartet, quin = quintet, sept = septet, m = multiplet), coupling constants in Hertz (Hz), integration.

Infrared spectra were recorded using a Bruker Tensor 27 FT-IR spectrometer.

High-resolution mass spectrometric data were obtained on an Agilent 6210 time-of-flight HPLC/MS spectrometer (ESI-TOF).

Chiral GC analysis was performed using an Agilent 7890A GC system using commercially available columns. Chiral HPLC analysis was performed using an Agilent 1200 series quaternary HPLC system using commercially available CHIRALCEL analytical columns (4.6 x 250 mm).

Optical rotations were measured using a 1 mL cell with a 5 cm path length on a Jasco P-2000 digital polarimeter.

1.10.3 Optimization Studies

General procedure for optimization of N-alkyl group and HF loading

Catalyst **1b** (15.4 mg, 20.0 μmol, 20.0 mol %), cinnamamide (100 μmol, 1.00 equiv), and dichloromethane (200 μL) were combined in a polyethylene tube at room temperature. Pyridinium poly(hydrogen fluoride) (pyr•9HF, 70% hydrogen fluoride by weight, 50 or 100 equiv hydrogen fluoride) was added via syringe at -78 ˚C, followed by *m*-chloroperbenzoic acid (*m*CPBA, 77% by weight, 29.1 mg, 1.30 equiv). The reaction was warmed to 4 ˚C and stirred for 24 h at that temperature. The reaction was diluted with dichloromethane and poured slowly into a slurry of basic alumina in dichloromethane at -78 ˚C. The reaction was warmed to room temperature with stirring, filtered, and concentrated under reduced pressure. The crude product mixture was analyzed by ^{1}H NMR using nitrobenzene as an internal standard to determine the yield of product, by ^{19}F NMR to determine the product ratio, and by chiral GC to determine the enantiomeric excess.

General procedure for catalyst optimization

Catalyst (20.0 μmol, 20.0 mol %), cinnamamide **2n** (21.7 mg, 100 μmol, 1.00 equiv), and dichloromethane (200 μL) were combined in a polyethylene tube at room temperature. Pyridinium poly(hydrogen fluoride) (pyr•9HF, 70% hydrogen fluoride by weight, 30 or 50 equiv hydrogen fluoride) was added via syringe at -78 ˚C, followed by *m*-chloroperbenzoic acid (*m*CPBA, 77% by weight, 29.1 mg, 1.30 equiv). The reaction was warmed to 4 ˚C or room temperature and stirred for 24 h at that temperature. The reaction was diluted with dichloromethane and poured slowly into a slurry of basic alumina in dichloromethane at -78 ˚C.

The reaction was warmed to room temperature with stirring, filtered, and concentrated under reduced pressure. The crude product mixture was analyzed by ^{1}H NMR using nitrobenzene as an internal standard to determine the yield of product, by ^{19}F NMR to determine the product ratio, and by chiral GC to determine the enantiomeric excess.

1.10.4 Preparation and Characterization of Substrates

General Procedure A: To a stirred solution of carboxylic acid (1 equiv) in dichloromethane (0.1 M) was added 1-hydroxybenzotriazole hydrate (1.5 equiv) and *N*-(3-dimethylaminopropyl)-*N*′-ethylcarbodiimide hydrochloride (1.7 equiv). *N,N*-Diisopropylethylamine (4.0 equiv) and amine coupling partner (3.0 equiv) were added sequentially by syringe. After stirring for 12–18 h, the solution was diluted with dichloromethane (10 mL per 1.00 mmol of substrate) and washed with 1.0 M aqueous HCl (10 mL per 1.00 mmol of substrate), then with brine (10 mL per 1.00 mmol of substrate). The organic layer was dried over anhydrous $MgSO_4$, filtered, and concentrated under reduced pressure. The residue was purified by flash column chromatography on silica gel.

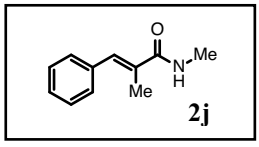

2j

Prepared according to General Procedure A using α-methylcinnamic acid (1.00 g, 6.17 mmol) and methylamine (2.0 M in THF, 9.25 mL, 18.5 mmol). After workup, the crude residue was purified by silica gel chromatography (50% ethyl acetate in hexanes) to give **2j** (959 mg, 89%) as a white solid.

^{1}H NMR (600 MHz, $CDCl_3$) δ 7.40 – 7.36 (m, 2H), 7.35 – 7.32 (m, 3H), 7.31 – 7.27 (m, 1H), 5.88 (br s, 1H), 2.95 (d, *J* = 4.9 Hz, 3H), 2.10 (d, *J* = 1.4 Hz, 3H); ^{13}C NMR (125.7 MHz, $CDCl_3$) δ 170.4, 136.3, 133.8, 132.1, 129.4, 128.5, 127.9, 26.9, 14.4; FTIR (thin film) ν 3311, 2937, 1649, 1611, 1531, 702 cm^{-1}; HRMS (ESI-TOF) Calc'd for $C_{11}H_{14}NO$ $[M+H]^+$: 176.1070; found 176.1068.

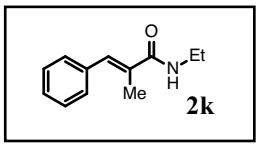

2k

Prepared according to General Procedure A using α-methylcinnamic acid (1.00 g, 6.17 mmol) and ethylamine (2.0 M in THF, 9.25 mL, 18.5 mmol). After workup, the crude residue was purified by silica gel chromatography (20 to 50% ethyl acetate in hexanes) to give **2k** (1.006 g, 86%) as a white solid.

^{1}H NMR (500 MHz, $CDCl_3$) δ 7.40 – 7.35 (m, 2H), 7.35 – 7.27 (m, 4H), 5.84 (br s, 1H), 3.43 (qd, *J* = 7.3, 5.6 Hz, 2H), 2.10 (d, *J* = 1.4 Hz, 3H), 1.23 (t, *J* = 7.3 Hz, 3H); ^{13}C NMR (125.7 MHz, $CDCl_3$) δ 169.6, 136.4, 133.7, 132.3, 129.4, 128.5, 127.9, 35.0, 15.1, 14.4; FTIR (thin film) ν 3291, 2968, 2943, 2876, 1641, 1617, 1532, 705 cm^{-1}; HRMS (ESI-TOF) Calc'd for $C_{12}H_{16}NO$ $[M+H]^+$: 190.1226; found 190.1225.

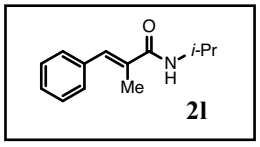

2l

Prepared according to General Procedure A using α-methylcinnamic acid (1.00 g, 6.17 mmol) and isopropylamine (1.51 mL, 18.5 mmol). After workup, the crude residue was purified by silica gel chromatography (30% ethyl acetate in hexanes) to give **2l** (1.054 g, 84%) as a white solid.

^{1}H NMR (500 MHz, $CDCl_3$) δ 7.40 – 7.35 (m, 2H), 7.35 – 7.27 (m, 4H), 5.67 (br s, 1H), 4.20 (m, 1H), 2.09 (d, *J* = 1.4 Hz, 3H), 1.24 (d, *J* = 6.5 Hz, 6H); ^{13}C NMR (125.7 MHz, $CDCl_3$) δ 169.0, 136.3, 133.7, 132.5, 129.4, 128.5, 127.9, 41.9, 23.0, 14.4; FTIR (thin film) ν 3295, 2975, 1638, 1614, 1530, 1358, 706 cm^{-1}; HRMS (ESI-TOF) Calc'd for $C_{13}H_{18}NO$ $[M+H]^+$: 204.1383; found 204.1382.

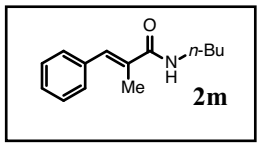

Prepared according to General Procedure A using α-methylcinnamic acid (1.00 g, 6.17 mmol) and *n*-butylamine (1.83 mL, 18.5 mmol). After workup, the crude residue was purified by silica gel chromatography (30% ethyl acetate in hexanes) to give **2m** (1.269 g, 95%) as a white solid.

^{1}H NMR (500 MHz, $CDCl_3$) δ δ 7.40 – 7.35 (m, 2H), 7.33 (dd, *J* = 6.7, 1.5 Hz, 3H), 7.31 – 7.27 (m, 1H), 5.85 (br s, 1H), 3.39 (td, *J* = 7.2, 5.7 Hz, 2H), 2.10 (d, *J* = 1.4 Hz, 3H), 1.63 – 1.51 (m, 4H), 1.41 (dq, *J* = 14.6, 7.4 Hz, 2H), 0.96 (t, *J* = 7.4 Hz, 3H); ^{13}C NMR (125.7 MHz, $CDCl_3$) δ 169.7, 136.4, 133.7, 132.4, 129.4, 128.5, 127.9, 39.9, 31.9, 20.3, 14.5, 13.9; FTIR (thin film) ν 3296, 2959, 2934, 2872, 1638, 1613, 1527, 706 cm^{-1}; HRMS (ESI-TOF) Calc'd for $C_{14}H_{20}NO$ $[M+H]^+$: 218.1539; found 218.1539.

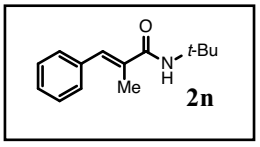

Prepared according to General Procedure A using α-methylcinnamic acid (3.00 g, 18.5 mmol) and *tert*-butylamine (5.83 mL, 55.5 mmol). After workup, the crude residue was purified by silica gel chromatography (20% ethyl acetate in hexanes) to give **2n** (3.538 g, 88%) as a white solid.

^{1}H NMR (500 MHz, $CDCl_3$) δ 7.40 – 7.34 (m, 2H), 7.33 – 7.27 (m, 3H), 7.25 (s, 1H), 5.70 (br s, 1H), 2.06 (d, *J* = 1.4 Hz, 3H), 1.44 (s, 9H);^{13}C NMR (125.7 MHz, $CDCl_3$) δ 169.2, 136.5, 133.6, 133.0, 129.4, 128.4, 127.8, 51.5, 29.0, 14.5; FTIR (thin film) ν 3315, 2967, 1647, 1619, 1527, 1450, 702 cm^{-1}; HRMS (ESI-TOF) Calc'd for $C_{14}H_{20}NO$ $[M+H]^+$: 218.1539; found 218.1539.

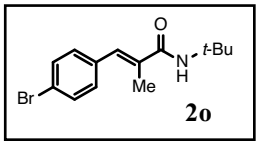

2o

To a stirred solution of ethyl (*E*)-3-(4-bromophenyl)-2-methylacrylate[61] (1.275 g, 4.74 mmol) in THF (13.5 mL) and ethanol (13.5 mL) was added 1.0 M aqueous NaOH (13.5 mL). After 21 h, 1.0 M aqueous HCl (20 mL) and ethyl acetate (40 mL) were sequentially added. The organic layer was washed with brine (20 mL), dried over anhydrous $MgSO_4$, and concentrated under reduced pressure to afford (*E*)-3-(4-bromophenyl)-2-methylacrylic acid, which was used without further purification. The title compound was prepared according to General Procedure A using (*E*)-3-(4-bromophenyl)-2-methylacrylic acid (1.062 g, 4.41 mmol) and *tert*-butylamine (1.39 mL, 13.2 mmol). After workup, the crude residue was purified by silica gel chromatography (30% ethyl acetate in hexanes) to give **2o** (1.087 g, 83%) as a white solid.

^{1}H NMR (500 MHz, $CDCl_3$) δ 7.53 – 7.47 (m, 2H), 7.20 – 7.16 (m, 3H), 5.68 (s, 1H), 2.03 (d, *J* = 1.4 Hz, 3H), 1.43 (s, 9H); ^{13}C NMR (125.7 MHz, $CDCl_3$) δ 168.9, 135.4, 134.2, 131.9, 131.6, 130.9, 121.8, 51.6, 28.9, 14.5; FTIR (thin film) ν 3323, 2968, 1649, 1622, 1527, 1487, 1221 cm^{-1}; HRMS (ESI-TOF) Calc'd for $C_{14}H_{19}BrNO$ $[M+H]^+$: 296.0645; found 296.0643.

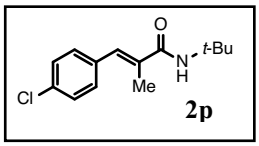

2p

Prepared according to General Procedure A using (*E*)-3-(4-chlorophenyl)-2-methylacrylic acid[62] (785 mg, 3.99 mmol) and *tert*-butylamine (1.26 mL, 12.0 mmol). After workup, the crude residue was purified by silica gel chromatography (10 to 30% diethyl ether in hexanes) to give **2p** (739 mg, 74%) as a white solid.

[61] Hu, X.-H.; Zhang, J.; Yang, X.-F.; Xu, Y.-H.; Loh, T.-P. *J. Am. Chem. Soc.* **2015**, *137*, 3169–3172.

[62] Basavaiah, D.; Krishnamacharyulu, M.; Suguna Hyma, R.; Sarma, P. K. S.; Kumaragurubaran, N. *J. Org. Chem.* **1999**, *64*, 1197–1200.

^{1}H NMR (500 MHz, $CDCl_3$) δ 7.34 (d, J = 8.5 Hz, 2H), 7.24 (d, J = 8.5 Hz, 2H), 7.20 (s, 1H), 5.68 (br s, 1H), 2.04 (d, J = 1.4 Hz, 3H), 1.43 (s, 9H); ^{13}C NMR (125.7 MHz, $CDCl_3$) δ 168.9, 134.9, 134.1, 133.6, 131.8, 130.6, 128.7, 51.6, 28.9, 14.5; FTIR (thin film) ν 3314, 2968, 2922, 1648, 1621, 1528, 1452, 1091 cm^{-1}; HRMS (ESI-TOF) Calc'd for $C_{14}H_{19}ClNO$ $[M+H]^+$: 252.1150; found 252.1146.

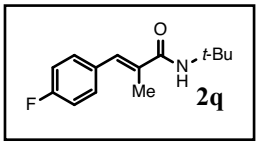

2q

Prepared according to General Procedure A using (*E*)-3-(4-fluorophenyl)-2-methylacrylic acid (300 mg, 1.67 mmol) and *tert*-butylamine (0.53 mL, 5.01 mmol). After workup, the crude residue was purified by silica gel chromatography (35% diethyl ether in hexanes) to give **2q** (350 mg, 89%) as a white solid.

^{1}H NMR (500 MHz, $CDCl_3$) δ 7.32 – 7.27 (m, 2H), 7.22 (s, 1H), 7.09 – 7.03 (m, 2H), 5.68 (s, 1H), 2.04 (d, J = 1.5 Hz, 3H), 1.43 (s, 9H); ^{13}C NMR (125.7 MHz, $CDCl_3$) δ 169.0, 162.2 (d, J = 247.9 Hz), 133.4, 132.5 (d, J = 3.6 Hz), 132.0, 131.1 (d, J = 8.1 Hz), 115.5 (d, J = 21.5 Hz), 51.5, 29.0, 14.5; ^{19}F NMR (470.4 MHz, $CDCl_3$) δ -113.69 (tt, J = 8.6, 5.4 Hz); FTIR (thin film) ν 3317, 2968, 2926, 1651, 1622, 1508, 1226 cm^{-1}; HRMS (ESI-TOF) Calc'd for $C_{14}H_{19}FNO$ $[M+H]^+$: 236.1445; found 236.1443.

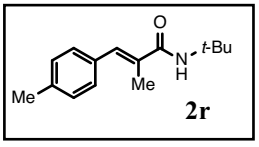

2r

Prepared according to General Procedure A using (*E*)-2-methyl-3-(*p*-tolyl)acrylic acid[6362] (500 mg, 2.84 mmol) and *tert*-butylamine (0.90 mL, 8.52 mmol). After workup, the crude residue was purified by silica gel chromatography (0 to 20% diethyl ether in hexanes) to give **2r** (532 mg, 81%) as a white solid.

[63] See ref. 62.

^{1}H NMR (500 MHz, $CDCl_3$) δ 7.22 (m, J = 8.1 Hz, 3H), 7.20 – 7.15 (m, 2H), 5.68 (s, 1H), 2.36 (s, 3H), 2.06 (d, J = 1.4 Hz, 3H), 1.43 (s, 9H); ^{13}C NMR (125.7 MHz, $CDCl_3$) δ 169.4, 137.7, 133.6, 133.0, 132.8, 129.4, 129.2, 51.5, 29.0, 21.4, 14.5; FTIR (thin film) ν 3298, 2972, 2951, 2918, 1646, 1619, 1527, 1512, 1451, 1224, 812 cm^{-1}; HRMS (ESI-TOF) Calc'd for $C_{15}H_{22}NO$ $[M+H]^+$: 232.1696; found 232.1694.

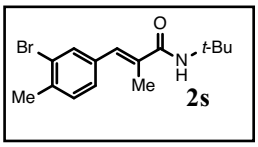

2s

Triethyl 2-phosphonopropionate (1.63 mL, 7.54 mmol, 1.5 equiv) was slowly added to a dispersion of sodium hydride (349 mg, 8.53 mmol, 1.7 equiv) in THF (7.50 mL) at 0 ˚C. The resulting mixture was stirred for 1 h. The mixture was then cooled to -78 ˚C, and 3-bromo-4-methylbenzaldehyde (1.00 g, 5.02 mmol, 1.0 equiv) was slowly added. After stirring at room temperature for 15 h, the mixture was poured over saturated aqueous ammonium chloride, and the phases were separated. The aqueous phase was extracted with diethyl ether, and the combined organic layers were washed with brine, dried over anhydrous magnesium sulfate, and concentrated under reduced pressure. The crude residue was purified by silica gel chromatography (0 to 10% ethyl acetate in hexanes). The resulting colorless oil (1.275 g, 4.74 mmol) was dissolved in THF (13.5 mL) and ethanol (13.5 mL) To the stirred solution was added 1.0 M aqueous NaOH (13.5 mL). After 21 h, 1.0 M aqueous HCl (20 mL) and ethyl acetate (40 mL) were sequentially added. The organic layer was washed with brine (20 mL), dried over anhydrous $MgSO_4$, and concentrated under reduced pressure to afford (*E*)-3-(3-bromo-4-methylphenyl)-2-methylacrylic acid, which was used without further purification. The spectral data for this compound were in accordance with the literature.[64] The title compound was prepared according to General Procedure A using (*E*)-3-(3-bromo-4-

[64] See ref. 39.

methylphenyl)-2-methylacrylic acid (896 mg, 3.51 mmol) and *tert*-butylamine (1.10 mL, 10.5 mmol). After workup, the crude residue was purified by silica gel chromatography (25% ethyl acetate in hexanes) to give **2s** (979.4 mg, 90%) as a white solid.

^{1}H NMR (500 MHz, $CDCl_3$) δ 7.49 (d, *J* = 1.6 Hz, 1H), 7.24 – 7.21 (m, 1H), 7.18 – 7.13 (m, 2H), 2.40 (s, 3H), 2.05 (d, *J* = 1.4 Hz, 3H), 1.43 (s, 9H); ^{13}C NMR (125.7 MHz, $CDCl_3$) δ 168.9, 137.5, 135.9, 134.2, 133.0, 131.4, 130.7, 128.3, 124.9, 51.6, 29.0, 22.9, 14.5; FTIR (thin film) ν 3308, 2967, 2922, 1649, 1619, 1527, 1221 cm^{-1}; HRMS (ESI-TOF) Calc'd for $C_{15}H_{21}BrNO$ $[M+H]^+$: 310.0801; found 310.0800.

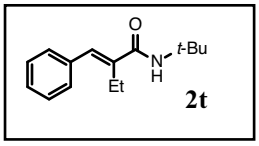

2t

Prepared according to General Procedure A using (*E*)-2-benzylidenebutanoic acid[65] (723 mg, 4.10 mmol) and *tert*-butylamine (1.29 mL, 12.3 mmol). After workup, the crude residue was purified by silica gel chromatography (10% ethyl acetate in hexanes) to give **2t** (816.6 mg, 86%) as a white solid.

^{1}H NMR (500 MHz, $CDCl_3$) δ 7.39 – 7.34 (m, 2H), 7.32 – 7.27 (m, 3H), 7.01 (s, 1H), 5.70 (br s, 1H), 2.51 (q, *J* = 7.5 Hz, 2H), 1.44 (s, 9H), 1.13 (t, *J* = 7.5 Hz, 3H); ^{13}C NMR (125.7 MHz, $CDCl_3$) δ 169.5, 141.6, 136.4, 131.0, 128.9, 128.5, 127.7, 51.5, 29.0, 21.4, 13.6; FTIR (thin film) ν 3310, 2965, 1642, 1619, 1536, 700 cm^{-1}; HRMS (ESI-TOF) Calc'd for $C_{15}H_{22}NO$ $[M+H]^+$: 232.1696; found 232.1695.

[65] Gensler, W. J.; Berman, E. *J. Am. Chem. Soc.* **1958**, *80*, 4949–4954.

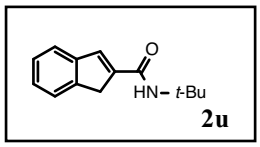

2u

Prepared according to General Procedure A using 1*H*-indene-2-carboxylic acid (200 mg, 1.25 mmol) and *tert*-butylamine (0.39 mL, 3.75 mmol). After workup, the crude residue was purified by silica gel chromatography (10% ethyl acetate in hexanes) to give **2u** (212 mg, 79%) as a white solid.

^{1}H NMR (500 MHz, $CDCl_3$) δ 7.51 – 7.44 (m, 2H), 7.36 (td, *J* = 1.8, 0.7 Hz, 1H), 7.33 – 7.27 (m, 2H), 5.73 (br s, 1H), 3.65 – 3.63 (m, 2H), 1.46 (s, 9H); ^{13}C NMR (125.7 MHz, $CDCl_3$) δ 164.5, 143.9, 143.3, 142.6, 134.9, 127.0, 126.9, 124.6, 122.8, 51.6, 38.4, 29.1; FTIR (thin film) ν 3246, 3069, 3055, 2980, 2960, 2929, 1628, 1588, 1563, 1532, 1270, 1218, 758, 713 cm^{-1}; HRMS (ESI-TOF) Calc'd for $C_{14}H_{18}NO$ $[M+H]^+$: 216.1383; found 216.1380.

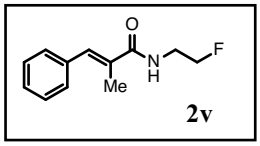

2v

Prepared according to General Procedure A using α-methylcinnamic acid (1.00 g, 6.17 mmol) and 2-fluoroethylamine hydrochloride (1.84 g, 18.5 mmol). After workup, the crude residue was purified by silica gel chromatography (50% diethyl ether in hexanes) to give **2v** (1.037 g, 81%) as a white solid.

^{1}H NMR (500 MHz, $CDCl_3$) δ 7.42 – 7.37 (m, 3H), 7.36 – 7.28 (m, 3H), 6.24 (br s, 1H), 4.59 (dt, *J* = 47.5, 4.7 Hz, 2H), 3.72 (ddt, *J* = 28.5, 5.7, 4.6 Hz, 2H), 2.12 (d, *J* = 1.4 Hz, 3H); ^{13}C NMR (125.7 MHz, $CDCl_3$) δ 169.8, 136.1, 134.6, 131.7, 129.5, 128.5, 128.1, 83.0 (d, *J* = 166.2 Hz), 40.5 (d, *J* = 19.5 Hz), 14.4; ^{19}F NMR (470.4 MHz, $CDCl_3$) δ -224.2 (tt, *J* = 47.3, 28.4 Hz, 1F); FTIR (thin film) ν 3279, 3052, 2960, 1643, 1619, 1531, 705 cm^{-1}; HRMS (ESI-TOF) Calc'd for $C_{12}H_{15}FNO$ $[M+H]^+$: 208.1132; found 208.1129.

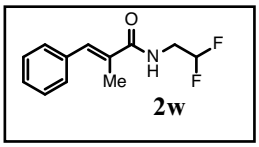

2w

Prepared according to General Procedure A using α-methylcinnamic acid (1.00 g, 6.17 mmol) and with the following modification: 2.0 equiv of 2,2-difluoroethan-1-amine (0.87 mL, 12.3 mmol) were used. After workup, the crude residue was purified by silica gel chromatography (10 to 50% diethyl ether in hexanes) to give **2w** (1.094 g, 79%) as a white solid.

^{1}H NMR (500 MHz, $CDCl_3$) δ 7.42 – 7.37 (m, 3H), 7.36 – 7.30 (m, 3H), 6.10 (br s, 1H), 5.94 (tt, J = 56.3, 4.2 Hz, 1H), 3.77 (tdd, J = 14.8, 6.2, 4.2 Hz, 2H), 2.13 (d, J = 1.4 Hz, 3H); ^{13}C NMR (125.7 MHz, $CDCl_3$) δ 170.0, 135.9, 135.2, 131.2, 129.5, 128.6, 128.3, 113.8 (t, J = 241.3 Hz), 42.4 (t, J = 26.5 Hz), 14.4; ^{19}F NMR (470.4 MHz, $CDCl_3$) δ -122.9 (dt, J = 56.4, 14.8 Hz, 2F); FTIR (thin film) ν 3290, 1646, 1616, 1524, 1113, 1057, 695 cm^{-1}; HRMS (ESI-TOF) Calc'd for $C_{12}H_{14}F_2NO$ $[M+H]^+$: 226.1038; found 226.1035.

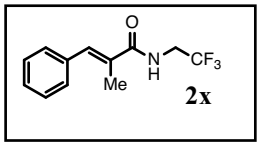

2x

Prepared according to General Procedure A using α-methylcinnamic acid (1.00 g, 6.17 mmol) and 2,2,2-trifluoroethan-1-amine (1.45 mL, 18.5 mmol). After workup, the crude residue was purified by silica gel chromatography (20 to 50% ethyl acetate in hexanes) to give **2x** (1.365 g, 91%) as a white solid.

^{1}H NMR (500 MHz, $CDCl_3$) δ 7.44 – 7.37 (m, 3H), 7.37 – 7.30 (m, 3H), 6.10 (br s, 1H), 4.07 (qd, J = 9.1, 6.4 Hz, 2H), 2.14 (d, J = 1.4 Hz, 3H); ^{13}C NMR (125.7 MHz, $CDCl_3$) δ 169.6, 135.7, 135.5, 131.1, 129.5, 128.6, 128.4, 124.4 (q, J = 278.4 Hz), 41.2 (q, J = 34.6 Hz), 14.4; ^{19}F NMR (470.4 MHz, $CDCl_3$) δ -72.4 (t, J = 9.2 Hz, 3F); FTIR (thin film) ν 3277, 1649, 1625, 1532, 1258, 1153 cm^{-1}; HRMS (ESI-TOF) Calc'd for $C_{12}H_{13}F_3NO$ $[M+H]^+$: 244.0944; found 244.0942.

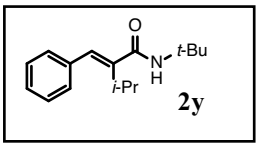

2y

Prepared according to General Procedure A using (*E*)-2-benzylidene-3-methylbutanoic acid[66] (187 mg, 0.98 mmol) and *tert*-butylamine (0.31 mL, 2.94 mmol). After workup, the crude residue was purified by silica gel chromatography (20% ethyl acetate in hexanes) to give **2y** (153 mg, 63%) as a white solid.

^{1}H NMR (500 MHz, $CDCl_3$) δ 7.38 – 7.33 (m, 2H), 7.29 – 7.25 (m, 3H), 6.65 (s, 1H), 5.57 (s, 1H), 3.08 – 2.97 (m, 1H), 1.43 (s, 9H), 1.23 (d, J = 6.9 Hz, 6H); ^{13}C NMR (125.7 MHz, $CDCl_3$) δ 170.7, 147.0, 136.2, 128.8, 128.5, 128.3, 127.5, 51.6, 36.5, 29.0, 28.4, 21.7; FTIR (thin film) ν 3312, 2973, 2922, 1640, 1617, 1532, 702 cm^{-1}; HRMS (ESI-TOF) Calc'd for $C_{16}H_{24}NO$ $[M+H]^+$: 246.1852; found 246.1850.

[66] Hoen, R.; Boogers, J. A. F.; Bernsmann, H.; Minnaard, A. J.; Meetsma, A.; Tiemersma-Wegman, T. D.; de Vries, A. H. M.; de Vries, J. G.; Feringa, B. L. *Angew. Chem., Int. Ed.* **2005**, *44,* 4209–4212.

1.10.5 Synthesis and Characterization of 1,2-Difluorides

General Procedure B: A polyethylene conical tube equipped with a stir bar was charged with the alkene substrate (1 equiv), catalyst **1b** (20.0 mol%), and dichloromethane (2.00 mL per 1.00 mmol of substrate) at room temperature. The resulting mixture was cooled to -78 ˚C, and pyridinium poly(hydrogen fluoride) (pyr•9HF, 70% hydrogen fluoride by weight, 50 equiv hydrogen fluoride) was added via syringe, followed by *m*-chloroperbenzoic acid (*m*CPBA, 77% by weight, 1.30 equiv). The tube was sealed, and the mixture was warmed to 4 ˚C and stirred for 24 h. The mixture was then cooled to -78 ˚C, diluted with dichloromethane (10.0 mL per 1.00 mmol of substrate), and pipetted slowly into a suspension of basic alumina (10 g per 1.00 mmol of substrate) in dichloromethane (50 mL per 1.00 mmol of substrate) at -78 ˚C. The resulting suspension was warmed to room temperature with stirring. The suspension was then filtered, and the filter cake was washed with dichloromethane (200 mL per 1.00 mmol of substrate). The combined filtrates were concentrated under reduced pressure. The crude product mixture was analyzed by ^{19}F NMR to determine the ratio of 1,2-difluoride to 1,1-difluoride. The 1,1-difluoride products were assigned by analogy to previously reported 1,1-difluorides.[67] The crude product mixture was then purified by flash column chromatography on silica gel, and pure 1,2-difluoride was isolated and characterized.

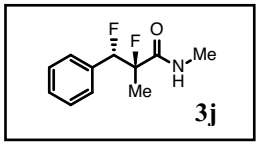

3j

Prepared according to General Procedure B using **2j** (175 mg, 1.00 mmol). Analysis of the crude product mixture by ^{19}F NMR indicated a 1,2:1,1 ratio of 3.3:1.0. After workup, the crude residue was purified by silica gel chromatography (10 to 30% diethyl ether in hexanes) to give **3j** (108 mg, 51%) as a white solid. **3j** was determined to be of

[67] See ref. 39.

94% e.e. by chiral GC analysis (β-Cyclosil, 40 → 200 ˚C, 1 ˚/min, 7 psi, t_R(major) = 94.910 min, t_R(minor) = 96.848 min).

^{1}H NMR (500 MHz, $CDCl_3$) δ 7.36–7.31 (m, 5H), 5.99 (br s, 1H), 5.72 (dd, *J* = 44.1, 25.7 Hz, 1H), 2.63 (dd, *J* = 5.1, 0.6 Hz, 3H), 1.79 (dd, *J* = 22.5, 1.8 Hz, 3H); ^{13}C NMR (125.7 MHz, $CDCl_3$) δ 170.0 (dd, *J* = 19.4, 7.3 Hz), 135.8 (dd, *J* = 23.0, 1.3 Hz), 129.0, 128.1, 127.1 (d, *J* = 7.2 Hz), 98.5 (dd, *J* = 196.1, 23.0 Hz), 94.4 (dd, *J* = 184.2, 19.4 Hz), 25.8, 20.2 (dd, *J* = 24.4, 5.3 Hz); ^{19}F NMR (470.4 MHz, $CDCl_3$) δ -171.42 – -171.71 (m, 1F), -196.87 (dd, *J* = 44.2, 9.7 Hz, 1F); FTIR (thin film) ν 3342, 1658, 1552, 729 cm^{-1}; HRMS (ESI-TOF) Calc'd for $C_{11}H_{14}F_2NO$ $[M+H]^+$: 214.1038; found 214.1036; $[\alpha]_D^{22}$ = –37.7 (c = 0.030, $CHCl_3$).

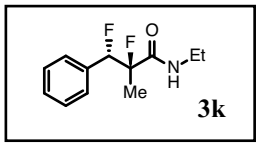

3k

Prepared according to General Procedure B using **2k** (189 mg, 1.00 mmol). Analysis of the crude product mixture by ^{19}F NMR indicated a 1,2:1,1 ratio of 4.3:1.0. After workup, the crude residue was purified by silica gel chromatography (5 to 20% diethyl ether in hexanes) to give **3k** (138 mg, 61%) as a white solid. **3k** was determined to be of 95% e.e. by chiral GC analysis (β-Cyclosil, 40 → 200 ˚C, 1.5 ˚/min, 14 psi, t_R(major) = 60.848 min, t_R(minor) = 61.554 min).

^{1}H NMR (500 MHz, $CDCl_3$) δ 7.34–7.33 (m, 5H), 5.96 (br s, 1H), 5.71 (dd, *J* = 44.2, 25.7 Hz, 1H), 3.22 – 3.11 (m, 1H), 3.11 – 3.00 (m, 1H), 1.79 (dd, *J* = 22.5, 1.6 Hz, 3H), 0.87 (dd, *J* = 7.7, 7.0 Hz, 3H); ^{13}C NMR (125.7 MHz, $CDCl_3$) δ 169.2 (dd, *J* = 19.2, 7.3 Hz), 134.2 (d, *J* = 21.8 Hz), 129.0, 128.1, 127.2 (d, *J* = 7.1 Hz), 98.2 (dd, *J* = 196.3, 22.7 Hz), 94.4 (dd, *J* = 184.6, 19.2 Hz), 33.9, 20.1 (dd, *J* = 24.4, 5.0 Hz), 14.5; ^{19}F NMR (470.4 MHz, $CDCl_3$) δ -171.60 (dtdd, *J* = 48.8, 22.4, 9.7, 5.4 Hz, 1F), -196.61 (ddd, *J* = 44.1, 10.0, 1.8 Hz, 1F); FTIR (thin film) ν 3336,

1651, 1550, 1109, 693 cm^{-1}; HRMS (ESI-TOF) Calc'd for $C_{12}H_{16}F_2NO$ $[M+H]^+$: 228.1194; found 228.1192; ; $[\alpha]_D^{21}$ = –12.7 (c = 0.069, $CHCl_3$).

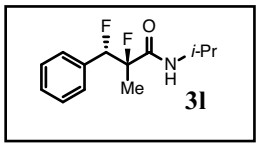

3l

Prepared according to General Procedure B using **2l** (203 mg, 1.00 mmol). Analysis of the crude product mixture by ^{19}F NMR indicated a 1,2:1,1 ratio of 4.8:1.0. After workup, the crude residue was purified by silica gel chromatography (0 to 12% diethyl ether in hexanes) to give **3l** (135 mg, 56%) as a white solid. **3l** was determined to be of 95% e.e. by chiral GC analysis (β-Cyclosil, 40 → 200 ˚C, 1.5 ˚/min, 14 psi, t_R(minor) = 59.224 min, t_R(major) = 59.726 min).

^1H NMR (500 MHz, $CDCl_3$) δ 7.35–7.33 (m, 5H), 5.69 (m, 2H), 4.03 – 3.67 (m, 1H), 1.79 (dd, *J* = 22.5, 1.7 Hz, 3H), 1.04 (d, *J* = 6.6 Hz, 3H), 0.75 (d, *J* = 6.5 Hz, 3H); ^{13}C NMR (125.7 MHz, $CDCl_3$) δ 168.3 (dd, *J* = 19.1, 7.1 Hz), 134.19 (d, *J* = 21.8 Hz), 129.0, 128.1, 127.3 (d, *J* = 7.3 Hz), 98.1 (dd, *J* = 196.4, 22.7 Hz), 94.5 (dd, *J* = 184.4, 18.9 Hz), 41.1, 22.4, 22.2, 20.1 (dd, *J* = 24.5, 4.9 Hz); ^{19}F NMR (470.4 MHz, $CDCl_3$) δ -171.43 – -171.76 (m, 1F), -196.40 (dd, *J* = 44.1, 9.8 Hz, 1F); FTIR (thin film) ν 3333, 1646, 1544, 720 cm^{-1}; HRMS (ESI-TOF) Calc'd for $C_{13}H_{18}F_2NO$ $[M+H]^+$: 242.1351; found 242.1348; ; $[\alpha]_D^{22}$ = –3.9 (c = 0.058, $CHCl_3$).

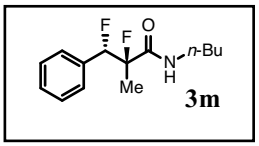

3m

Prepared according to General Procedure B using **2m** (217 mg, 1.00 mmol). Analysis of the crude product mixture by ^{19}F NMR indicated a 1,2:1,1 ratio of 6.9:1.0. After workup, the crude residue was purified by silica gel chromatography (2 to 16% diethyl ether in hexanes) to give **3m** (161 mg, 63%) as a white solid.

3m was determined to be of 94% e.e. by chiral GC analysis (CP-Chirasil-Dex CB, 120 ˚C, 14 psi, t_R(major) = 34.262 min, t_R(minor) = 35.790 min).

^{1}H NMR (500 MHz, $CDCl_3$) δ 7.35–7.33 (m, 5H), 5.97 (br s, 1H), 5.70 (dd, *J* = 44.1, 25.7 Hz, 1H), 3.19 – 3.09 (m, 1H), 2.99 (m, 1H), 1.79 (dd, *J* = 22.5, 1.7 Hz, 1H), 1.28 – 1.10 (m, 2H), 1.10 – 0.94 (m, 2H), 0.82 – 0.77 (m, 3H); ^{13}C NMR (125.7 MHz, $CDCl_3$) δ 169.2 (dd, *J* = 19.0, 7.2 Hz), 134.2 (d, *J* = 21.6 Hz), 129.0 (d, *J* = 1.7 Hz), 128.1, 127.3 (d, *J* = 7.0 Hz), 98.3 (dd, *J* = 196.3, 22.9 Hz), 94.5 (dd, *J* = 184.0, 19.0 Hz), 38.7, 31.2, 20.2 (dd, *J* = 24.4, 5.0 Hz), 19.7, 13.7; ^{19}F NMR (470.4 MHz, $CDCl_3$) δ -171.50 – -171.73 (m, 1F), -196.19 (ddd, *J* = 44.1, 9.6, 1.8 Hz, 1F); FTIR (thin film) ν 3341, 2955, 1652, 1545 cm^{-1}; HRMS (ESI-TOF) Calc'd for $C_{14}H_{20}F_2NO$ $[M+H]^+$: 256.1507; found 256.1506; $[\alpha]_D^{21}$ = –13.5 (c = 0.11, $CHCl_3$).

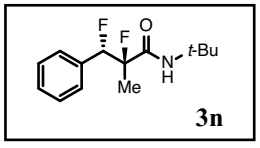

3n

Prepared according to General Procedure B using **2n** (217 mg, 1.00 mmol). Analysis of the crude product mixture by ^{19}F NMR indicated a 1,2:1,1 ratio of 39:1.0. After workup, the crude residue was purified by silica gel chromatography (2 to 10% diethyl ether in hexanes) to give **3n** (207 mg, 81%) as a white solid. **3n** was determined to be of 96% e.e. by chiral GC analysis (β-Cyclosil, 40 → 200 ˚C, 1.5 ˚/min, 14 psi, t_R(minor) = 57.689 min, t_R(major) = 58.359 min).

^{1}H NMR (500 MHz, $CDCl_3$) δ 7.38 – 7.32 (m, 5H), 5.77 (br s, 1H), 5.68 (dd, *J* = 55, 25 Hz, 1H), 1.77 (dd, *J* = 22.5, 1.7 Hz, 3H), 1.14 (s, 9H); ^{13}C NMR (125.7 MHz, $CDCl_3$) δ 168.4 (dd, *J* = 17.6, 7.2 Hz), 134.2 (d, *J* = 21.9 Hz), 129.0, 128.1, 127.5 (d, *J* = 6.8 Hz), 97.9 (dd, *J* = 197.3, 22.5 Hz), 94.6 (dd, *J* = 184.0, 19.0 Hz), 51.2, 28.4, 20.2 (dd, *J* = 24.6, 5.0 Hz); ^{19}F NMR (470.4 MHz, $CDCl_3$) δ -169.28 – -169.57 (m, 1F), -196.25 (dd, *J* = 44.1, 9.7 Hz, 1F); FTIR (thin film) ν

3443, 3387, 2970, 1682, 1528, 1022, 714 cm^{-1}; HRMS (ESI-TOF) Calc'd for $C_{14}H_{20}F_2NO$ $[M+H]^+$: 256.1507; found 256.1505; $[\alpha]_D^{21} = -11.0$ (c = 0.048, $CHCl_3$).

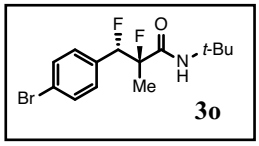

3o

Prepared according to General Procedure B using **2o** (296 mg, 1.00 mmol). Analysis of the crude product mixture by ^{19}F NMR indicated a 1,2:1,1 ratio of >100:1.0. After workup, the crude residue was purified by silica gel chromatography (2 to 10% diethyl ether in hexanes) to give **3o** (289 mg, 83%) as a white solid. **3o** was determined to be of 98% e.e by chiral HPLC analysis (AD-H, 1 mL/min, 2% IPA/hexanes, 220 nm, t_R(major) = 6.280 min, t_R(minor) = 8.468 min).

^1H NMR (500 MHz, $CDCl_3$) δ 7.50 – 7.46 (m, 2H), 7.25 – 7.21 (m, 2H), 5.81 (br s, 1H), 5.67 (dd, *J* = 44.1, 25.5 Hz, 1H), 1.75 (dd, *J* = 22.5, 1.7 Hz, 3H), 1.18 (s, 9H); ^{13}C NMR (125.7 MHz, $CDCl_3$) δ 168.3 (dd, *J* = 17.7, 7.2 Hz), 133.3 (d, *J* = 22.1 Hz), 131.3, 129.1 (d, *J* = 6.6 Hz), 123.2 (d, *J* = 1.9 Hz), 97.7 (dd, *J* = 197.5, 22.4 Hz), 93.9 (dd, *J* = 184.5, 19.2 Hz), 51.4, 28.5, 20.2 (dd, *J* = 24.5, 5.0 Hz); ^{19}F NMR (470.4 MHz, $CDCl_3$) δ -169.33 – -169.89 (m, 1F), -197.08 (dd, *J* = 44.1, 10.1 Hz, 1F); FTIR (thin film) ν 3440, 2972, 1682, 1528, 1012, 777 cm^{-1}; HRMS (ESI-TOF) Calc'd for $C_{14}H_{19}BrF_2NO$ $[M+H]^+$: 334.0613; found 334.0610; $[\alpha]_D^{22} = -0.7$ (c = 0.19, $CHCl_3$).

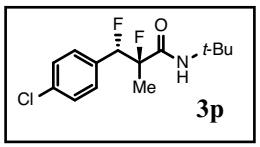

3p

Prepared according to General Procedure B using **2p** (252 mg, 1.00 mmol). Analysis of the crude product mixture by ^{19}F NMR indicated a 1,2:1,1 ratio of 86:1.0. After workup, the crude residue was purified by silica gel chromatography (2 to 6% diethyl ether in hexanes) to give **3p** (243 mg, 84%) as a white solid. **3p** was determined to be of

97% e.e. by chiral GC analysis (β-Cyclosil, 40 → 200 ˚C, 0.2 ˚/min, 14 psi, t_R(minor) = 402.049 min, t_R(major) = 403.697 min).

^{1}H NMR (500 MHz, $CDCl_3$) δ 7.35 – 7.28 (m, 4H), 5.81 (br s, 1H), 5.69 (dd, *J* = 44.1, 25.5 Hz, 1H), 1.76 (dd, *J* = 22.5, 1.7 Hz, 3H), 1.17 (s, 9H); ^{13}C NMR (125.7 MHz, $CDCl_3$) δ 168.3 (dd, *J* = 17.7, 7.2 Hz), 135.0 (d, *J* = 1.8 Hz), 132.8 (d, *J* = 22.4 Hz), 128.9 (d, *J* = 6.8 Hz), 128.3, 97.8 (dd, *J* = 197.5, 22.6 Hz), 93.9 (dd, *J* = 184.3, 19.2 Hz), 51.4, 28.4, 20.2 (dd, *J* = 24.5, 5.1 Hz); ^{19}F NMR (470.4 MHz, $CDCl_3$) δ -169.44 – -169.74 (m, 1F), -196.72 (dd, *J* = 44.2, 9.9 Hz, 1F); FTIR (thin film) ν 3441, 2969, 1681, 1530, 779 cm^{-1}; HRMS (ESI-TOF) Calc'd for $C_{14}H_{19}ClF_2NO$ $[M+H]^+$: 290.1118; found 290.1115; $[\alpha]_D^{21}$ = –2.2 (c = 0.14, $CHCl_3$).

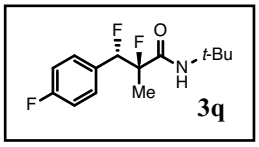

3q

Prepared according to General Procedure B using **2q** (235 mg, 1.00 mmol). Analysis of the crude product mixture by ^{19}F NMR indicated a 1,2:1,1 ratio of 16:1.0. After workup, the crude residue was purified by silica gel chromatography (2 to 8% diethyl ether in hexanes) to give **3q** (197 mg, 72%) as a white solid. **3q** was determined to be of 98% e.e. by chiral GC analysis (β-Cyclosil, 40 → 200 ˚C, 1.5 ˚/min, 14 psi, t_R(minor) = 57.213 min, t_R(major) = 57.730 min).

^{1}H NMR (500 MHz, $CDCl_3$) δ 7.35 (dd, *J* = 8.1, 5.6 Hz, 2H), 7.08 – 6.99 (m, 2H), 5.79 (br s, 1H), 5.68 (dd, *J* = 43.9, 25.6 Hz, 1H), 1.76 (dd, *J* = 22.5, 1.7 Hz, 3H), 1.15 (s, 9H); ^{13}C NMR (125.7 MHz, $CDCl_3$) δ 168.4 (dd, *J* = 17.7, 7.2 Hz), 163.2 (d, *J* = 247.8 Hz), 130.1 (d, *J* = 22.8 Hz), 129.8 – 129.3 (m), 115.1 (d, *J* = 21.7 Hz), 97.9 (dd, *J* = 197.5, 22.6 Hz), 94.0 (dd, *J* = 184.0, 18.9 Hz), 51.3, 28.4, 20.2 (dd, *J* = 24.7, 4.8 Hz); ^{19}F NMR (470.4 MHz, $CDCl_3$) δ -112.66 (ttd, *J* = 8.1, 5.3, 2.5 Hz, 1F), -169.70 – -170.01 (m, 1F), -195.10 (dd, *J* = 44.0, 10.0 Hz, 1F); FTIR

(thin film) ν 3388, 2984, 1663, 1532, 1228, 788 cm^{-1}; HRMS (ESI-TOF) Calc'd for $C_{14}H_{19}F_3NO$ $[M+H]^+$: 274.1413; found 274.1413; $[\alpha]_D^{22} = -8.1$ (c = 0.11, $CHCl_3$).

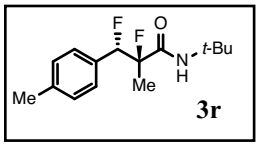

3r

Prepared according to General Procedure B using **2r** (231 mg, 1.00 mmol) and with the following modification: 25 equiv hydrogen fluoride were used. Analysis of the crude product mixture by ^{19}F NMR indicated a 1,2:1,1 ratio of 2.2:1.0. After workup, the crude residue was purified by silica gel chromatography (1 to 7% diethyl ether in hexanes) to give **3r** (107 mg, 40%) as a white solid. **3r** was determined to be of 98% e.e by chiral HPLC analysis (AD-H, 1 mL/min, 2% IPA/hexanes, 220 nm, t_R(major) = 6.029 min, t_R(minor) = 7.590 min).

^1H NMR (500 MHz, $CDCl_3$) δ 7.24 (d, *J* = 7.9 Hz, 2H), 7.14 (d, *J* = 7.8 Hz, 2H), 5.80 (br s, 1H), 5.65 (dd, *J* = 44.0, 25.8 Hz, 2H), 2.35 (d, *J* = 0.9 Hz, 3H), 1.75 (dd, *J* = 22.4, 1.7 Hz, 3H), 1.15 (s, 9H); ^{13}C NMR (125.7 MHz, $CDCl_3$) δ 168.57 (dd, *J* = 17.6, 7.1 Hz), 138.83 (d, *J* = 1.7 Hz), 131.30 (d, *J* = 22.1 Hz), 128.75, 127.38 (dd, *J* = 7.7, 1.3 Hz), 98.04 (dd, *J* = 197.0, 22.7 Hz), 94.57 (dd, *J* = 183.4, 19.2 Hz), 51.24, 28.43, 21.34, 20.21 (dd, *J* = 24.5, 5.1 Hz); ^{19}F NMR (470.4 MHz, $CDCl_3$) δ -169.08 – -169.31 (m, 1F), -195.50 (dd, *J* = 44.2, 9.7 Hz, 1F); FTIR (thin film) ν 3441, 2965, 1684, 1526, 1034, 777 cm^{-1}; HRMS (ESI-TOF) Calc'd for $C_{15}H_{22}F_2NO$ $[M+H]^+$: 270.1664; found 270.1661; $[\alpha]_D^{22} = -5.8$ (c = 0.053, $CHCl_3$).

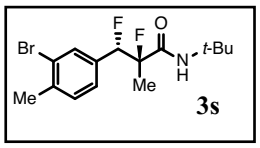

Prepared according to General Procedure B using **2s** (310 mg, 1.00 mmol). Analysis of the crude product mixture by ^{19}F NMR indicated a 1,2:1,1 ratio of 79:1.0. After workup, the crude residue was purified by silica gel chromatography (2 to 10% diethyl ether in hexanes) to give **3s** (289 mg, 83%) as a white solid. **3s** was determined to be of 98% e.e. by chiral GC analysis (β-Cyclosil, 40 → 200 ˚C, 1.5 ˚/min, 14 psi, t_R(minor) = 82.246 min, t_R(major) = 82.683 min).

^{1}H NMR (500 MHz, $CDCl_3$) δ 7.51 (s, 1H), 7.20 (dd, *J* = 1.3, 0.7 Hz, 2H), 5.83 (s, 1H), 5.66 (dd, *J* = 44.1, 25.6 Hz, 1H), 2.39 (d, *J* = 1.0 Hz, 3H), 1.75 (dd, *J* = 22.5, 1.8 Hz, 3H), 1.19 (s, 9H); ^{13}C NMR (125.7 MHz, $CDCl_3$) δ 168.4 (dd, *J* = 17.7, 7.3 Hz), 138.7, 133.7 (d, *J* = 22.3 Hz), 131.0 (d, *J* = 7.2 Hz), 130.4, 126.2 (d, *J* = 7.0 Hz), 124.6, 97.9 (dd, *J* = 197.5, 22.5 Hz), 93.6 (dd, *J* = 184.7, 19.3 Hz), 51.5, 28.5, 22.9, 20.2 (dd, *J* = 24.6, 5.3 Hz); ^{19}F NMR (470.4 MHz, $CDCl_3$) δ -169.23 – -169.52 (m, 1F), -197.31 (dd, *J* = 43.8, 9.9 Hz, 1F); FTIR (thin film) ν 3401, 2976, 1665, 1531, 1048, 781 cm^{-1}; HRMS (ESI-TOF) Calc'd for $C_{15}H_{21}BrF_2NO$ $[M+H]^+$: 348.0769; found 348.0767; $[\alpha]_D^{22}$ = +5.0 (c = 0.23, $CHCl_3$).

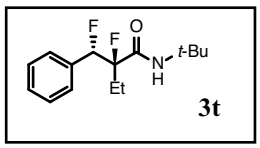

Prepared according to General Procedure B using **2t** (231 mg, 1.00 mmol). Analysis of the crude product mixture by ^{19}F NMR indicated a 1,2:1,1 ratio of >100:1.0. After workup, the crude residue was purified by silica gel chromatography (2 to 6% diethyl ether in hexanes) to give **3t** (156 mg, 58%) as a colorless oil. **3t** was determined to be of 95% e.e. by chiral GC analysis (β-Cyclosil, 40 → 200 ˚C, 1.5 ˚/min, 14 psi, t_R(minor) = 64.469 min, t_R(major) = 65.011 min).

^{1}H NMR (500 MHz, $CDCl_3$) δ 7.38 – 7.31 (m, 5H), 5.78 (br s, 1H), 5.69 (dd, *J* = 44.3, 25.8 Hz, 1H), 2.30 – 2.18 (m, 1H), 2.18 – 2.09 (m, 1H), 1.14 (s, 9H), 0.98 (t, *J* = 7.4 Hz, 3H); ^{13}C NMR (125.7 MHz, $CDCl_3$) δ 167.4 (dd, *J* = 17.8, 7.1 Hz), 134.4 (d, *J* = 22.0 Hz), 129.0 (d, *J* = 1.8 Hz), 128.0, 127.5 (d, *J* = 6.4 Hz), 100.8 (dd, *J* = 200.2, 21.8 Hz), 94.6 (dd, *J* = 183.8, 18.9 Hz), 51.4, 28.4, 26.4 (dd, *J* = 23.2, 4.4 Hz), 7.4 (d, *J* = 3.8 Hz); ^{19}F NMR (470.4 MHz, $CDCl_3$) δ -181.01 – -181.20 (m, 1F), -196.00 (dd, *J* = 44.3, 10.0 Hz, 1F); FTIR (thin film) ν 3444, 2973, 1681, 1526, 1457, 717 cm^{-1}; HRMS (ESI-TOF) Calc'd for $C_{15}H_{22}F_2NO$ $[M+H]^+$: 270.1664; found 270.1663; $[\alpha]_D^{22}$ = –2.5 (c = 0.076, $CHCl_3$).

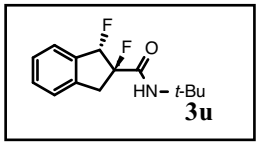

3u

Prepared according to General Procedure B using **2u** (215 mg, 1.00 mmol). Analysis of the crude product mixture by ^{19}F NMR indicated a 1,2:1,1 ratio of >100:1.0. After workup, the crude residue was purified by silica gel chromatography (5–20% diethyl ether in hexanes) to give **3u** (108 mg, 43%) as a pale yellow solid. **3u** was determined to be of 77% e.e by chiral GC analysis (β-Cyclosil, 40 → 200 ˚C, 1.5 ˚/min, 14 psi, t_R(minor) = 76.993 min, t_R(major) = 77.287 min).

^{1}H NMR (500 MHz, $CDCl_3$) δ 7.46–7.42 (m, 1H), 7.40–7.35 (m, 1H), 7.33–7.27 (m, 1H), 6.26 (s, 1H), 5.99 (dd, *J* = 54.9, 19.2 Hz, 1H), 3.93 (dd, *J* = 18.2, 17.1 Hz, 1H), 3.20 (ddd, *J* = 23.5, 17.1, 1.9 Hz, 1H), 1.42 (s, 9H); ^{13}C NMR (125.7 MHz, $CDCl_3$) δ 166.1 (dd, *J* = 20.6, 3.0 Hz), 141.0 (dd, *J* = 5.1, 2.1 Hz), 136.2 (dd, *J* = 19.5, 4.4 Hz), 130.7 (d, *J* = 3.6 Hz), 127.8 (d, *J* = 2.9 Hz), 125.6, 124.9 (d, *J* = 1.8 Hz), 103.8 (dd, *J* = 196.5, 22.3 Hz), 99.9 (dd, *J* = 190.1, 35.7 Hz), 51.9, 40.1 (d, *J* = 24.5 Hz), 28.8; ^{19}F NMR (470.4 MHz, $CDCl_3$) δ -156.56 – -156.72 (m, 1F), -179.96 (dd, *J* = 54.5, 4.9 Hz, 1F); FTIR (thin film) ν 3439, 3351, 2969, 2932, 1686, 1526, 1227,

1018, 753 cm^{-1}; HRMS (ESI-TOF) Calc'd for $C_{14}H_{18}F_2NO$ $[M+H]^+$: 254.1351; found 254.1349; ; $[\alpha]_D^{22}$ = 51.9 (c = 0.079, $CHCl_3$).

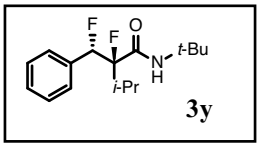

3y

Prepared according to General Procedure B using **2y** (49.1 mg, 0.20 mmol). Analysis of the crude product mixture by ^{19}F NMR indicated a 1,2:1,1 ratio of >100:1.0. After workup, the crude residue was purified by silica gel chromatography (10% diethyl ether in hexanes) to give **3y** (24.7 mg, 44%) as a colorless oil. **3y** was determined to be of 97% e.e by chiral GC analysis (CP-Chirasil-Dex CB, 40 → 160 ˚C, 1.5 ˚/min, 14 psi, t_R(minor) = 69.959 min, t_R(major) = 70.983 min).

^1H NMR (500 MHz, $CDCl_3$) δ 7.39 – 7.30 (m, 5H), 5.95 (dd, *J* = 44.1, 26.9 Hz, 1H), 5.75 (s, 1H), 2.51 (dpd, *J* = 17.5, 6.9, 1.4 Hz, 1H), 1.27 (d, *J* = 7.0 Hz, 3H), 1.13 (s, 9H), 1.05 (dd, *J* = 6.9, 1.1 Hz, 3H); ^{13}C NMR (125.7 MHz, $CDCl_3$) δ 167.0 (dd, *J* = 18.0, 7.9 Hz), 134.6 (d, *J* = 21.8 Hz), 128.9 (d, *J* = 1.6 Hz), 128.0, 127.7 (d, *J* = 7.6 Hz), 101.7 (dd, *J* = 199.6, 21.9 Hz), 93.2 (dd, *J* = 183.6, 18.8 Hz), 51.4, 32.7 (dd, *J* = 23.4, 3.3 Hz), 28.5, 17.9 (d, *J* = 8.6 Hz), 17.0; ^{19}F NMR (470.4 MHz, $CDCl_3$) δ -174.72 – -174.94 (m), -197.81 (dd, *J* = 44.1, 10.0 Hz); FTIR (thin film) ν 3445, 2971, 1681, 1524, 1456, 1021, 716 cm^{-1}; HRMS (ESI-TOF) Calc'd for $C_{16}H_{24}F_2NO$ $[M+H]^+$: 284.1820; found 284.1819.

1.10.6 Derivatization of 1,2-Difluoride Products

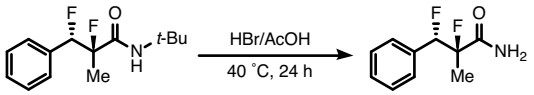

3n **3b**

3b: To a screw-cap vial charged with **3n** (51.1 mg, 0.20 mmol) and a stir bar, hydrogen bromide solution (1.00 mL, 33 wt. % in acetic acid) was added. The vial was capped tightly with a Teflon-lined cap and warmed to 40 ˚C for 24 h. The reaction mixture was then cooled to room temperature and diluted with ethyl acetate (10 mL). Saturated aqueous $NaHCO_3$ was added slowly until the aqueous layer reached pH = 8. The layers were separated, and the organic layer was washed with water (3 × 5 mL), washed with brine (5 mL), dried over anhydrous $MgSO_4$, and concentrated. The resulting residue was purified by flash column chromatography on silica gel (50% ethyl acetate in hexanes) to give **3b** as a white solid (35.4 mg, 89%). **3b** was determined to be of 96% e.e by chiral GC analysis (β-Cyclosil, 40 → 200 ˚C, 1.5 ˚/min, 14 psi, t_R(major) = 67.968 min, t_R(minor) = 68.946 min).

^{1}H NMR (500 MHz, $CDCl_3$) δ 7.40 – 7.33 (m, 5H), 5.96 (br s, 1H), 5.71 (dd, *J* = 44.1, 25.2 Hz, 1H), 5.19 (br s, 1H), 1.81 (dd, *J* = 22.3, 1.7 Hz, 3H); ^{13}C NMR (125.7 MHz, DMSO-d_6) δ 171.0 (dd, *J* = 21.2, 6.8 Hz), 134.4 (d, *J* = 21.5 Hz), 128.9, 128.0, 127.3 (d, *J* = 7.2 Hz), 96.9 (dd, *J* = 196.1, 22.6 Hz), 94.2 (dd, *J* = 179.5, 19.6 Hz), 20.4 (dd, *J* = 25.2, 3.9 Hz); ^{19}F NMR (470.4 MHz, $CDCl_3$) δ -168.84 – -169.24 (m, 1F), -195.80 (dd, *J* = 44.1, 9.7 Hz, 1F); FTIR (thin film) ν 3394, 3189, 1661, 1639, 1112, 1038, 674 cm^{-1}; HRMS (ESI-TOF) Calc'd for $C_{10}H_{12}F_2NO$ $[M+H]^+$: 200.0881; found 200.0880; $[\alpha]_D^{22}$ = –103 (c = 0.0062, $CHCl_3$).

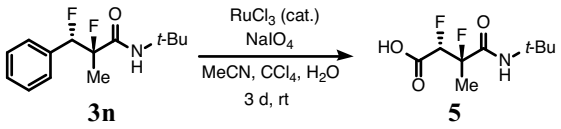

5: A catalytic amount of ruthenium trichloride hydrate and sodium periodate (770 mg, 3.6 mmol, 18 equiv) were added to a vigorously stirred solution of **3n** (51.1 mg, 0.20 mmol, 1.0 equiv) in carbon tetrachloride (0.75 mL), acetonitrile (0.75 mL), and water (2.0 mL). The reaction vessel was equipped with a vent needle, and the biphasic mixture was stirred for 72 h at room temperature. After 72 h, the reaction mixture was cooled to 0 ˚C and diethyl ether (10 mL) was added. The organic layer was separated, and the aqueous layer was extracted with diethyl ether (3 × 5 mL). The combined organic layers were dried over anhydrous $MgSO_4$ and concentrated under reduced pressure to afford **5** (33.1 mg, 74%) as a tan solid. **5** was determined to be of 96% e.e. by chiral GC analysis of its corresponding methyl ester **S-1**. To prepare methyl ester **S-1**, a solution of (diazomethyl)trimethylsilane (2.0 M in diethyl ether, 16.0 µL, 0.032 mmol, 1.5 equiv) was added dropwise via syringe to a stirred solution of **5** (5.0 mg, 0.022 mmol, 1 equiv) in benzene (150 µL) and methanol (43 µL) at room temperature. After 30 minutes, acetic acid (5 µL) was added dropwise via syringe to quench the unreacted (diazomethyl)trimethylsilane, and an aliquot of the reaction mixture was subjected to chiral GC analysis (β-Cyclosil, 40 → 200 ˚C, 1 ˚/min, 20 psi, t_R(major) = 53.977 min, t_R(minor) = 54.311 min).

^{1}H NMR (500 MHz, $CDCl_3$) δ 6.29 (br s, 1H), 5.30 (dd, *J* = 47.7, 24.5 Hz, 1H), 1.72 (dd, *J* = 23.0, 1.9 Hz, 3H), 1.40 (s, 9H); ^{13}C NMR (125.7 MHz, acetone-d_6) δ 168.5 (dd, *J* = 18.7, 6.4 Hz), 166.8 (dd, *J* = 25.7, 5.7 Hz), 97.8 (dd, *J* = 195.4, 20.7 Hz), 91.0 (dd, *J* = 192.2, 22.4 Hz), 51.9, 28.7, 20.8 (dd, *J* = 23.9, 7.6 Hz); ^{19}F NMR (470.4 MHz, DMSO-d_6) δ -161.51 (pd, *J* =

23.5, 11.0 Hz, 1F), -202.93 (dd, J = 46.4, 11.6 Hz, 1F); FTIR (thin film) ν 3434, 2972, 1758, 1654, 1540, 1230, 1221, 1191, 1083 cm^{-1}; HRMS (ESI-TOF) Calc'd for $C_9H_{16}F_2NO_3$ $[M+H]^+$: 224.1093; found 224.1092; $[\alpha]_D^{22}$ = 3.7 (c = 0.029, $CHCl_3$).

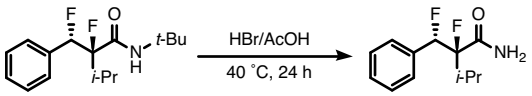

3y **3a**

3a: To a screw-cap vial charged with **3y** (10.0 mg, 0.035 mmol) and a stir bar, hydrogen bromide solution (0.50 mL, 33 wt. % in acetic acid) was added. The vial was capped tightly and warmed to 40 ˚C for 24 h. The reaction mixture was then cooled to room temperature and diluted with ethyl acetate. Saturated aqueous $NaHCO_3$ was added slowly until the aqueous layer reached pH = 8. The layers were separated, and the organic layer was washed with water (3 × 5 mL), washed with brine (5 mL), dried over anhydrous $MgSO_4$, and concentrated. The resulting residue was purified by flash column chromatography on silica gel (0 to 10% diethyl ether in dichloromethane) to give **3a** as a white solid. The spectral data for **3a** were in accordance with the literature.[68] $[\alpha]_D^{21}$ = +14.3 (c = 0.00275, $CHCl_3$). The absolute stereochemistry of **3a** was assigned by comparison of the sign of the optical rotation with the literature value. The assignment of absolute stereochemistry was confirmed by verifying that the major and minor enantiomer of product eluted in the same order as previously reported (β-Cyclosil, 120 → 200 ˚C, 1 ˚/min, 7 psi, t_R(major) = 46.538 min, t_R(minor) = 47.017 min).

[68] See ref. 35.

1.10.7 Measurement of Product Ratios for Selected Cinnamamides

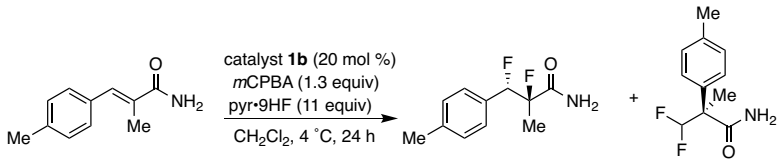

The reaction was conducted according to General Procedure B using (*E*)-2-methyl-3-(*p*-tolyl)acrylamide[69] (175.2, 1.00 mmol) and with the following modifications: 100 equiv of hydrogen fluoride were used, and the reaction was quenched after 72 h. Analysis of the crude product mixture by ^{19}F NMR indicated a 1,2:1,1 ratio of 1.0:36.

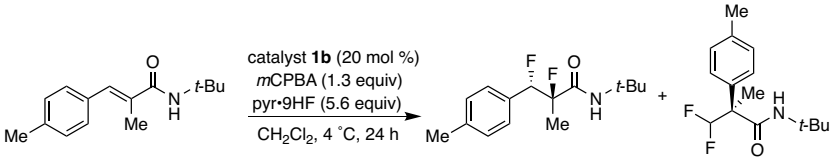

The reaction was conducted according to General Procedure B using **2r** (12.9 mg, 0.056 mmol). Analysis of the crude product mixture by ^{19}F NMR indicated a 1,2:1,1 ratio of 1.4:1.0.

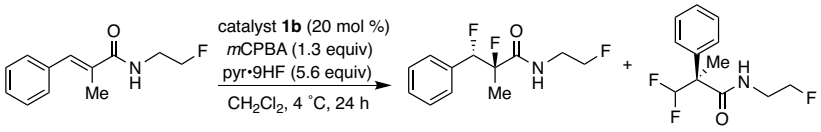

The reaction was conducted according to General Procedure B using **2v** (207.3 mg, 1.00 mmol). Analysis of the crude product mixture by ^{19}F NMR indicated a 1,2:1,1 ratio of 3.4:1.0.

[69] Pastushak, N. O.; Dombrovskii, A. V. *Zhurnal Obshchei Khimii* **1964**, *34,* 3110.

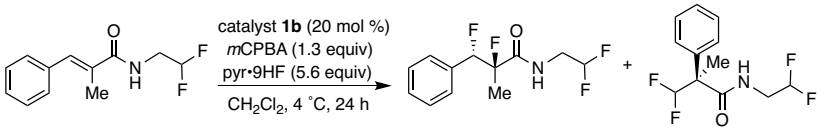

The reaction was conducted according to General Procedure B using **2w** (225.2 mg, 1.00 mmol). Analysis of the crude product mixture by ^{19}F NMR indicated a 1,2:1,1 ratio of 2.1:1.0.

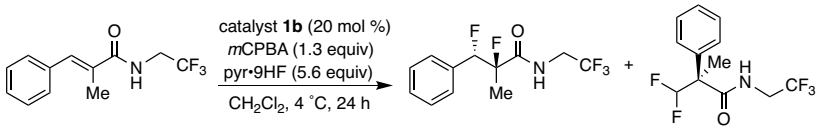

The reaction was conducted according to General Procedure B using **2x** (243.2 mg, 1.00 mmol). Analysis of the crude product mixture by ^{19}F NMR indicated a 1,2:1,1 ratio of 1.1:1.0.

1.10.8 Correlations Between Product Ratios and Steric and Electronic Parameters for Amide *N*-Substituents

Steric and electronic parameters for the amide *N*-substituents of **2b** and **2j**–**n** were plotted versus the product ratio (ln(1,2 : 1,1)) obtained for each substrate.

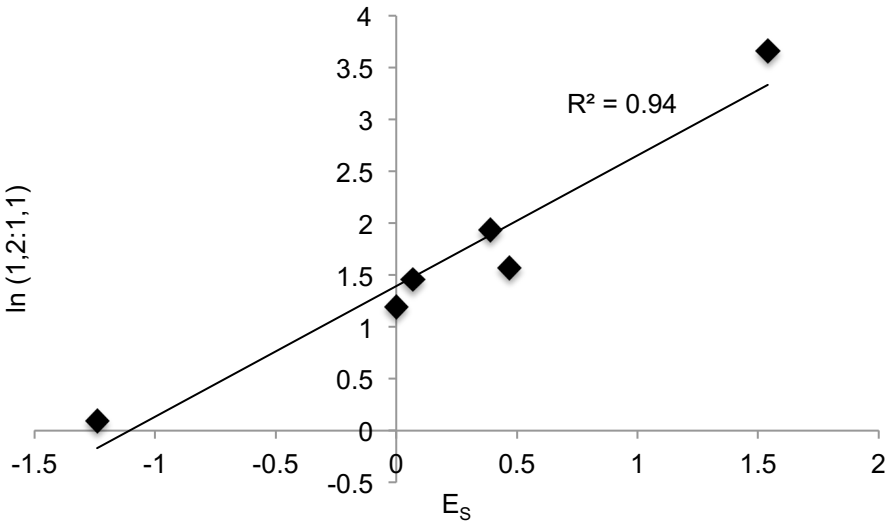

Figure 1.22 Correlation with Taft Steric Parameter.[70,71]

[70] (a) Taft, R. W., Jr. *J. Am. Chem. Soc.* **1952**, *74*, 2729–2732. (b) Taft, R. W., Jr. In *Steric Effects in Organic Chemistry*, ed. M. S. Newman, Wiley, New York, **1956**, pp 556–675.

[71] Sigman, M. S.; Miller, J. J. *J. Org. Chem.* **2009**, *74,* 7633–7643.

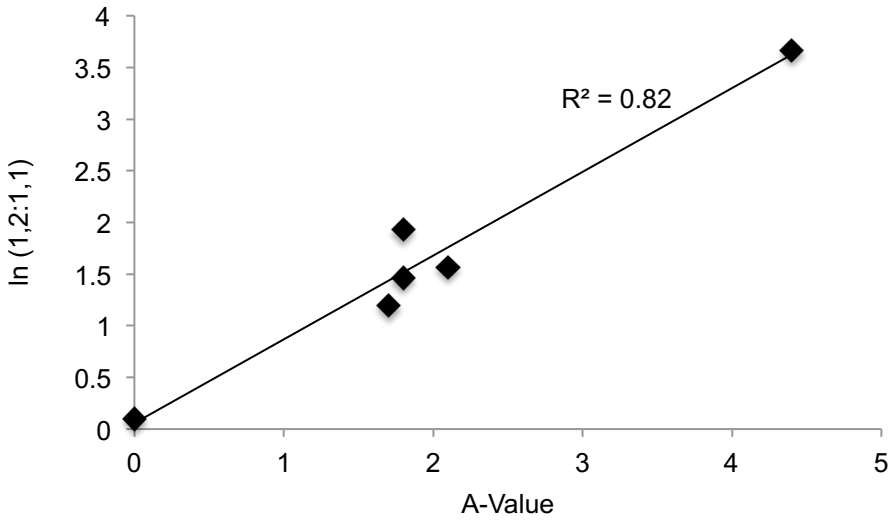

Figure 1.23 Correlation with A-Value.[72]

[72] (a) Hirsch, J. A. *Topics in Stereochemistry*, **1967**, *3*, 199–222. (b) Jensen, F. R.; Bushweller, C. H. *Adv. Alicyclic Chem* **1971**, *3*, 139. (c) Eliel, E. L.; Wilen, S. H.; *Stereochemistry of Organic Compounds,* Wiley, **1993**, p, 696. (d) Eliel, E. L.; Wilen, S. H.; Doyle, M. P. *Basic Organic Stereochemistry*, Wiley, **2001**, p. 443.

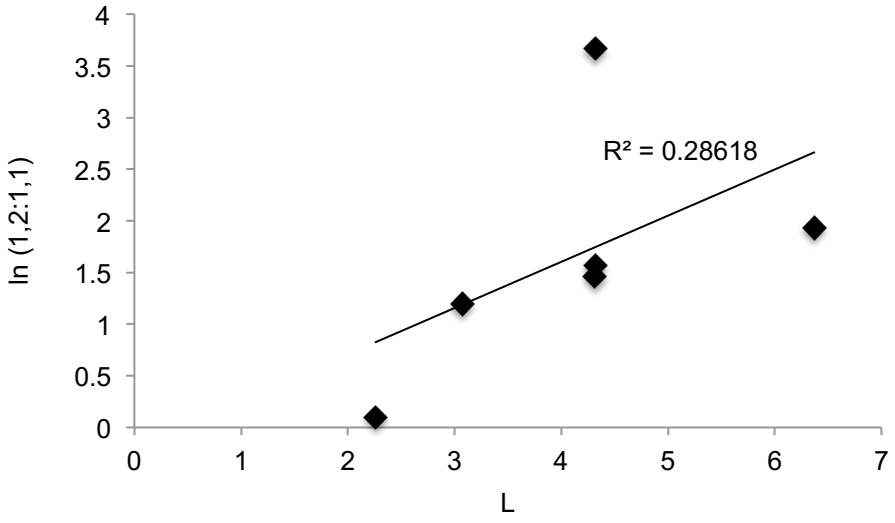

Figure 1.24 Correlation with Sterimol L.[73]

[73] Sterimol parameters were obtained using Molecular Modeling Pro Version 6.3.6.

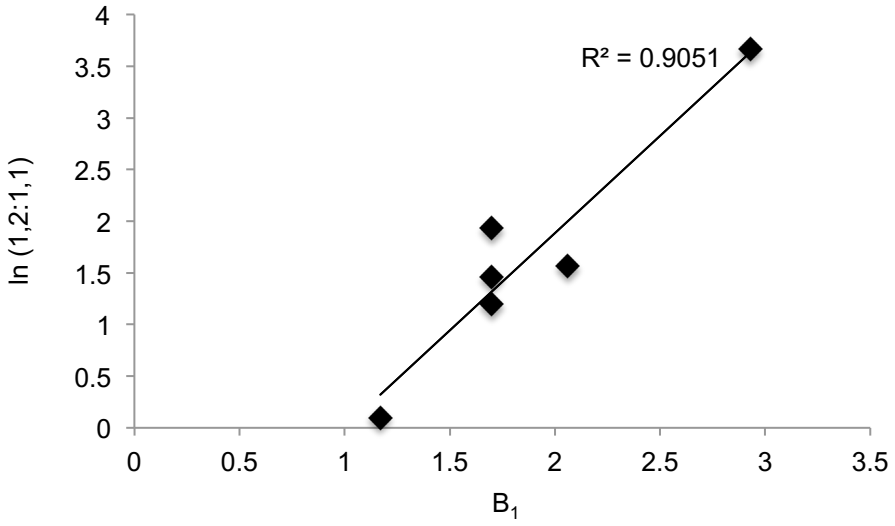

Figure 1.25 Correlation with Sterimol B_1.

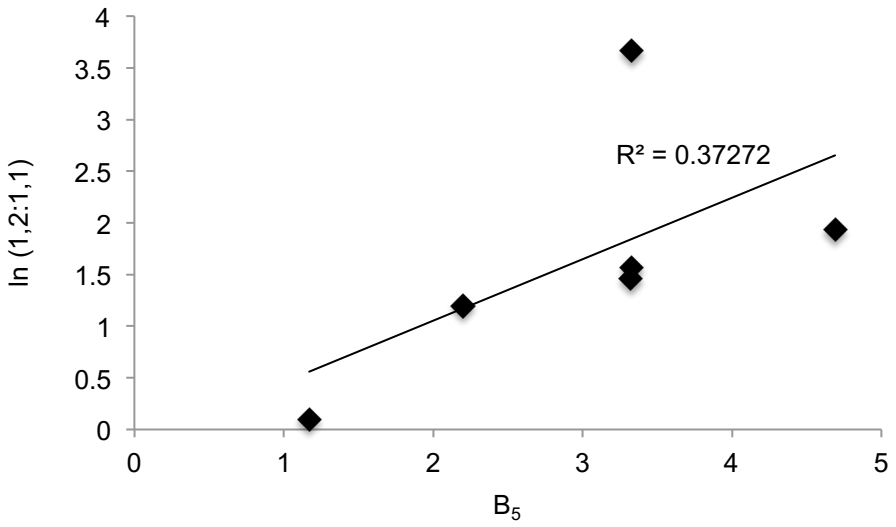

Figure 1.26 Correlation with Sterimol B_5.

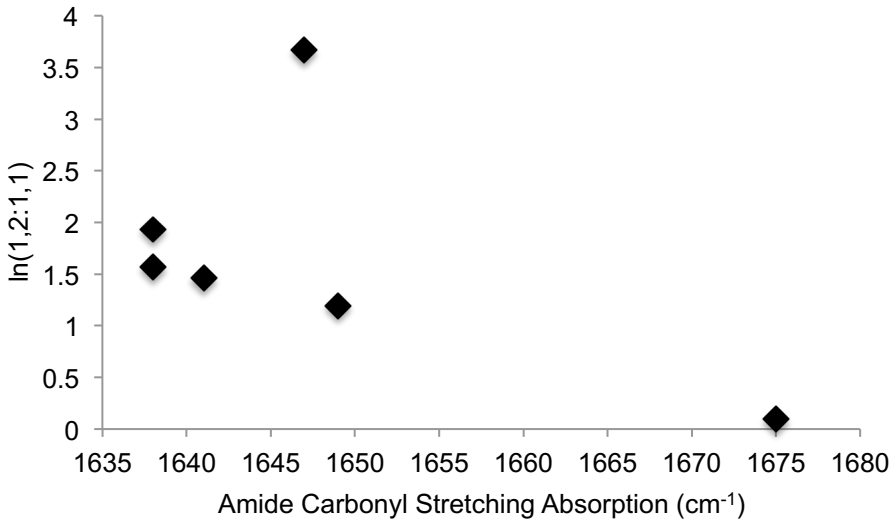

Figure 1.27 Correlation with Amide Carbonyl Stretching Absorption.[74]

[74] The amide carbonyl IR stretching absorption for **2b** was obtained from: Lewis, F. D.; Elbert, J. E.; Upthagrove, A. L.; Hale, P. D. *J. Org. Chem.* **1991**, *56,* 553–561.

Chapter 2

Stoichiometric Studies of Iodoarene Difluorides

2.1 Introduction

Despite the growing popularity of hypervalent iodine catalysis in synthetic chemistry, mechanistic studies of aryliodine(III)-promoted reactions have been extremely limited. Existing mechanistic hypotheses have been predominantly informed by computational analysis.[1] In the case of the iodoarene difluoride-catalyzed difluorination reactions developed in our group, mechanistic study has been hampered by the presence of corrosive HF-pyridine in large quantities, the biphasic nature of the reaction medium, and the necessity of including the

[1] For representative computational studies of fluorinative hypervalent iodine-promoted reactions, see: (a) Zhou, B.; Yan, T.; Xue, X.-S.; Cheng, J.-P. *Org. Lett.* **2016**, *18*, 6128–6131. (b) Ulmer, A.; Brunner, C.; Arnold, A. M.; Pöthig, A.; Gulder, T. *Chem. –Eur. J.* **2016**, *22*, 3660–3664. (c) Yan, T.; Zhou, B.; Xue, X.-S.; Cheng, J.-P. *J. Org. Chem.* **2016**, *81*, 9006–9011. (d) Zhou, B.; Xue, X.-S.; Cheng, J.-P. *Tetrahedron Lett.* **2017**, *58*, 1287–1291. (e) Zhou, B.; Haj, M. K.; Jacobsen, E. N.; Houk, K. N.; Xue, X.-S. *J. Am. Chem. Soc.* **2018**, *140*, 15206–15218.

stoichiometric oxidant *m*CPBA, which generates insoluble byproducts as it turns over catalyst over the course of the reaction. Development of methodology for preparing the key iodoarene difluoride intermediate free of HF-pyridine and *m*CPBA and for carrying out stoichiometric studies of the difluorination reaction under homogeneous conditions could potentially provide important new insights into the mechanism of this transformation. This chapter describes efforts towards (1) the efficient synthesis of chiral iodoarene difluorides, and (2) the development of a 1,2-difluorination reaction of alkenes using stoichiometric quantities of these compounds. Section 2.2 reviews methods reported in the literature for the synthesis of iodoarene difluorides. In section 2.3, we report the synthesis of chiral iodoarene difluorides with xenon difluoride. Sections 2.4 and 2.5 describe the stoichiometric use of these chiral iodoarene difluorides to accomplish the 1,2-difluorination of alkenes under the biphasic HF-pyridine/dichloromethane conditions employed in the catalytic reaction as well as under novel, HF-free conditions.

2.2 Synthesis of Iodoarene Difluorides

Three general approaches have been developed for the synthesis of iodoarene difluorides: (1) deoxyfluorination of an iodosylarene, (2) ligand exchange at a tricoordinate iodine(III) center, and (3) direct oxidative addition to an aryl iodide using strong fluorinating reagents.[2]

The deoxyfluorination approach requires the preparation of iodosylarenes, which can be synthesized from aryl iodides by perborate oxidation to form a diacetoxy derivative, followed by basic hydrolysis. Alternatively, basic hydrolysis to an iodosylarene can proceed from the iodoarene dichloride, which can be prepared by reaction of an aryl iodide with chlorine gas. Treatment of freshly prepared iodosylarenes with aqueous HF forms the corresponding

[2] For a detailed review of the synthesis and properties of iodoarene difluorides and other polyvalent iodine compounds, see: Zhdankin, V. V. *Hypervalent Iodine Chemistry: Preparation, Structure, and Synthetic Applications of Polyvalent Iodine Compounds.* John Wiley and Sons, Ltd: Chichester, West Sussex, **2014**.

iodoarene difluorides (Scheme 2.1). The groups of Wirth and Hara have employed this strategy to prepare *para*-iodotoluene difluoride in high yields.[3] However, because iodoarene difluorides are hygroscopic and susceptible to hydrolysis, isolating them from a reaction mixture containing aqueous HF poses a challenge. The highly acidic reaction medium also presents a limitation in cases where the substrate contains acid-sensitive functionality.

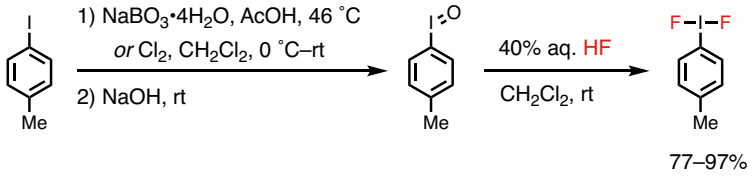

Scheme 2.1 Synthesis of $ArIF_2$ via deoxyfluorination of iodosylarenes with aq. HF.

A milder approach for the conversion of iodosylarenes to iodoarene difluorides developed by Yagupolskii, Lyalin, and coworkers relies on sulfur tetrafluoride as the fluoride source (Scheme 2.2).[4] Sulfur tetrafluoride, a highly toxic and corrosive gas, may be inconvenient for use on a laboratory scale. However, because this method employs a gaseous reagent and volatile solvent, the iodoarene difluoride product may be isolated straightforwardly by evaporation of the volatile reaction components under anhydrous conditions. In addition, this method does not require acidic reaction conditions, allowing its extension to more complex and sensitive substrates.

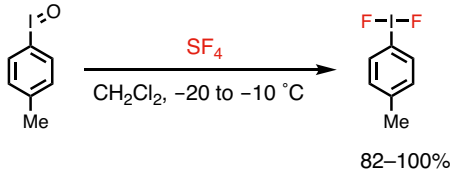

Scheme 2.2 Synthesis of $ArIF_2$ via deoxyfluorination of iodosylarenes with SF_4.

[3] (a) Arrica, M. A.; Wirth, T. *Eur. J. Org. Chem.* **2005**, 395–403. (b) Sawaguchi, M.; Ayuba, S.; Hara, S. *Synthesis* **2002**, *13*, 1802–1803.

[4] Lyalin, V. V.; Orda, V. V.; Alekseeva, L. A.; Yagupolskii, L. M. *Zhurnal Organicheskoi Khimii* **1970**, *6*, 329.

Carpenter pioneered a classical method for the preparation of iodoarene difluorides by ligand exchange. In his method, treatment of iodoarene dichlorides in dichloromethane with aqueous HF in the presence of yellow mercuric oxide yields iodoarene difluorides (Scheme 2.3).[5] Similar to previously described methods, the use of aqueous HF presents an obstacle to product isolation; however, Carpenter demonstrated that the dichloromethane phase of the reaction mixture solubilizes the product and can be used directly to difluorinate styrenes. While this method can be used to convert a variety of iodoarene dichlorides to their corresponding difluorides, its use of an excess of toxic mercuric oxide to sequester chloride ions from the solution is a serious disadvantage.

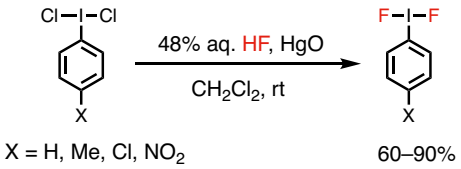

Scheme 2.3 Carpenter's method for synthesis of $ArIF_2$ from $ArICl_2$ via ligand exchange.

An alternative ligand exchange approach, developed by DiMagno and coworkers, starts from iodoarene diacetates.[6] In this method, treatment of phenyliodine(III) diacetate (PIDA) in acetonitrile with two equivalents of anhydrous TBAF yields iodobenzene difluoride quantitatively (Scheme 2.4).[7] This protocol does not offer any means for isolation of the iodoarene difluoride from solution.

[5] Carpenter, W. *J. Org. Chem.* **1966**, *31*, 2688–2689.

[6] Sun, H.; Wang, B.; DiMagno, S. G. *Org. Lett.* **2008**, *10*, 4413–4416.

[7] Commercial sources of TBAF contain water. Anhydrous TBAF can be prepared via nucleophilic aromatic substitution of hexafluorobenzene with tetrabutylammonium cyanide in aprotic solvents at low temperature. See: Sun, H.; DiMagno, S. G. *J. Am. Chem. Soc.* **2005**, *127*, 2050–2051.

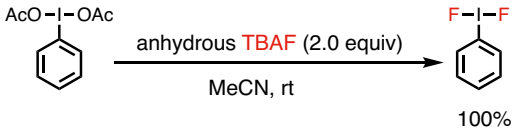

Scheme 2.4 Synthesis of $ArIF_2$ from $ArI(OAc)_2$ via ligand exchange.

Dutton and coworkers have demonstrated the generation of iodobenzene difluoride via ligand exchange on Weiss's reagent ($[PhI(pyridine)_2][OTf^-]_2$).[8] Treatment of Weiss's reagent with potassium fluoride in the presence of the potassium chelating agent 18-crown-6 resulted in rapid formation of iodobenzene difluoride (Scheme 2.5). The authors also showed that a variety of M–F complexes display similar reactivity with Weiss's reagent.

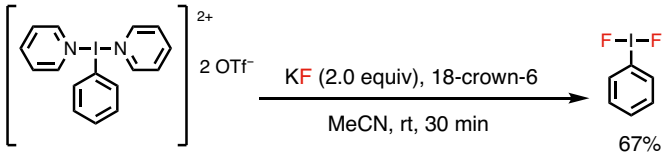

Scheme 2.5 Synthesis of $ArIF_2$ from Weiss's reagent via ligand exchange.

Shreeve and coworkers have developed a synthesis of iodoarene difluorides employing direct oxidation with Selectfluor (Figure 2.1).[9] A unique feature of their approach is that it uses molecular iodine and an arene as starting materials, rather than beginning with an aryl iodide.[10] Consequently, the scope of this approach is limited to electron-rich arenes, with the best results obtained for arenes bearing multiple alkyl groups that direct the site of iodination.

[8] Albayer, M.; Sharp-Bucknall, L.; Withanage, N.; Armendariz-Vidales, G.; Hogan, C. F.; Dutton, J. L. *Inorg. Chem.* **2020**, *59*, 2765–2770.

[9] Ye, C.; Twamley, B.; Shreeve, J. M. *Org. Lett.* **2005**, *7*, 3961–3964.

[10] Iodination of sterically hindered alkyl-substituted benzenes with elemental iodine can be mediated with Selectfluor. See: Stavber, S.; Kralj, P.; Zupan, M. *Synthesis* **2002**, 598–600.

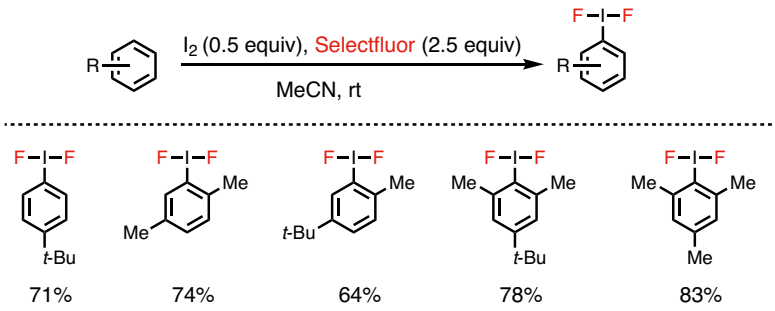

Figure 2.1 Shreeve and coworkers's method for synthesis of $ArIF_2$ by treatment of arenes with I_2 and Selectfluor.

Shreeve and coworkers also explored the direct oxidation of iodobenzene and *para*-iodotoluene to their corresponding iodoarene difluorides with Selectfluor. While NMR monitoring of these reactions indicated that they proceeded quantitatively, isolated yields were low (Scheme 2.6). The authors note that addition of trace quantities of triethylamine trihydrofluoride prior to workup improved isolated yields; they speculate that HF stabilizes the iodoarene difluoride product.[11]

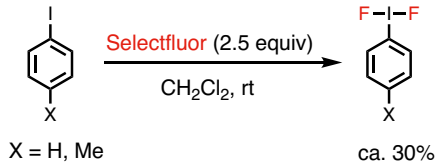

Scheme 2.6 Shreeve and coworkers's method for synthesis of $ArIF_2$ by treatment of ArI with Selectfluor.

Building on these reports, the Gilmour group has developed an efficient protocol for preparing *para*-iodotoluene difluoride using Selectfluor and an additional fluoride source.[12] In direct contrast to observations in the literature, Gilmour and coworkers note that, in their hands, treatment of *p*-iodotoluene with Selectfluor resulted in incomplete conversion to *para*-

[11] The authors did not provide isolated yields obtained using this protocol.

[12] Sarie, J. C.; Thiehoff, C.; Mudd, R. J.; Daniliuc, C. G.; Kehr, G.; Gilmour, R. *J. Org. Chem.* **2017**, *82*, 11792–11798.

iodotoluene difluoride. However, addition of a second fluoride source resulted in improved conversions. After surveying a variety of reaction conditions and fluoride sources, the authors concluded that optimal results were obtained upon treatment of *p*-iodotoluene in acetonitrile with large excesses of Selectfluor and cesium fluoride.[13] They proceeded to examine the scope of the reaction under these conditions (Figure 2.2). Arenes bearing highly electron-withdrawing groups were challenging to oxidize using this method, with conversions after 48 h of ca. 10–15%. Conversion of electron-rich and mildly electron-deficient aryl iodides to their corresponding iodoarene difluorides proceeded much more efficiently. However, the authors comment that the most electron-rich products (derived from *p*-OBn and *p*-OMe iodobenzene) were unstable and could not be isolated.

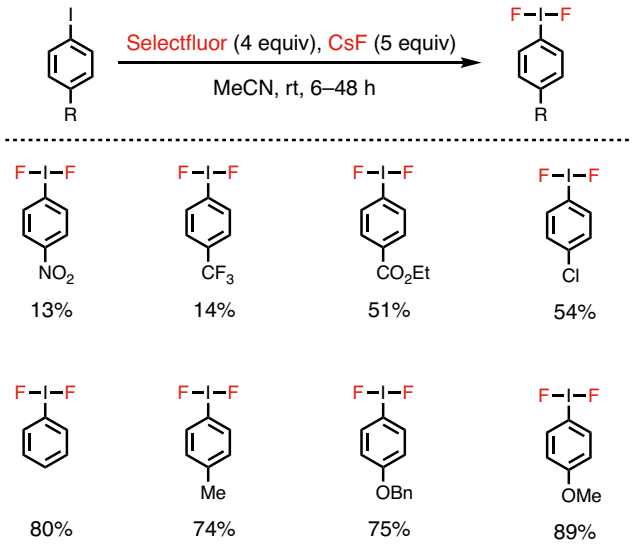

Figure 2.2 Gilmour and coworkers's method for synthesis of $ArIF_2$ by treatment of ArI with Selectfluor and CsF.

[13] The highest conversions were achieved with substoichiometric triethylamine trihydrofluoride as the fluoride source. To avoid the hazards of HF reagents, the authors tested other fluoride sources. They found that while TBAF•$3H_2O$ decomposed Selectfluor and shut down conversion, LiF successfully promoted the reaction, and the more soluble CsF gave conversions comparable to those achieved with triethylamine trihydrofluoride.

Togni and coworkers found that treatment of *ortho*-substituted, electron-deficient aryl iodides with trichloroisocyanuric acid (TCICA) and potassium fluoride led to formation of iodoarene difluorides in good yields (Scheme 2.7).[14] Importantly, *meta*- and *para*-substituted iodoarene difluorides could not be isolated using this approach; instead, oxidation of aryl iodides lacking an *ortho* substituent resulted in formation of $ArIF_4$ compounds. The authors propose that the *ortho* substituent hinders further oxidation of iodine(III) to iodine(V), resulting in the observed substitution-pattern-controlled access to each of these oxidation states.

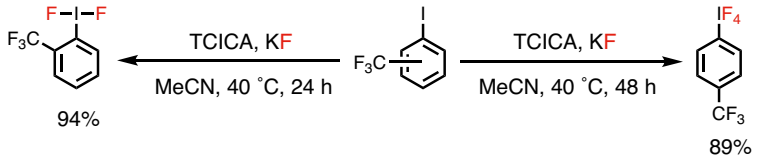

Scheme 2.7 Togni and coworkers's method for synthesis of $ArIF_2$ and $ArIF_4$ by treatment of ArI with TCICA and KF. The oxidation state accessed is controlled by the arene substitution pattern.

The powerful fluorinating reagent xenon difluoride (XeF_2) directly oxidizes aryl iodides to their corresponding iodoarene difluorides.[15] Treatment of a variety of simple aryl iodides with XeF_2 in the presence of anhydrous HF results in clean conversion to the iodoarene difluoride (Scheme 2.8). In some cases, no HF additive is required to promote the reaction, as has been demonstrated in the synthesis of some heteroaromatic iododifluorides with XeF_2.[16] Because xenon gas is the only byproduct generated in this reaction, this method is uniquely suitable for preparation and isolation of pure iodoarene difluorides.

---

[14] Häfliger, J.; Pitts, C. R.; Bornemann, D.; Käser, R.; Santschi, N.; Charpentier, J.; Otth, E.; Trapp, N.; Verel, R.; Lüthi, H. P.; Togni, A. *Chem. Sci.* **2019**, *10*, 7251–7259.

[15] (a) Zupan, M.; Pollak, A. *J. Fluorine Chem.* **1976**, *7*, 445–447. (b) Gregorčič, A.; Zupan, M. *Bull. Chem. Soc. Jpn.* **1977**, *50*, 517–520.

[16] Abo-Amer, A.; Frohn, H.-F.; Steinberg, C.; Westphal, U. *J. Fluorine Chem.* **2006**, *127*, 1311–1323.

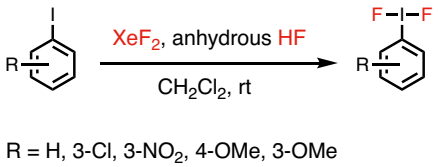

Scheme 2.8 Synthesis of $ArIF_2$ via direct oxidation with XeF_2.

2.3 Synthesis of Chiral Iodoarene Difluorides with Xenon Difluoride

Because of our interest in using chiral iodoarene difluorides for stoichiometric mechanistic studies, we aimed to develop a method of preparation that would allow us to isolate the desired compounds free of any contaminants introduced during their synthesis. Methods employing XeF_2 seemed well suited to this purpose, and so we initiated our efforts by attempting to prepare an iodoarene difluoride using XeF_2 as the oxidant and iodobenzene (**1a**) as a model substrate (Scheme 2.9). We found that at room temperature in dichloromethane solvent, **1a** cleanly converted to iodobenzene difluoride (**2a**). The reaction rate was highly concentration-dependent. Unlike in many previously reported examples of iodoarene difluoride synthesis with XeF_2, no HF additive was required to promote oxidation.

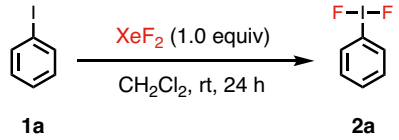

Scheme 2.9 Oxidation of iodobenzene (**1a**) with XeF_2.

We proceeded to apply these conditions to the oxidation of chiral aryl iodide catalyst **1b**. We found that iodoarene difluoride **2b** can be generated cleanly and quantitatively in dichloromethane by using XeF_2 as a stoichiometric oxidant (Scheme 2.10). Full consumption of XeF_2 requires a reaction time of ca. 26 h. Importantly, the stability of the product in

dichloromethane solution is limited; NMR monitoring shows that if the reaction mixture is allowed to stand for longer than 26 h, the concentration of product in solution slowly diminishes.

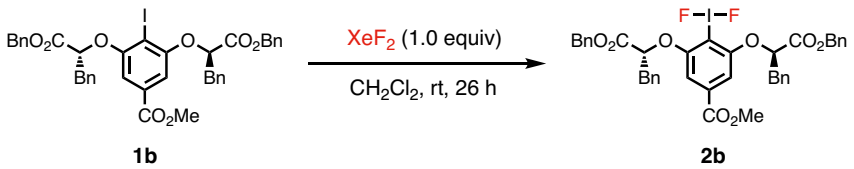

Scheme 2.10 Oxidation of catalyst **1b** with XeF_2.

Due to its high cost and proclivity for directly fluorinating alkenes, XeF_2 is not an attractive alternative fluoride source or oxidant for use in catalytic alkene fluorination.[17] However, it is an ideal reagent for stoichiometric generation of the key iodoarene difluoride intermediate. Because the only byproduct of its reaction with aryl iodide is xenon gas, the resulting iodoarene difluoride can either be used directly as a freshly prepared solution in dichloromethane, or it can be isolated by simple solvent evaporation.

2.4 Stoichiometric 1,2-Difluorination in Biphasic HF-Pyridine/Dichloromethane

Having developed a method for independently preparing the iodoarene difluoride that the catalytic reaction generates *in situ*, we aimed to evaluate the stoichiometric reactivity of this species. We began by running the stoichiometric reaction between cinnamamide **3** and iodoarene difluoride **2b** in a biphasic mixture of HF-pyridine and dichloromethane (Scheme 2.11). Using the same proportion of HF-pyridine to dichloromethane that proved optimal in the catalytic reaction, **3** cleanly converted to 1,2-difluoride **4**, with a small amount of the 1,1-difluoride **5**

[17] We attempted to develop a catalytic, HF-free difluorination reaction of substrate **3** using 20 mol % aryl iodide **1b**, stoichiometric XeF_2 as the oxidant, and hexafluoroisopropanol (HFIP) as the solvent (for discussion of stoichiometric reaction development in HFIP, see Section 2.5 of this thesis). The diastereoselectivity of the reaction under these conditions suffered due to a strong XeF_2-mediated background reaction that favored *syn* 1,2-difluorination. Efforts to outcompete this background reaction by modulating temperature or by slow addition of oxidant or substrate were unsuccessful. The highest d.r. achieved was 1.2 : 1.0 (favoring the *syn* diastereomer), and the highest e.e. achieved for the *anti* 1,2-difluoride product was 45%.

resulting from aryl migration also formed. The 1,2-difluoride **4** was produced in 97% e.e., closely matching the 96% e.e. obtained in the catalytic reaction of the same substrate.

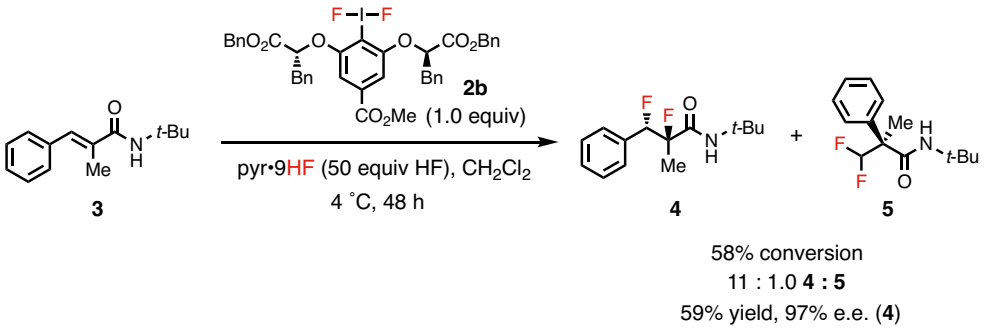

Scheme 2.11 Reaction between **3** and stoichiometric **2b** in biphasic HF-pyridine/dichloromethane.

Most of the catalytic fluorination reactions developed in our group require a large excess of HF-pyridine to proceed efficiently, resulting in biphasic reaction mixtures. The role of each phase of the reaction mixture in the catalytic cycle has remained unclear. With the ability to prepare and isolate the key iodoarene difluoride intermediate, we endeavored to explore its reactivity in each phase of the catalytic reaction mixture separately. To generate the two phases, HF-pyridine and dichloromethane were stirred vigorously for 30 min. After separation of the layers, the reaction between cinnamamide substrate **3** and stoichiometric **2b** was attempted in each layer: a dichloromethane layer presumed to be saturated in HF-pyridine, and an HF-pyridine layer presumed to be saturated in dichloromethane.

No reaction took place in the dichloromethane phase (Scheme 2.12A). In the HF-pyridine phase, however, difluorination proceeded to give results that closely matched those observed in the stoichiometric reaction run under biphasic conditions (compare Scheme 2.12B and Scheme 2.11). These results indicate that for the catalytic difluorination of cinnamamides, the steps involving substrate fluorination likely occur in the HF-pyridine layer. While the dichloromethane

phase may play a role in other portions of the catalytic cycle, such as aryl iodide oxidation, it does not promote the fluoroiodination and subsequent reaction of cinnamamide substrates.

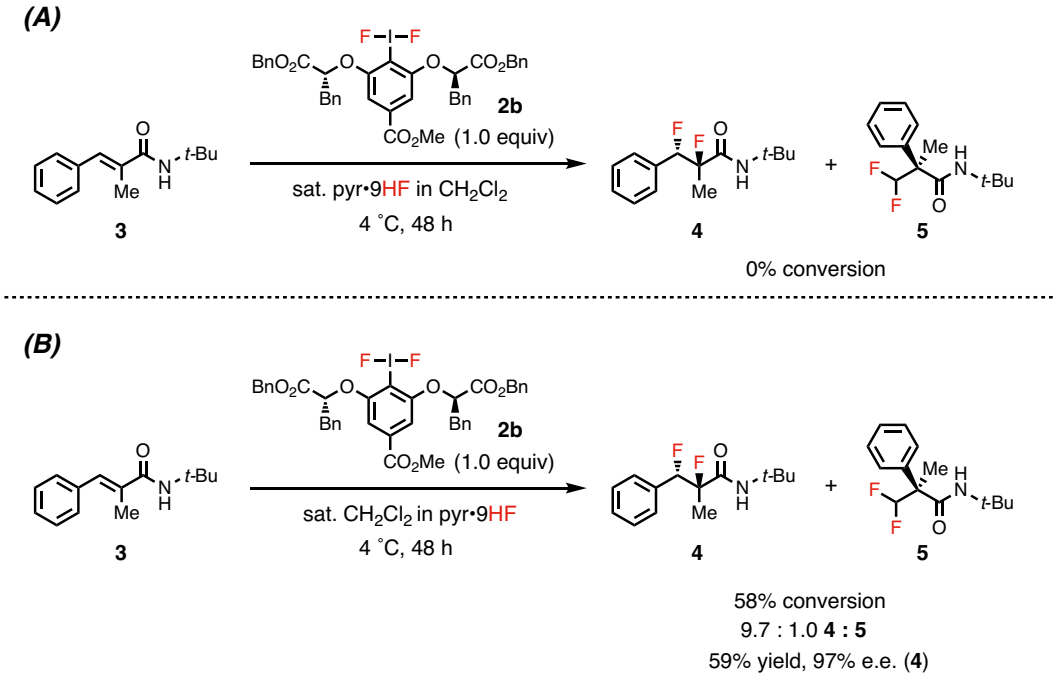

Scheme 2.12 Reaction between **3** and stoichiometric **2b** in each phase of the reaction mixture. (A) Reaction in the dichloromethane layer. (B) Reaction in the HF-pyridine layer.

We also found that the stoichiometric difluorination reaction proceeds in neat HF-pyridine (Scheme 2.13). However, conversions and yields were lower in this reaction, and 1,2-product selectivity was poor. These results suggest that, while the dichloromethane phase itself does not appear to play a role in the substrate fluorination portion of the catalytic cycle, the presence of dichloromethane in the HF-pyridine layer may be significant.

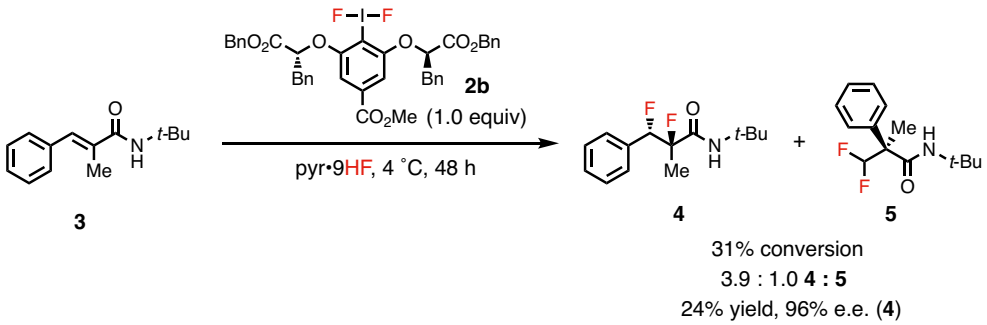

Scheme 2.13 Reaction between **3** and stoichiometric **2b** in neat HF-pyridine.

Notably, the stoichiometric reactions described here produce lower ratios of 1,2-difluoride to 1,1-difluoride than the catalytic reaction of the same substrate. As described in Chapter 1, the ratio of HF to amine has been found to have a significant impact on product ratios.[18] We found that this parameter also influenced product ratios in the stoichiometric reaction: doping in pyridine to reach an HF : amine ratio of 4.5 : 1.0 increased the product ratio from ca. 10 : 1.0 to 33 : 1.0 (Scheme 2.14). Added pyridine may attenuate the acidity of the HF layer and enhance the nucleophilicity of fluoride. While this result suggests that the stoichiometric reaction is responsive to the same parameters that affect product ratio in the catalytic reaction, it does not account for the original observation of unusually low product ratios in the stoichiometric reaction.

[18] See also: Scheidt, F.; Schäfer, M.; Sarie, J.; Daniliuc, C.; Molloy, J.; Gilmour, R. *Angew. Chem., Int. Ed.* **2018**, *57*, 16431–16435.

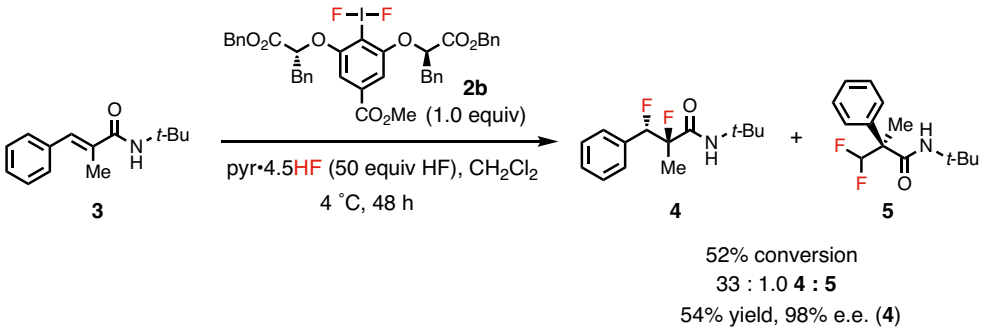

Scheme 2.14 Reaction between **3** and stoichiometric **2b** in biphasic HF-pyridine/dichloromethane with added pyridine.

A key difference between the catalytic reaction and the stoichiometric reaction is the absence of *m*CPBA in the stoichiometric reaction. Specifically, the catalytic reaction employs commercially available *m*CPBA without purification, even though commercial sources of *m*CPBA are only ca. 77% pure and contain large quantities of water. We hypothesized that, similarly to amine additives, water may attenuate the acidity of the HF-pyridine phase, thereby affecting product ratio. Doping in an equivalent of water confirmed that water does indeed shift the product ratio towards 1,2-difluoride (Scheme 2.15).

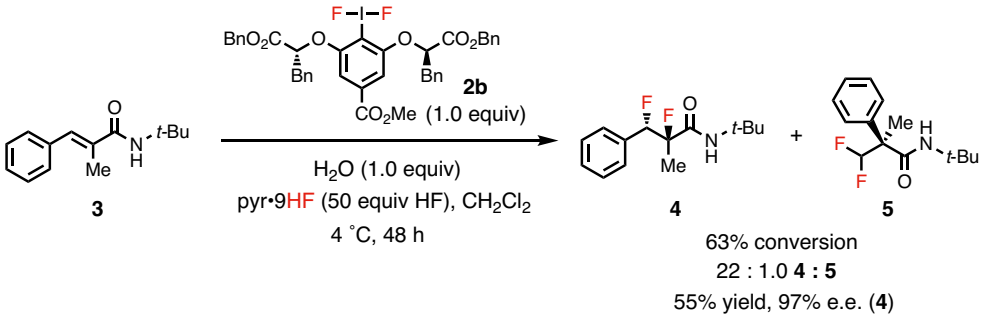

Scheme 2.15 Reaction between **3** and stoichiometric **2b** in biphasic HF-pyridine/dichloromethane with added water.

As previously described, we have observed that at lower HF loadings, higher ratios of 1,2- to 1,1-difluoride are obtained. Together, these data suggest a plausible interpretation for the

dependence of product ratio on HF-pyridine loading in the catalytic difluorination of cinnamamides. In these reactions, a fixed quantity of *m*CPBA is added to the reaction mixture, carrying with it a fixed quantity of water. It is plausible that the water introduced in this manner partitions exclusively into the highly polar HF-pyridine layer of the biphasic reaction mixture. When a large volume of HF-pyridine is used, this additional water content would not be expected to dramatically affect the composition of the HF-pyridine layer. However, if a smaller volume of HF-pyridine is used, the quantities of water introduced with *m*CPBA could be sufficient to significantly attenuate the acidity of the HF-pyridine layer.

An additional way in which stoichiometric reaction outcomes deviate from observations of the catalytic reaction is that the yields of the stoichiometric reaction are low (ca. 55–60% compared to ca. 80% in the catalytic reaction). Because conversion and yield track closely in the stoichiometric reaction run in biphasic HF-pyridine/dichloromethane, substrate decomposition or diversion into byproducts does not account for the low yields. However, we hypothesized that decomposition of the iodoarene difluoride may take place under the reaction conditions. To probe this catalyst decomposition hypothesis, we preincubated iodoarene difluoride **2b** in a stirred mixture of HF-pyridine and dichloromethane at 4 ˚C for 24 h, then added substrate and stirred the reaction mixture for an additional 24 h (Scheme 2.16). At the end of this process, no 1,2-difluoride product **4** could be detected, and no consumption of starting material had taken place. These results are consistent with iodoarene difluoride degradation under the reaction conditions.

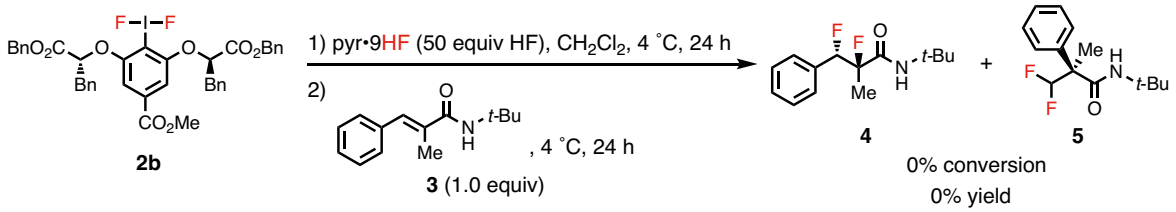

Scheme 2.16 Preincubation of **2b** in biphasic HF-pyridine/dichloromethane followed by stoichiometric reaction with **3**.

We performed a single-turnover experiment using 0.2 equiv of iodoarene difluoride **2b** to determine if catalyst degradation is operative under these conditions (Scheme 2.17). Substrate conversion in this experiment (19%) closely matched the 20 mol % catalyst loading used in the experiment, suggesting a competition between a difluorination pathway that is ordered in substrate **3** and a catalyst degradation pathway that is not.

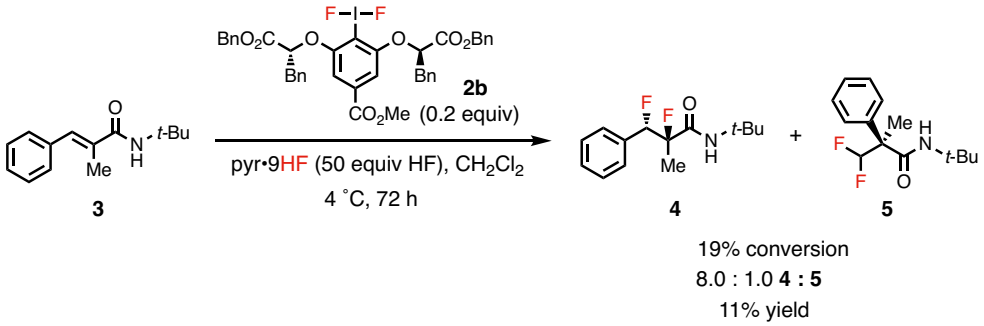

Scheme 2.17 Single-turnover experiment in biphasic HF-pyridine/dichloromethane.

2.5 Stoichiometric, HF-Free 1,2-Difluorination

Our initial stoichiometric studies in biphasic HF-pyridine/dichloromethane indicated that in the catalytic reaction, HF serves not only as a fluoride source for generation of the iodoarene difluoride, but also as the phase in which difluorination of the substrate takes place. Having developed a method for independently preparing the iodoarene difluoride without using HF-pyridine, we aimed to determine if this species could be activated under HF-free conditions to

react with alkenes. These studies could provide critical insights into the requirements for achieving alkene fluorination and aid in development of catalytic conditions that minimize or eliminate the use of HF. In addition, the ability to perform the stoichiometric, enantiodetermining step under HF-free, homogeneous conditions might enable future kinetic studies.

Brønsted and Lewis acids have been shown to enhance the reactivity of aryl-λ^3-iodanes. Cotter and coworkers demonstrated that trichloroacetic acid catalyzes the chlorination of alkenes with iodobenzene dichloride.[19] Shafir and coworkers have investigated the role of boron trifluoride diethyl etherate in the activation of PIDA using computational modeling, spectroscopic studies, and X-ray crystallography.[20] In both cases, activation is proposed to involve coordination of the acid to a ligand on iodine(III). Presumably, this mode of activation could also apply to the activation of iodoarene difluorides by HF observed in our work.

Table 2.1 Solvent effects in the hypervalent iodine-promoted arene azidation developed by Kita and coworkers.

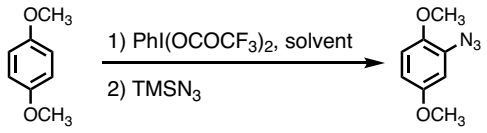

entry	solvent	yield (%)
1	HFIP	68
2	TFE	60
3	MeCN	27
4	CH_2Cl_2	5

[19] Cotter, J. L.; Andrews, L. J.; Keefer, R. M. *J. Am. Chem. Soc.* **1962**, *84*, 793–797.

[20] Izquierdo, S.; Essafi, S.; del Rosal, I.; Vidossich, P.; Pleixats, R.; Vallribera, A.; Ujaque, G.; Lledós, A.; Shafir, A. *J. Am. Chem. Soc.* **2016**, *138*, 12747–12750.

A number of reports have demonstrated the utility of hexafluoroisopropanol (HFIP) as a solvent in iodine(III)-promoted reactions. In their development of an azidation of aromatic compounds promoted by phenyliodine(III) bis(trifluoroacetate) and trimethylsilyl azide, Kita and coworkers found that satisfactory yields could only be achieved with HFIP or trifluoroethanol (TFE) as the reaction solvent (Table 2.1).[21] This approach was later extended to include acetate and β-dicarbonyl compounds as nucleophiles.[22] The proposed mechanism for these transformations involves generation of aryl radical cations, which HFIP, a highly polar but poorly nucleophilic solvent, may be uniquely suited to stabilize.

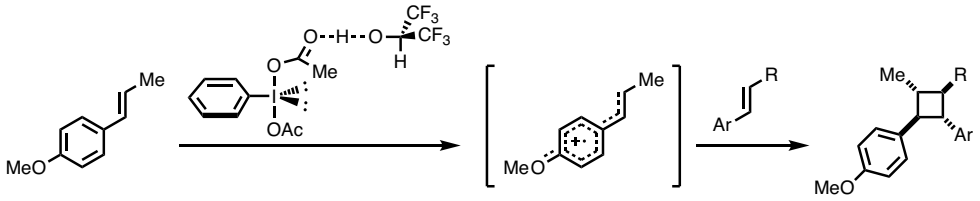

Scheme 2.18 Dimerization of styrenes developed by Donohoe and coworkers. The reaction is catalyzed by PIDA and is proposed to involve formation of a hydrogen-bonded adduct between PIDA and HFIP.

Fluoroalcohol solvents have also found application in a variety of other hypervalent iodine-promoted transformations. Kita and coworkers developed hypervalent iodine-catalyzed oxidative couplings that give optimal results in HFIP or TFE solvent.[23] In their development of oxidative rearrangements promoted by (poly)cationic hypervalent iodine reagents, Wengryniuk and coworkers found a blend of HFIP and dichloromethane to be the optimal solvent

[21] Kita, Y.; Tohma, H.; Inagaki, M.; Hatanaka, K.; Yakura, T. *Tetrahedron Lett.* **1991**, *32*, 4321–4324.

[22] Kita, Y.; Tohma, H.; Hatanaka, K.; Takada, T.; Fujita, S.; Mitoh, S.; Sakurai, H.; Oka, S. *J. Am. Chem. Soc.* **1994**, *116*, 3684–3691.

[23] (a) Ito, M.; Kubo, H.; Itani, I.; Morimoto, K.; Dohi, T.; Kita, Y. *J. Am. Chem. Soc.* **2013**, *135*, 14078–14081. (b) Morimoto, K.; Sakamoto, K.; Ohshika, T.; Dohi, T.; Kita, Y. *Angew. Chem. Int. Ed.* **2016**, *55*, 3652–3656.

combination for the ring expansion of alcohols to form seven- and eight-membered cyclic acetals.[24] Donohoe and coworkers have reported that PIDA catalyzes the dimerization of electron-rich styrenes (Scheme 2.18).[25] No reaction took place in conventional solvents; reactivity was only observed in HFIP and, to a lesser degree, in TFE. In a collaborative study, the Donohoe and Compton laboratories investigated the role of HFIP in this transformation.[26] Contrary to the conventional explanation that HFIP owes its unique utility in hypervalent iodine oxidation reactions to its ability to stabilize radical cation and other highly polar intermediates, the new study proposed that HFIP enhances the oxidizing ability of PIDA by hydrogen bonding to the acetate ligands on iodine. Using cyclic voltammetry, the authors showed that reduction of PIDA is significantly more facile in HFIP than in acetonitrile. The authors also presented MS data and NMR studies, including NOE and DOSY experiments, to support the proposal that HFIP and PIDA form a hydrogen-bonded adduct.

A recent report demonstrates the ability of HFIP to activate hypervalent fluoroiodane reagents.[27] Stuart and coworkers found that use of HFIP as the solvent enabled the fluoroiodane-promoted fluorination of 1,3-ketoesters without inclusion of an HF-amine additive (Scheme 2.19A). In addition, this reagent combination effected the fluorocyclization of unsaturated carboxylic acids without transition metals (Scheme 2.19B). The authors propose that HFIP activates the fluoroiodane via formation of a hydrogen-bonded adduct.

---

[24] (a) Kelley, B. T.; Walters, J. C.; Wengryniuk, S. E. *Org. Lett.* **2016**, *18*, 1896–1899. (b) Walters, J. C.; Tierno, A. F.; Dubin, A. H.; Wengryniuk, S. E. *Eur. J. Org. Chem.* **2018**, 1460–1464.

[25] Colomer, I.; Barcelos, R. C.; Donohoe, T. J. *Angew. Chem. Int. Ed.* **2016**, *55*, 4748–4752.

[26] Colomer, I.; Batchelor-McAuley, C.; Odell, B.; Donohoe, T. J. Compton, R. G. *J. Am. Chem. Soc.* **2016**, *138*, 8855–8861.

[27] Minhas, H. K.; Riley, W.; Stuart, A. M.; Urbonaite, M. *Org. Biomol. Chem.* **2018**, *16*, 7170–7173.

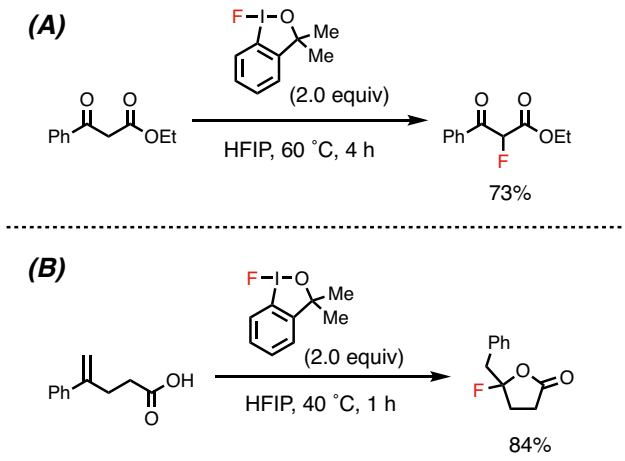

Scheme 2.19 (A) Fluorination of 1,3-ketoesters with a fluoroiodane in HFIP, developed by Stuart and coworkers. (B) Fluorocyclization of unsaturated carboxylic acids with a fluoroiodane in HFIP, developed by Stuart and coworkers.

We found that the iodoarene difluoride intermediate **2b** can be generated by treatment of **1b** with XeF_2 in HFIP , and that addition of cinnamamide substrate **3** to the resulting solution forms the desired 1,2-difluoride **4** (Scheme 2.20). This stoichiometric reaction takes place under HF-free, homogeneous conditions and proceeds with high 1,2-chemoselectivity and enantioselectivity slightly exceeding that obtained in the catalytic system employing *m*CPBA and biphasic HF-pyridine/dichloromethane.[28] This observation suggests that the stoichiometric reaction in HFIP proceeds through the same mechanism that is operative in the catalytic reaction.

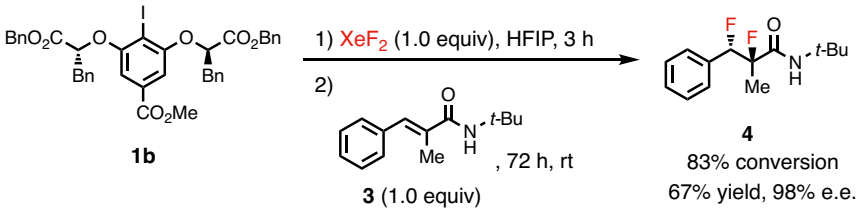

Scheme 2.20 Reaction between between **3** and stoichiometric **2b** in HFIP.

[28] The ratio of 1,2-difluoride to 1,1-difluoride obtained for stoichiometric reactions in HFIP is >100 : 1.0.

We aimed to use our newly developed conditions for HF- and oxidant-free 1,2-difluorination of cinnamamides with stoichiometric iodoarene difluorides to probe the *para*-ester catalyst effect observed in previous work. In reactions requiring high HF-pyridine loadings, the presence of an ester or other highly electron-withdrawing substituent *para* to the iodine substituent on a chiral resorcinol-derived catalyst is essential for obtaining high enantioselectivity. However, chiral aryl iodides lacking a *para*-ester substituent serve as highly enantioselective catalysts for some reactions that proceed at lower HF loadings. We have attributed this effect to catalyst degradation that takes place to a significant degree at high HF loadings but not at lower HF loadings.[29] To test this hypothesis, we prepared the iodoarene difluorides of representative chiral aryl iodides **1b–e**. After performing the stoichiometric reaction of each iodoarene difluoride with **3** in HFIP, we compared the enantiomeric enrichment of 1,2-difluoride product **4** obtained by this method to that obtained in the catalytic reaction with HF-pyridine/*m*CPBA (Figure 2.3). In the catalytic reaction with HF-pyridine/*m*CPBA, use of catalyst **1c** gave products with ca. 50% lower e.e. than when using catalyst **1b**. However, in the stoichiometric reaction in HFIP use of both catalysts gave products with 98% e.e.[30] Catalysts **1d** and **1e** also displayed this pattern; under the catalytic conditions, *para*-ester-bearing catalyst **1d** afforded product with much higher enantioselectivity than catalyst **1e**, but in HFIP, their corresponding iodoarene difluorides promoted the reaction with similar levels of enantioselectivity. This experiment confirms the hypothesis that the *para*-ester substituent does not change the catalyst's inherent enantioselectivity, but rather renders the catalyst more resistant to degradation pathways that are competitive under high HF loadings.

[29] Section 1.4 of this thesis provides a more detailed description of this effect and relevant references.

[30] Catalyst **1c** reacted vigorously with XeF_2 and showed extreme susceptibility to decomposition upon treatment with XeF_2. To mitigate these problems, the oxidation was conducted at 4 ˚C, and substrate was added within 30 min of beginning the oxidation. Nevertheless, this reaction afforded very low yields of **4**.

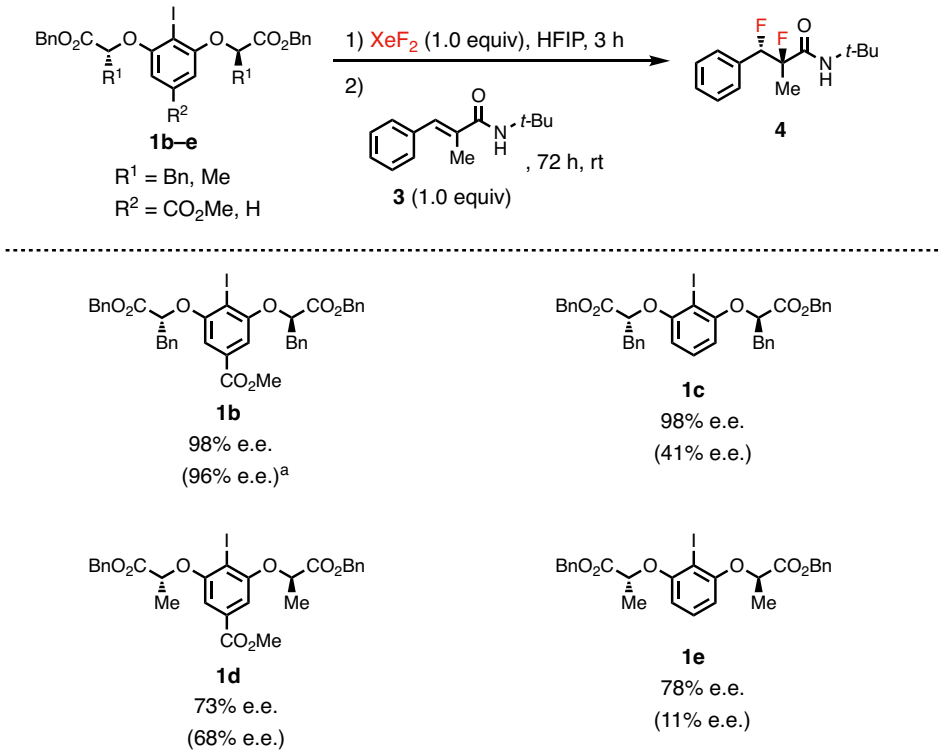

Figure 2.3 Comparison of 1,2-difluoride e.e. obtained in stoichiometric vs. catalytic reactions. Stoichiometric reactions were conducted on a 0.10 mmol scale. Results from catalytic reaction are shown in parentheses. Unless otherwise noted, catalytic reactions were conducted on a 0.10 mmol scale with 5.6 equiv HF-pyridine. [a]Catalytic reaction conducted on 1.00 mmol scale.

While the stoichiometric reaction between iodoarene difluoride **2b** and cinnamamide **3** initially gave promising results, subsequent attempts to replicate these results revealed that yields were irreproducible and that conversions exceeded yields by 15–30% (Scheme 2.21).[31] In order to use this reaction to study the mechanism of the catalytic reaction, reproducibility would need to be established, and any byproducts formed in the reaction would need to be accounted for and characterized. The remainder of this section focuses on efforts to achieve these aims as well as to explore other conditions for HF-free, stoichiometric 1,2-difluorination.

[31] Fluorination reactions of other substrates with stoichiometric chiral iodoarene difluorides suffered from low yields to an even greater extent (see Experimental Information).

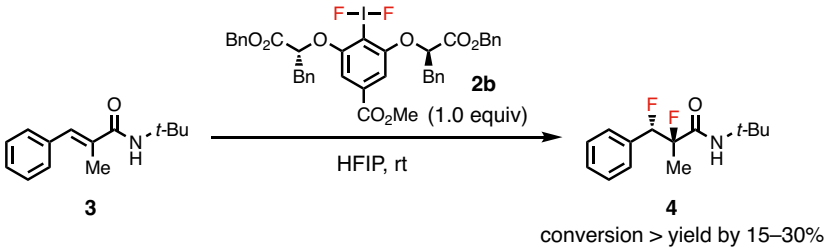

Scheme 2.21 Discrepancy between conversion and yield in the reaction between between **3** and stoichiometric **2b** in HFIP.

The known sensitivity of iodoarene difluorides and the hygroscopicity of HFIP prompted us to investigate water as a potential culprit for the poor reproducibility of the stoichiometric difluorination in HFIP and the discrepancies between conversion and yield observed in this reaction. Addition of two equivalents of water to the stoichiometric reaction of **3** resulted in significantly diminished alkene conversion and 1,2-difluoride yield (Scheme 2.22A). However, using rigorously dried HFIP in the reaction did not resolve the conversion vs. yield discrepancy, nor did running the reaction under air-free and moisture-free conditions in a glovebox (Scheme 2.22B).

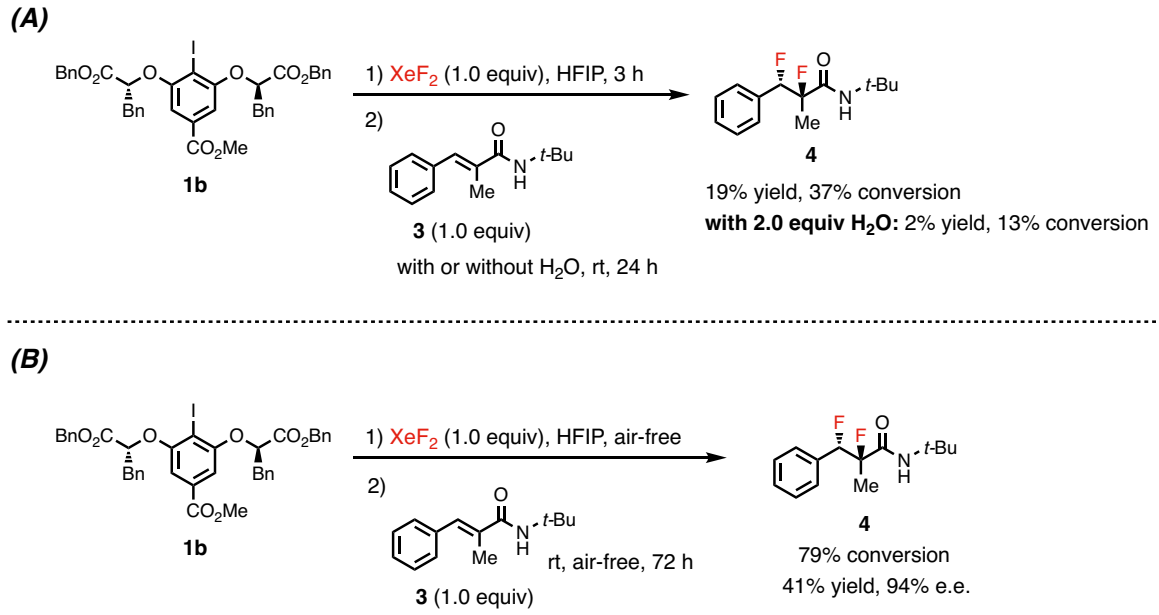

Scheme 2.22 (A) Reaction between **3** and stoichiometric **2b** in HFIP with and without added water. (B) Reaction between **3** and stoichiometric **2b** in HFIP under air- and moisture-free conditions in a glovebox.

Next, we considered the possibility that HFIP may be a non-innocent participant in the reaction, resulting in unproductive consumption of substrate. We surveyed a variety of other additives to determine if compounds other than HFIP could activate iodoarene difluorides to promote the 1,2-difluorination reaction more cleanly (Table 2.2). Nonafluoro-*tert*-butyl alcohol gave results comparable to those obtained with HFIP, while TFE failed to promote the desired reaction altogether (entries 1–2). While stronger acids such as trifluoroacetic acid and boron trifluoride diethyl etherate were competent to activate the iodoarene difluoride towards reaction with the substrate, reactions using these acids afforded product in lower yields and enantioselectivities than did the reaction in HFIP; in addition, both reactions show a large discrepancy between conversion of substrate and yield of product (entries 3–4).

Table 2.2 Survey of non-HF additives for promoting 1,2-difluorination of 3 with stoichiometric 2b.

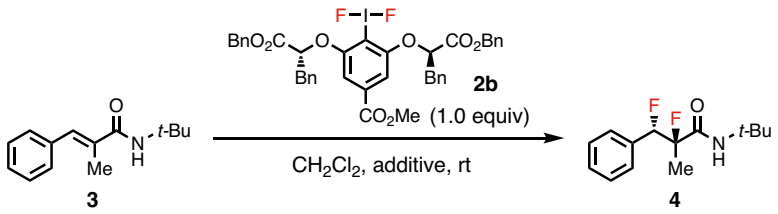

entry	additive	conversion (%)	yield of **4** (%)	e.e. (%)
1[a]	nonafluoro-*tert*-butyl alcohol	67	47	98
2[a]	TFE	–	0	–
3	TFA	78	24	96
4	BF_3•Et_2O	43	28	91

[a] Reaction run in neat additive with no CH_2Cl_2.

To aid in identification of any discrete byproducts formed in the reaction, we performed the stoichiometric reaction with fluorinated substrate **5** (Scheme 2.23). Use of a fluorinated substrate allowed us to track formation of 1,2-difluoride **6** and any additional products by monitoring the aryl fluoride region of the ^{19}F NMR spectrum. While multiple fluorinated byproducts were observed by ^{19}F NMR, collectively they account for only ca. 10% of the starting material added; this suggests that decomposition pathways such as oligomerization may be taking place.

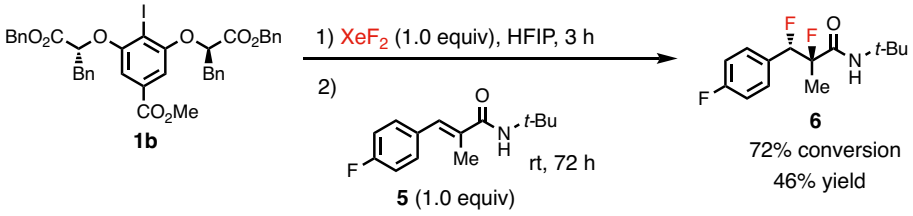

Scheme 2.23 Reaction between fluorinated substrate **5** and stoichiometric **2b** in HFIP.

We performed a single-turnover experiment using 0.2 equiv of iodoarene difluoride **2b** to determine if substrate conversion to the desired product proceeds more cleanly when an excess

of substrate is present (Scheme 2.24). While substrate conversion in this experiment was equivalent to catalyst loading, the yield of 1,2-difluoride **4** obtained was far below the theoretical maximum of 20%. This data suggests that the discrepancies between conversion and yield observed in the stoichiometric reaction in HFIP result at least in part from iodoarene difluoride-mediated, undesired substrate consumption pathways.

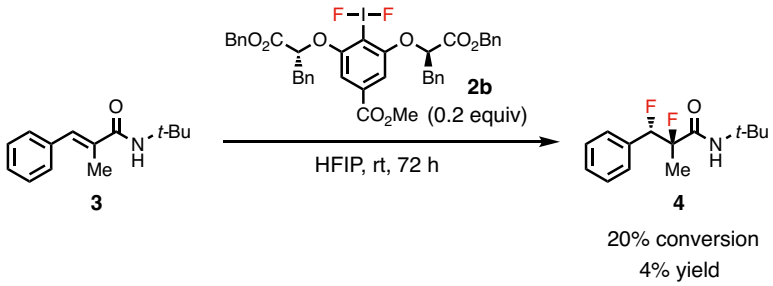

Scheme 2.24 Single-turnover experiment in HFIP.

2.6 Conclusions and Outlook

Iodoarene difluorides are generated *in situ* as key intermediates in aryl iodide-catalyzed fluorination reactions. We have developed a method for preparing these compounds independent of the HF-pyridine/*m*CPBA reagent combination employed to access them catalytically, instead using XeF_2 to directly oxidize chiral aryl iodides to their corresponding iodoarene difluorides. When used stoichiometrically in biphasic HF-pyridine/dichloromethane or in the HF-pyridine layer alone, these compounds recapitulate their catalytic reactivity. Studies performed in these systems have provided preliminary insight into the reasons that many of the catalytic fluorination reactions developed in our group require large excesses of HF. In addition, we have discovered that HF is not an essential component for promoting the reaction between an iodoarene difluoride and an alkene. The stoichiometric reaction between a chiral iodoarene difluoride and a cinnamamide substrate in HFIP yields the 1,2-difluoride product with very high

enantioselectivity. After additional optimization and characterization, kinetic studies of this stoichiometric, homogeneous reaction could be undertaken, potentially yielding mechanistic insights into aryl iodide-catalyzed fluorination that would have been challenging to obtain through study of the heterogeneous catalytic system.

2.7 Experimental Information

2.7.1 General Experimental Procedures and Note of Caution

General Experimental Procedures

All reactions for the preparation of substrates and catalysts were performed in standard, dry glassware fitted with rubber septa under an inert atmosphere of nitrogen unless otherwise described. All difluorination reactions were performed in polyethylene tubes sealed with a high density polyethylene cap under an atmosphere of air. Stainless steel gas-tight syringes or cannulae were used to transfer air- and moisture-sensitive liquids. Reported concentrations refer to solution volumes at room temperature. Concentration of organic solutions under reduced pressure was performed using house vacuum (ca. 40 mm Hg) at 30 ºC. Column chromatography was performed with SiliaFlash® P60 (40-63μm, 60 Å) silica gel from Silicycle. Thin layer chromatography (TLC) was used for reaction monitoring, and product detection was performed using pre-coated glass plates covered with 0.20 mm silica gel with fluorescent indicator; plates were visualized by exposure to UV light (λ = 254 nm) or by staining with potassium permanganate or ninhydrin.

Note of Caution

Pyridine•9HF is a corrosive and toxic substance that will corrode glassware. Safe handling can be conducted with plastic syringes and metal needles, with $NaHCO_3$ (aq.) or NaOH (aq.) employed to quench excess HF. Though reactions should not be conducted in glassware when employing pyridine•9HF, glassware may be used to quench reactions provided sufficient quantities of base are present. Always handle pyridine•9HF while wearing gloves and in a fume

hood. As a precautionary measure, have calcium gluconate gel nearby and apply immediately and liberally on skin exposed to pyridine•9HF.

Xenon difluoride is a corrosive and toxic substance that will corrode glassware. Always handle XeF_2 while wearing gloves and in a fume hood. Do not use weigh paper; instead, add XeF_2 to a tared PTFE container inside a fume hood and weigh the capped container.

2.7.2 Materials and Instrumentation

Materials

Reagents were purchased in reagent grade from commercial suppliers and used as received, unless otherwise described. Anhydrous solvents (benzene, dichloromethane, diethyl ether, *N, N*-dimethylformamide, tetrahydrofuran, and toluene) were prepared by passing the solvent through an activated alumina column. Triethylamine and diisopropylethylamine were distilled over calcium hydride at atmospheric pressure. Hexafluoroisopropanol was dried over molecular sieves or distilled over CaH_2 prior to use.

Instrumentation

Proton nuclear magnetic resonance (^{1}H NMR) spectra were recorded on an Inova-500 spectrometer, are reported in parts per million downfield from tetramethylsilane, and are referenced to the residual protium resonances of the NMR solvent ($CDCl_3$: 7.26 [$CHCl_3$], acetone-d6: 2.05 [acetone-d5], DMSO-d6: 2.50 [DMSO-d5]). Proton-decoupled carbon-13 nuclear magnetic resonance (13C {1 H} NMR) spectra were recorded on an Inova-500 spectrometer, are reported in parts per million downfield from tetramethylsilane, and are referenced to the carbon resonances of the NMR solvent (CDCl3: 77.23, acetone-d6: 29.92, DMSO-d6: 39.61). Chemical shifts for fluorine-19 nuclear magnetic resonance (19F NMR) were recorded on an Inova-500 spectrometer, are reported in parts per million downfield from chlorotrifluoromethane, and are referenced to the fluorine resonance of chlorotrifluoromethane ($\delta = 0$). Data are represented as follows: chemical shift, multiplicity (br = broad, s = singlet, d = doublet, t = triplet, q = quartet, quin = quintet, sept = septet, m = multiplet), coupling constants in Hertz (Hz), integration.

Chiral GC analysis was performed using an Agilent 7890A GC system using commercially available columns. Chiral HPLC analysis was performed using an Agilent 1200 series quaternary HPLC system using commercially available CHIRALCEL analytical columns (4.6 x 250 mm).

2.7.3 Preparation of Iodoarene Difluorides

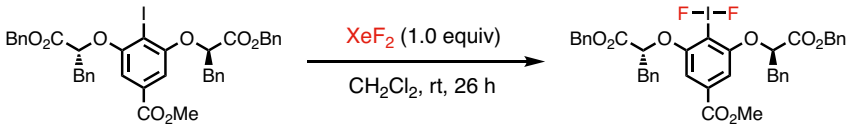

1b **2b**

Method A: To a solution of aryl iodide **1b** (231 mg, 0.30 mmol) in dichloromethane (900 µL) was added XeF_2 (51 mg, 0.30 mmol). After briefly mixing with a vortex mixer until XeF_2 was fully dissolved, the solution was allowed to stand until ^{1}H NMR indicated complete consumption of XeF_2 had taken place (ca. 26 h). The resulting yellow solution containing **2b** could be used directly, or **2b** could be isolated as a fluffy white or pale yellow solid by concentration of the solution under reduced pressure.

^{1}H NMR (500 MHz, CD_2Cl_2) δ 7.44 – 7.26 (m, 20H), 7.23 (s, 2H), 5.30 – 5.26 (m, 2H), 5.24 – 5.17 (m, 4H), 3.88 (s, 3H), 3.55 – 3.46 (m, 4H); ^{19}F NMR (470.4 MHz, CD_2Cl_2) δ -167.0 (s, 2F).

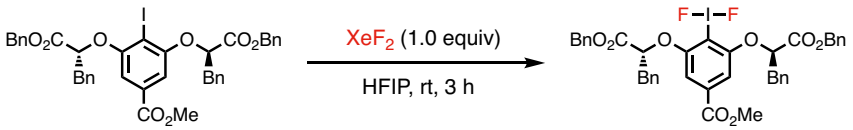

1b **2b**

Method B: To a solution of aryl iodide **1b** (77 mg, 0.10 mmol) in HFIP (250 µL) was added XeF_2 (17 mg, 0.10 mmol). After briefly mixing with a vortex mixer until XeF_2 was fully dissolved, the solution was allowed to stand for 3 h. The resulting bright yellow solution containing **2b** could be used directly, or **2b** could be isolated as a fluffy white or pale yellow solid by concentration of the solution under reduced pressure.

^{1}H NMR (500 MHz, CD_2Cl_2) δ 7.44 – 7.26 (m, 20H), 7.23 (s, 2H), 5.30 – 5.26 (m, 2H), 5.24 – 5.17 (m, 4H), 3.88 (s, 3H), 3.55 – 3.46 (m, 4H); ^{19}F NMR (470.4 MHz, CD_2Cl_2) δ -167.0 (s, 2F).

2.7.4 Difluorination with Stoichiometric Iodoarene Difluorides in HF-Pyridine/ Dichloromethane

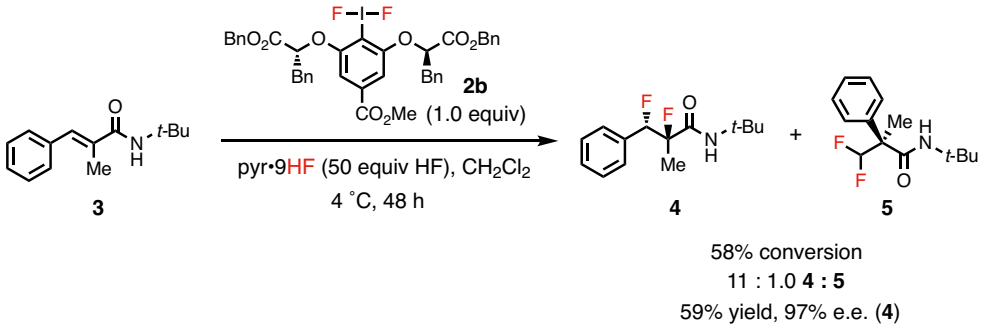

*Difluorination of **3** with Stoichiometric **2b** in HF-Pyridine/Dichloromethane:* To a polyethylene conical tube equipped with a stir bar was added a solution of iodoarene difluoride **2b** in dichloromethane (200 μL, 0.50 M) prepared using Method A. The solution was cooled to –78 ˚C, and cinnamamide substrate **3** (22 mg, 0.10 mmol) was added. Pyridinium poly(hydrogen fluoride) (130 μL) was added via syringe. The tube was sealed, and the mixture was warmed to 4 ˚C and stirred for 48 h. The reaction mixture was then diluted with dichloromethane and poured slowly into a slurry of basic alumina in dichloromethane at -78 ˚C. The resulting slurry was warmed to room temperature with stirring, filtered, and concentrated under reduced pressure. The crude product mixture was analyzed by ^{19}F NMR, with 1-fluorooctane used as an internal standard to determine the yield of product. The product ratio was determined by ^{19}F NMR, and the enantiomeric excess of **4** was determined by chiral GC (β-Cyclosil, 40 → 200 ˚C, 1.5 ˚/min, 14 psi).

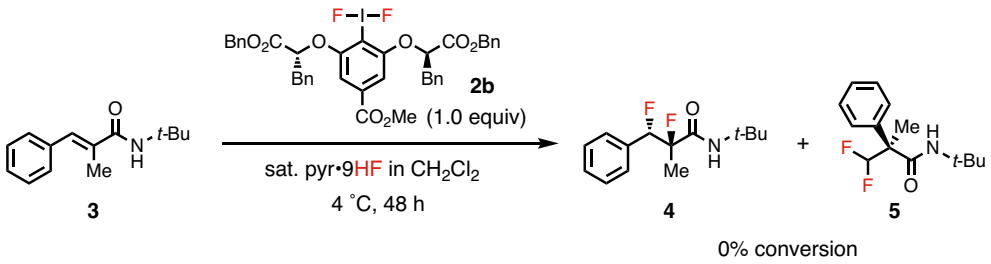

*Difluorination of **3** with Stoichiometric **2b** in the Dichloromethane Layer:* To a polyethylene conical tube equipped with a stir bar was added dichloromethane (600 μL). Pyridinium poly(hydrogen fluoride) (390 μL) was added via syringe, and the mixture was stirred for 30 min. After the stirring was stopped and the mixture was allowed to settle, a portion of the dichloromethane layer (200 μL) was withdrawn by syringe and added to a polyethylene conical tube in a –78 ˚C bath and containing a stir bar and iodoarene difluoride **2b** (81 mg, 0.10 mmol) isolated using Method A. Cinnamamide substrate **3** (22 mg, 0.10 mmol) was added, the tube was sealed, and the mixture was warmed to 4 ˚C and stirred for 48 h. The resulting slurry was warmed to room temperature with stirring, filtered, and concentrated under reduced pressure. The crude product mixture was analyzed by ^{19}F NMR, with 1-fluorooctane used as an internal standard to determine the yield of product.

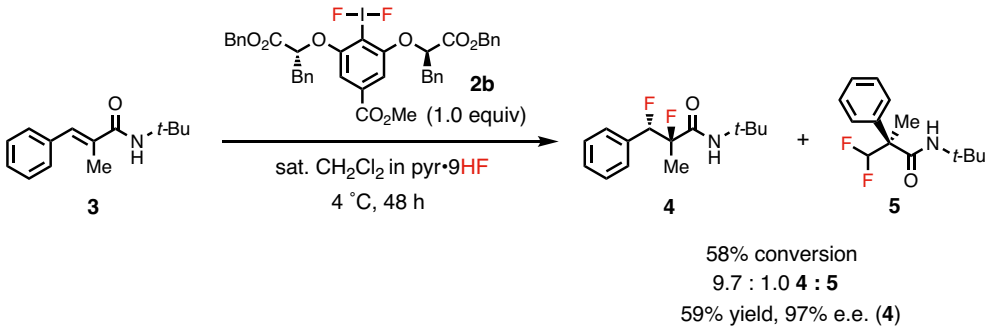

*Difluorination of **3** with Stoichiometric **2b** in the HF-Pyridine Layer:* To a polyethylene conical tube equipped with a stir bar was added dichloromethane (600 µL). Pyridinium poly(hydrogen fluoride) (390 µL) was added via syringe, and the mixture was stirred for 30 min. After the stirring was stopped and the mixture was allowed to settle, a portion of the pyridinium poly(hydrogen fluoride) layer (130 µL) was withdrawn by syringe and added to a polyethylene conical tube in a –78 ˚C bath and containing a stir bar and iodoarene difluoride **2b** (81 mg, 0.10 mmol) isolated using Method A. Cinnamamide substrate **3** (22 mg, 0.10 mmol) was added, the tube was sealed, and the mixture was warmed to 4 ˚C and stirred for 48 h. The resulting slurry was warmed to room temperature with stirring, filtered, and concentrated under reduced pressure. The crude product mixture was analyzed by ^{19}F NMR, with 1-fluorooctane used as an internal standard to determine the yield of product. The product ratio was determined by ^{19}F NMR, and the enantiomeric excess of **4** was determined by chiral GC (β-Cyclosil, 40 → 200 ˚C, 1.5 ˚/min, 14 psi).

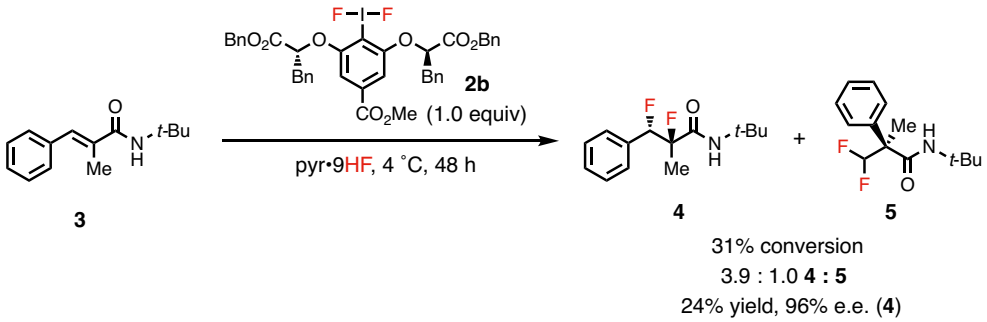

*Difluorination of **3** with Stoichiometric **2b** in Neat HF-Pyridine:* A polyethylene tube containing a stir bar and iodoarene difluoride **2b** (81 mg, 0.10 mmol) isolated using Method A was placed in a –78 ˚C bath. Pyridinium poly(hydrogen fluoride) (130 μL) was added via syringe, followed by cinnamamide substrate **3** (22 mg, 0.10 mmol). The tube was sealed, and the mixture was warmed to 4 ˚C and stirred for 48 h. The reaction mixture was then diluted with dichloromethane and poured slowly into a slurry of basic alumina in dichloromethane at -78 ˚C. The resulting slurry was warmed to room temperature with stirring, filtered, and concentrated under reduced pressure. The crude product mixture was analyzed by ^{19}F NMR, with 1-fluorooctane used as an internal standard to determine the yield of product. The product ratio was determined by ^{19}F NMR, and the enantiomeric excess of **4** was determined by chiral GC (β-Cyclosil, 40 → 200 ˚C, 1.5 ˚/min, 14 psi).

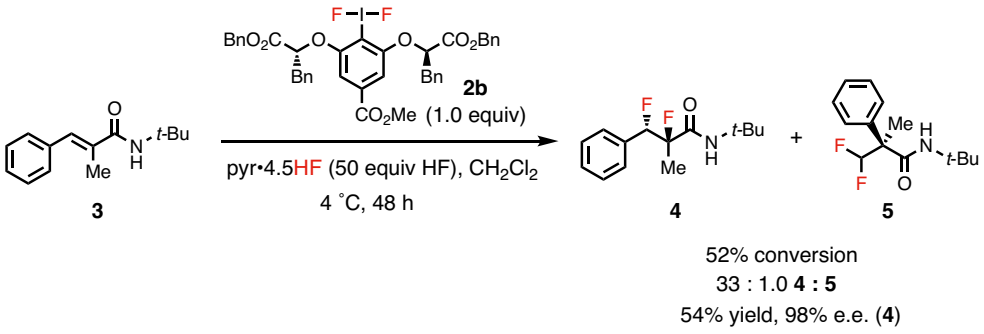

*Difluorination of **3** with Stoichiometric **2b** in HF-Pyridine/Dichloromethane with Added Pyridine:* To a polyethylene conical tube equipped with a stir bar was added a solution of iodoarene difluoride **2b** in dichloromethane (200 μL, 0.50 M) prepared using Method A. The solution was cooled to –78 ˚C, and pyridine (23 μL) was added, followed by addition of pyridinium poly(hydrogen fluoride) (130 μL) by syringe. Cinnamamide substrate **3** (22 mg, 0.10 mmol) was then added. The tube was sealed, and the mixture was warmed to 4 ˚C and stirred for 48 h. The reaction mixture was then diluted with dichloromethane and poured slowly into a slurry of basic alumina in dichloromethane at -78 ˚C. The resulting slurry was warmed to room temperature with stirring, filtered, and concentrated under reduced pressure. The crude product mixture was analyzed by ^{19}F NMR, with 1-fluorooctane used as an internal standard to determine the yield of product. The product ratio was determined by ^{19}F NMR, and the enantiomeric excess of **4** was determined by chiral GC (β-Cyclosil, 40 → 200 ˚C, 1.5 ˚/min, 14 psi).

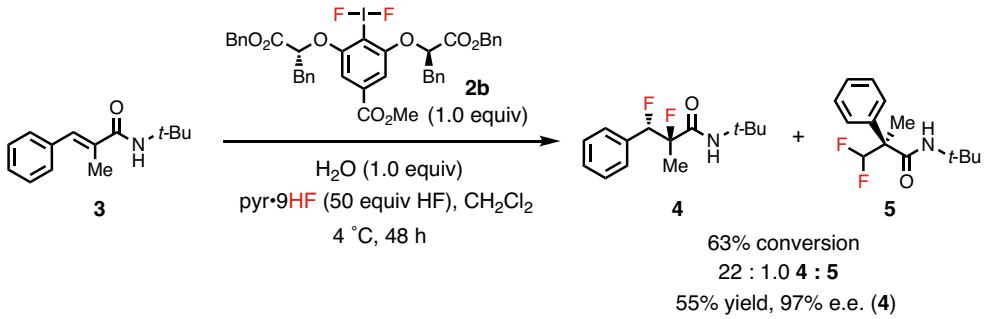

*Difluorination of **3** with Stoichiometric **2b** in HF-Pyridine/Dichloromethane with Added Water:* To a polyethylene conical tube equipped with a stir bar was added a solution of iodoarene difluoride **2b** in dichloromethane (200 μL, 0.50 M) prepared using Method A. The solution was cooled to –78 ˚C, and water (2 μL) was added, followed by cinnamamide substrate **3** (22 mg, 0.10 mmol). Pyridinium poly(hydrogen fluoride) (130 μL) was then added by syringe. The tube was sealed, and the mixture was warmed to 4 ˚C and stirred for 48 h. The reaction mixture was then diluted with dichloromethane and poured slowly into a slurry of basic alumina in dichloromethane at -78 ˚C. The resulting slurry was warmed to room temperature with stirring, filtered, and concentrated under reduced pressure. The crude product mixture was analyzed by ^{19}F NMR, with 1-fluorooctane used as an internal standard to determine the yield of product. The product ratio was determined by ^{19}F NMR, and the enantiomeric excess of **4** was determined by chiral GC (β-Cyclosil, 40 → 200 ˚C, 1.5 ˚/min, 14 psi).

2.7.5 Difluorination with Stoichiometric Iodoarene Difluorides in HFIP

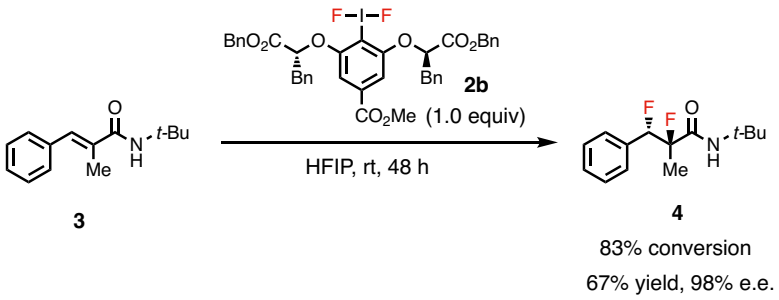

*Stoichiometric Difluorination using Iodoarene Difluoride **2b** in HFIP:* To a polyethylene conical tube equipped with a stir bar was added a solution of iodoarene difluoride **2b** in HFIP (250 μL, 0.40 M) prepared using Method B. Cinnamamide substrate **3** (22 mg, 0.10 mmol) was added, and the reaction mixture was stirred for 72 h. The reaction mixture was then concentrated under reduced pressure. The crude product mixture was analyzed by ^{1}H NMR, with nitrobenzene used as an internal standard to determine the yield of product. The enantiomeric excess of **4** was determined by chiral GC (β-Cyclosil, 40 → 200 ˚C, 1.5 ˚/min, 14 psi).

Comparison of 1,2-Difluoride e.e. Obtained in Stoichiometric vs. Catalytic Reactions

To a solution of aryl iodide **1b** or **1d–e** (0.10 mmol) in HFIP (200 μL) was added XeF_2 (17 mg, 0.10 mmol). After briefly mixing with a vortex mixer until XeF_2 was fully dissolved, the solution was allowed to stand for 1 h. Cinnamamide **3** (22 mg, 0.10 mmol) was added, and the reaction was stirred at rt for 24–48 h. The reaction mixture was concentrated under reduced pressure. The enantiomeric excess of **4** was determined by chiral GC (β-Cyclosil, 40 → 200 ˚C, 1.5 ˚/min, 14 psi).

To a polyethylene conical tube equipped with a stir bar was added XeF_2 (17 mg, 0.10 mmol) and HFIP (200 μL). After briefly mixing with a vortex mixer until XeF_2 was fully dissolved, the

solution was cooled to 4 ˚C. A solution of aryl iodide **1c** in HFIP (200 μL, 0.5 M) was added to the solution, which was then allowed to stand for 30 min at 4 ˚C. Cinnamamide **3** (22 mg, 0.10 mmol) was added, and the reaction was stirred at 4 ˚C. After 16 h, the solution had turned black. The reaction mixture was concentrated under reduced pressure. The enantiomeric excess of **4** was determined by chiral GC (β-Cyclosil, 40 → 200 ˚C, 1.5 ˚/min, 14 psi).

Stoichiometric Difluorination of Assorted Substrates using Iodoarene Difluoride ***2b*** *in HFIP:* To a polyethylene conical tube equipped with a stir bar was added a solution of iodoarene difluoride **2b** in HFIP (250 μL, 0.40 M) prepared using Method B. Alkene substrate (0.10 mmol) was added, and the reaction mixture was stirred at the specified temperature for the specified time period. The reaction mixture was then concentrated under reduced pressure. The crude product mixture was analyzed by ^{1}H NMR or ^{19}F NMR, with an internal standard used to determine the yield of product.

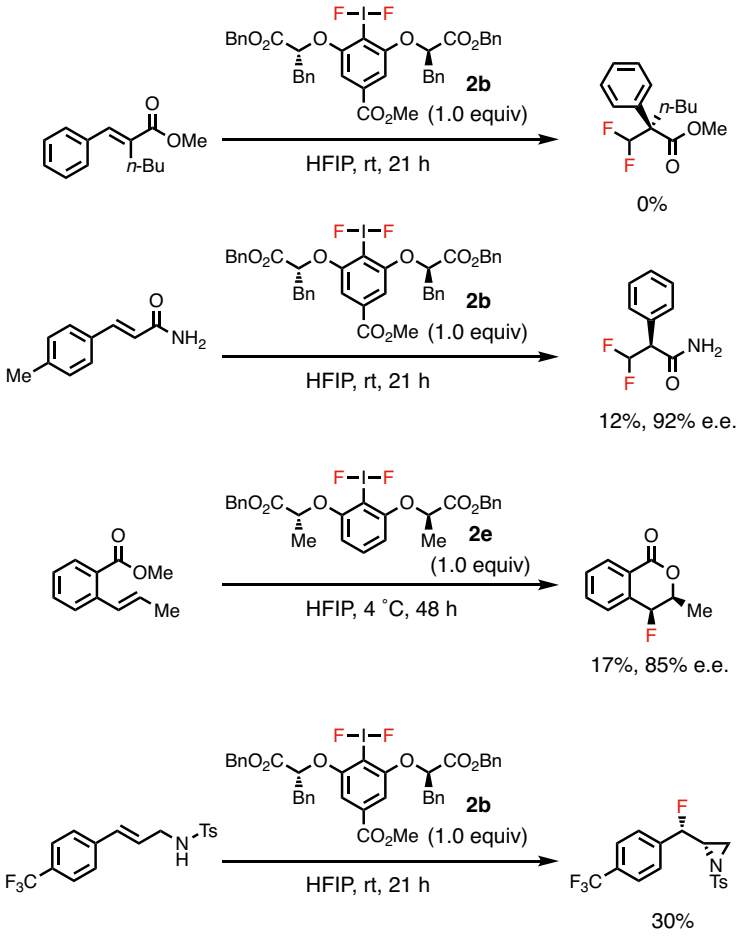

Scheme 2.25 Stoichiometric fluorination of assorted alkene substrates in HFIP.

Chapter 3

Studies Toward Electrocatalytic Difluorination of Alkenes

3.1 Introduction

Electrochemistry has long been known as a valuable technique for accomplishing redox chemistry on an industrial scale, with famous applications including the Chlor-alkali process for production of chlorine and sodium hydroxide, the Monsanto adiponitrile process, and the Simons electrochemical fluorination process.[1] More recently, electrochemistry has emerged as a

[1] (a) O'Brien, T. F.; Bommaraju, T. V.; Hine, F. *Handbook of Chlor-Alkali Technology*, Springer, **2005**. (b) Baizer, M. M.; Danly, D. E. *Chemtech.* **1980**, *10*, 161. (c) Simons, J. H. *J. Electrochem. Soc.* **1949**, *95*, 47–52.

powerful tool for use in synthetic organic methods development.[2] Electrochemistry obviates the need for stoichiometric oxidants and reductants and enables redox manipulations powered by sustainable energy sources. In addition, because the applied potential can be precisely controlled, electrochemical oxidation and reduction can aid in achieving the desired chemoselectivity in the presence of multiple redox-sensitive functional groups. Recent high-profile publications employing electrochemistry to accomplish organic transformations have inspired renewed enthusiasm for this approach in the synthetic community.[3]

We viewed electrochemical oxidation as an intriguing approach to generating iodoarene difluoride intermediates, and in this chapter, we report progress towards the application of this approach in the context of our group's catalytic fluorination chemistry.[4] Section 3.2 reviews precedent for the electrochemical generation of hypervalent iodine reagents and catalysts for mediating fluorination reactions. In Section 3.3, we report our efforts to develop an aryl iodide-catalyzed electrochemical difluorination of alkenes.

---

[2] For reviews of synthetic organic electrochemistry, see: (a) Moeller, K. D. *Tetrahedron* **2000**, *56*, 9572–9554. (b) Yoshida, J.; Kataoka, K.; Horcajada, R.; Nagaki, A. *Chem. Rev.* **2008**, *108*, 2265–2299. (c) Horn, E. J.; Rosen, B. R.; Baran, P. S. *ACS Cent. Sci.* **2016**, *2*, 302–308. (d) Yan, M.; Kawamata, Y.; Baran, P. S. *Chem. Rev.* **2017**, *117*, 13230–13319. (e) Yan, M.; Kawamata, Y.; Baran, P. S. *Angew. Chem. Int. Ed.* **2018**, *57*, 4149–4155. (f) Pletcher, D. *Electrochem. Commun.* **2018**, *88*, 1–4.

[3] For a selection of examples, see: (a) Xu, H.-C.; Moeller, K. D. *J. Am. Chem. Soc.* **2008**, *130*, 13542–13543. (b) Kirste, A.; Schnakenburg, G.; Stecker, F.; Fischer, A.; Waldvogel, S. R. *Angew. Chem. Int. Ed.* **2010**, *49*, 971–975. (c) Morofuki, T.; Shimizu, A.; Yoshida, J. *J. Am. Chem. Soc.* **2013**, *135*, 5000–5003. (d) Rosen, B. R.; Werner, E. W.; O'Brien, A. G.; Baran, P. S. *J. Am. Chem. Soc.* **2014**, *13s6*, 5571–5574. (e) Horn, E. J.; Rosen, B. R.; Chen, Y.; Tang, J.; Chen, K.; Eastgate, M. D.; Baran, P. S. *Nature* **2016**, *533*, 78–81. (f) Badalyan, A.; Stahl, S. S. *Nature* **2016**, *535*, 406–410. (g) Xiong, P.; Xu, H.-H.; Xu, H.-C. *J. Am. Chem. Soc.* **2017**, *139*, 2956–2959. (h) Fu, N.; Sauer, G. S.; Saha, A.; Loo, A.; Lin, S. *Science* **2017**, *357*, 575–579. (i) Sauer, G. S.; Lin, S. *ACS Catal.* **2018**, *8*, 5175–5187. (j) Peters, B. K.; Rodriguez, K. X.; Reisberg, S. H.; Beil, S. B.; Hickey, D. P.; Kawamata, Y.; Collins, M.; Starr, J.; Chen, L.; Udyavara, S.; Klunder, K.; Gorey, T. J.; Anderson, S. L.; Neurock, M.; Minteer, S. D.; Baran, P. S. *Science* **2019**, *363*, 838–845.

[4] This work was performed in collaboration with Thomas Keane and David Gygi in Daniel Nocera's laboratory at Harvard University.

3.2 Electrochemical Fluorination Reactions Mediated by Hypervalent Iodine

Due to their broad applicability, mild chemical properties, and straightforward synthetic accessibility, hypervalent iodine reagents have achieved widespread use as oxidants in synthetic chemistry. However, the efficient and environmentally benign reputation of these compounds is compromised to some extent by the stoichiometric chemical oxidants used to prepare them, such as *m*CPBA, Oxone, peracetic acid, hydrogen peroxide, or Selectfluor. Anodic oxidation represents an appealing alternative route to accessing these compounds in a direct fashion and without wasteful chemical oxidants. A number of reports have described the electrochemical generation of various hypervalent iodine reagents and their use as ex-cell or in-cell mediators in a broad range of reactions.[5]

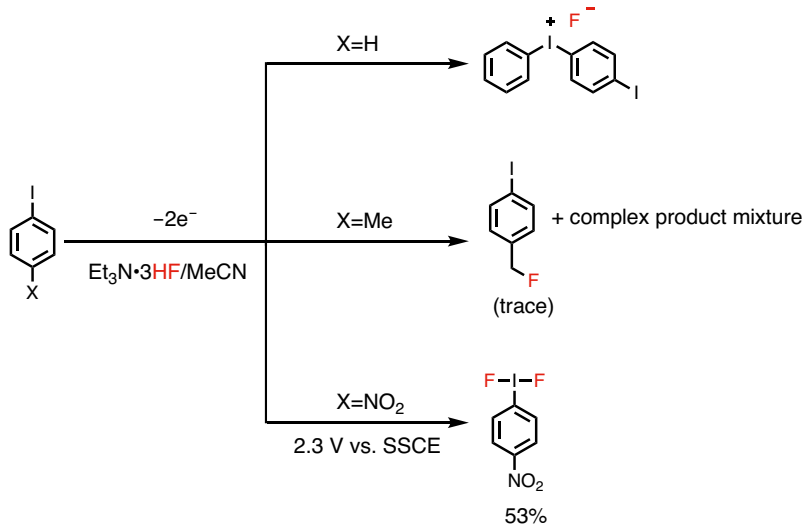

Scheme 3.1 Electrochemical oxidation of aryl iodides in $Et_3N•3HF$.

[5] For reviews, see: (a) Elsherbini, M.; Wirth, T. *Chem. Eur. J.* **2018**, *24*, 13399–13407. (b) Francke, R. *Curr. Opin. Electrochem.* **2019**, *15*, 83–88.

In 1960, Schmidt and Meinert reported that electrolysis of iodobenzene and silver fluoride in acetonitrile solution yielded iodobenzene difluoride.[6] However, Rozhkov found that this result could not be reproduced due to the poor conductivity exhibited by this solution.[7] Fuchigami and coworkers attempted to use triethylamine trihydrofluoride as an alternative fluoride source and achieved mixed results (Scheme 3.1).[8] Neither iodobenzene nor *p*-iodotoluene underwent oxidation to the aryl iodide difluoride, instead forming dimeric iodonium salts, off-target fluorination products, and a variety of other undesired species. While *p*-nitrobenzene could be oxidized to its corresponding iodoarene difluoride in acceptable yields, this reaction required a very high applied potential.

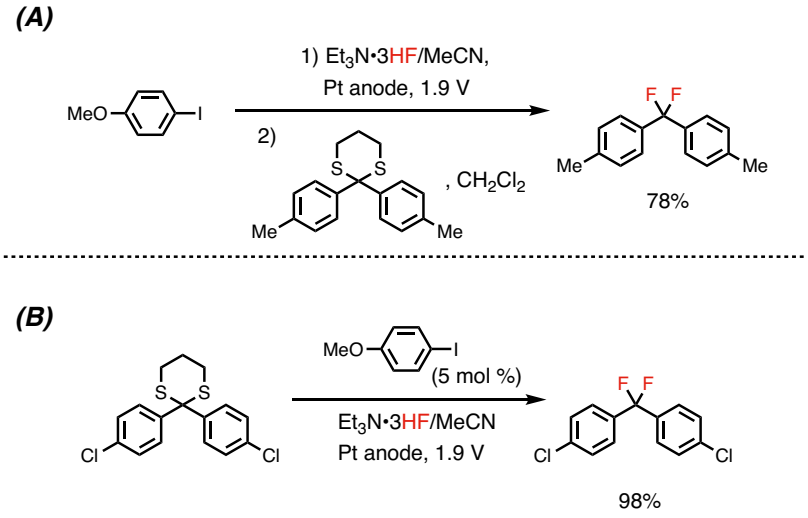

Scheme 3.2 Fuchigami's method for fluorodesulfurization of dithioketals promoted by an electrochemically generated iodoarene difluoride. (A) Ex-cell method. (B) In-cell method.

After establishing that iodoarene difluorides can be prepared via anodic oxidation, Fuchigami and coworkers demonstrated the utility of these compounds as both ex-cell and in-cell

[6] Schmidt, H.; Meinert, H. *Angew. Chem.* **1960**, *72*, 109–110.

[7] Rozhkov, I. *Russ. Chem. Rev.* **1976**, *45*, 615–629.

[8] Fuchigami, T.; Fujita, T. *J. Org. Chem.* **1994**, *51*, 7190–7192.

mediators for the *gem*-difluorination of dithioketals. To avoid the use of high applied potentials, the authors selected the electron-rich and therefore readily oxidized mediator *p*-iodoanisole. In the ex-cell example, electrolysis of *p*-iodoanisole with triethylamine trihydrofluoride affords the corresponding iodoarene difluoride; addition of substrate to the post-electrolytic solution resulted in fluorinative dithioketal cleavage (Scheme 3.2A). Adaptation of this approach to a catalytic, in-cell method proved straightforward, with excellent results achieved at a 5 mol % loading of *p*-iodoanisole (Scheme 3.2B). This example demonstrates the feasibility of achieving turnover in an electrocatalytic reaction involving iodoarene difluoride intermediates.

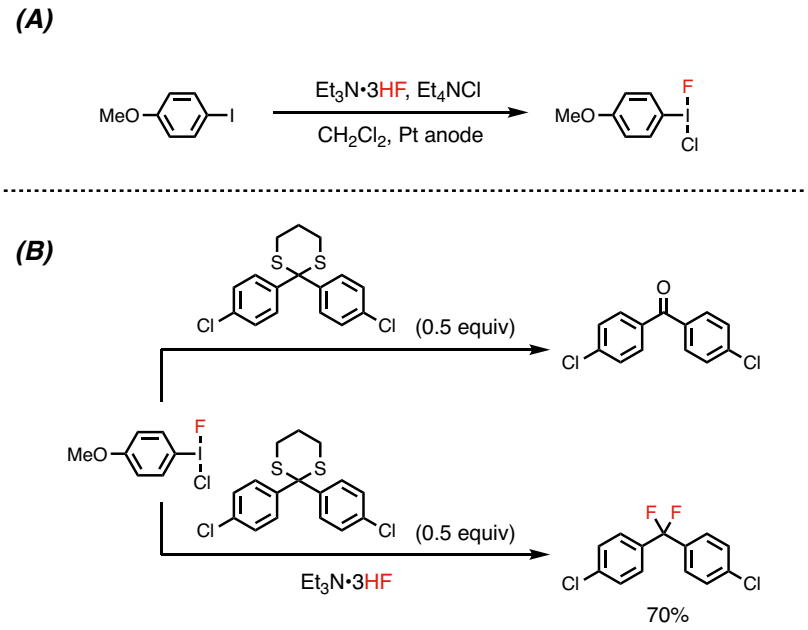

Scheme 3.3 Fuchigami's method for electrochemical oxidation of aryl iodides mediated by chloride. (A) Generation of an iodoarene chlorofluoride. (B) Reactivity of iodoarene chlorofluorides with dithioketals.

To extend the range of aryl iodides that could be employed in this electrochemical reaction, Fuchigami and coworkers investigated the use of chloride as a mediator for the indirect

anodic oxidation of aryl iodides.[9] In an attempt to prepare an aryl iodide difluoride via indirect anodic oxidation, the authors electrolyzed a solution of *p*-iodoanisole containing triethylamine trihydrofluoride and tetraethylammonium chloride in dichloromethane. Characterization data for the species produced in this electrolysis was inconsistent with the expected iodoarene difluoride product; rather, the product was assigned as an iodoarene chlorofluoride (Scheme 3.3A). This novel compound cleaved dithioketals to form the corresponding ketones; in the presence of triethylamine trihydrofluoride, however, fluorinative cleavage occurred to give *gem*-difluorides. (Scheme 3.3B). The in-cell reaction also proceeded efficiently, even at catalytic loadings of *p*-iodoanisole (Figure 3.1).

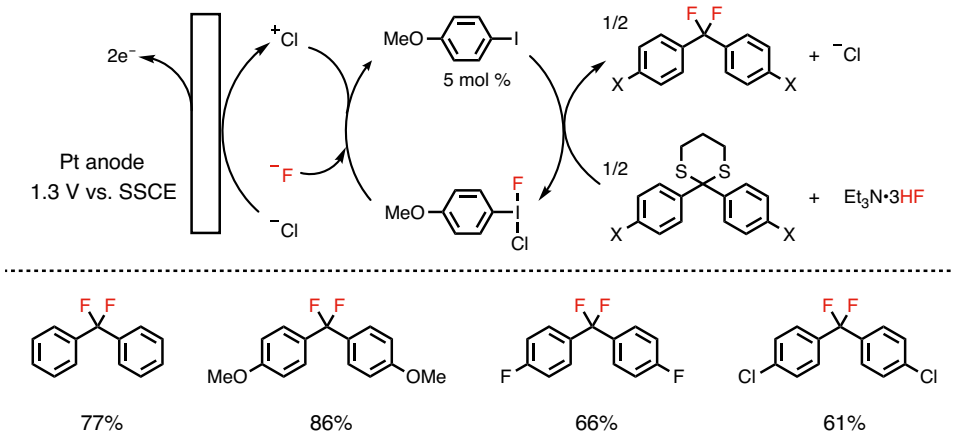

Figure 3.1 Fuchigami's method for electrocatalytic fluorodesulfurization of dithioketals.

Hara, Yoneda, and coworkers developed an electrochemical fluorination of β-dicarbonyl compounds that proceeds in the presence of *p*-iodotoluene, with triethylamine pentahydrofluoride serving as the fluoride source and solvent (Figure 3.2).[10] The reaction does not occur in the absence of *p*-iodotoluene, supporting the conclusion that *p*-iodotoluene

[9] Fujita, T.; Fuchigami, T. *Tetrahedron Lett.* **1996**, *37*, 4725–4728.

[10] Hara, S.; Hatakeyama, T.; Chen, S.-Q.; Ishi-I, K.; Yoshida, M.; Sawaguchi, M.; Fukuhara, T.; Yoneda, N. *J. Fluorine Chem.* **1998**, *87*, 189–192.

difluoride generated via electrochemical oxidation mediates the transformation. The authors note that rapid alternation of the anode and cathode was essential for suppression of severe anode passivation. The report includes a single catalytic example, in which a 71% yield of product could be obtained by using 0.5 equiv of *p*-iodotoluene in a divided cell.

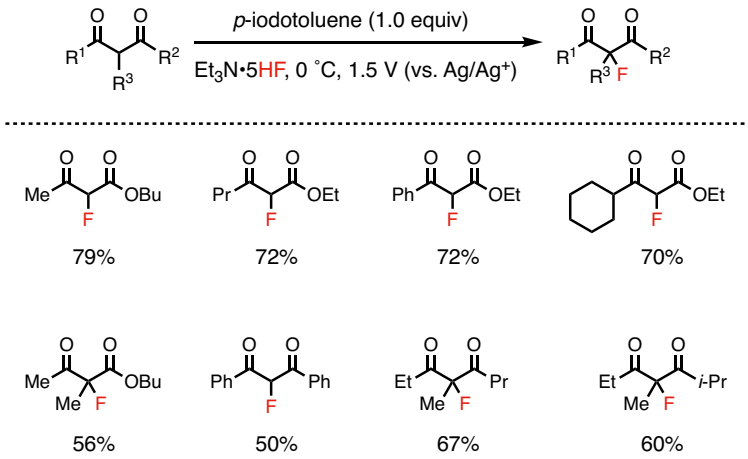

Figure 3.2 Hara and Yoneda's method for electrochemical fluorination of β-dicarbonyl compounds.

Building on early work investigating the electrochemical generation and *in situ* reactivity of hypervalent iodine compounds, Fuchigami and coworkers have pioneered the development of electrochemical fluorination reactions mediated by recyclable aryl iodides. A variety of sulfur compounds could be fluorinated using substoichiometric polystyrene-supported iodobenzene under previously developed electrochemical conditions.[11] In addition, benzylic fluorination and fluorodesulfurization reactions could be promoted by using a task-specific ionic liquid consisting of an aryl iodide containing an imidazolium moiety.[12] Both of these systems enabled convenient

[11] Sawamura, T.; Kuribayashi, S.; Inagi, S.; Fuchigami, T. *Adv. Synth. Catal.* **2010**, *352*, 2757–2760.

[12] Sawamura, T.; Kuribayashi, S.; Inagi, S.; Fuchigami, T. *Org. Lett.* **2010**, *12*, 644–646.

separation of the aryl iodide mediator from the reaction mixture and aided in avoidance of anode passivation.[13]

Waldvogel and coworkers developed the first reported method for alkene fluorofunctionalization using hypervalent iodine reagents generated *in situ* by anodic oxidation.[14] In their reaction, electrolysis of *N*-allylcarboxamides with *p*-iodotoluene and an HF source resulted in fluorinative cyclization to afford fluorinated oxazolines (Scheme 3.4A). Electrolysis of *N*-propargylamides with 2.0 equiv of *p*-iodotoluene under similar reaction conditions yielded fluorinated oxazoles (Scheme 3.4B).[15] In both of these methods, competing decomposition pathways resulting from direct anodic oxidation of certain substrates could be problematic.

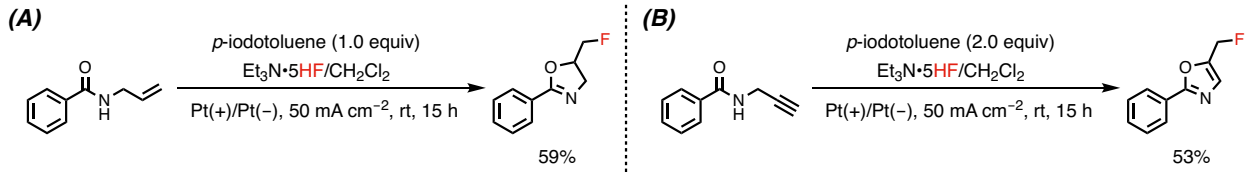

Scheme 3.4 Fluorinative cyclizations promoted by electrochemically generated hypervalent iodine reagents and developed by Waldvogel. (A) Synthesis of fluorinated oxazolines. (B) Synthesis of fluorinated oxazoles.

Lennox and coworkers recently reported a method in which electrochemically generated *p*-iodotoluene difluoride serves a stoichiometric mediator for the vicinal difluorination of alkenes.[16] Electron-poor substrates react cleanly under in-cell conditions, but electron-rich substrates with greater susceptibility to oxidation are incompatible with this method (Figure

[13] Anode passivation can occur to a greater degree when certain organic solvents are used. See: Shaaban, M. R.; Ishii, H.; Fuchigami, T. *J. Org. Chem.* **2000**, *65*, 8685–8689.

[14] Haupt, J. D.; Berger, M.; Waldvogel, S. R. *Org. Lett.* **2019**, *21*, 242–245.

[15] Herszman, J. D.; Berger, M.; Waldvogel, S. R. *Org. Lett.* **2019**, *21*, 7893–7896.

[16] Doobary, S.; Sedikides, A. T.; Caldora, H. P.; Poole, D. L.; Lennox, A. J. J. *Angew. Chem. Int. Ed.* **2020**, *59*, 1155–1160.

3.3A). For these substrates, the authors used an ex-cell approach, in which alkene is treated with a pregenerated solution of *p*-iodotoluene difluoride (Figure 3.3B). Use of catalytic *p*-iodotoluene resulted in decreased yields, an effect attributed to a rate of electrochemical oxidation (generation of *p*-iodotoluene difluoride) that exceeds the rate of the subsequent chemical steps (alkene fluorination).[17] The preliminary work towards electrocatalytic alkene difluorination described in this chapter was performed prior to the publication of the method reported by Lennox and coworkers.

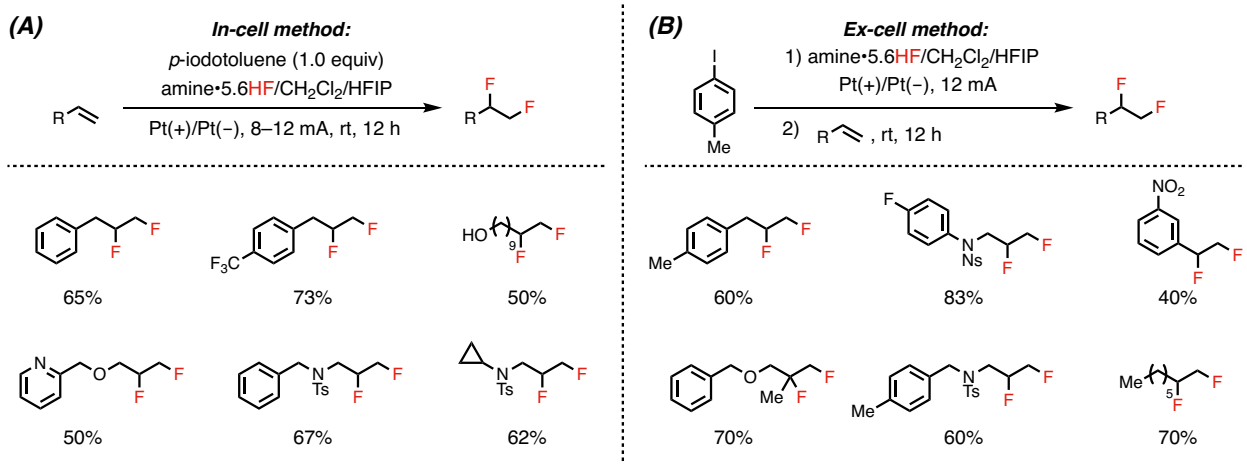

Figure 3.3 Alkene difluorination promoted by electrochemically generated *p*-iodotoluene difluoride and developed by Lennox. (A) In-cell method for electron-poor substrates. (B) Ex-cell method for electron-rich substrates.

3.3 Electrochemical Difluorination of Alkenes

In view of the promising literature precedent for electrochemical generation of iodoarene difluorides, we aimed to implement an electrocatalytic version of the alkene fluorination chemistry developed in our group. Electrochemical generation of the active iodoarene difluoride

[17] By applying five cycles of 0.7 F mol^{-1} and stirring for 6 h between the cycles, acceptable yields could be obtained at 20 mol % catalyst loading, but this approach was not adopted due to its impracticality.

in situ could potentially mitigate problems associated with the use of *m*CPBA as a stoichiometric oxidant: for example, fluorohydrin byproducts arise through direct oxidation of some electron-rich alkenes by *m*CPBA, and in some cases the carboxylic acid byproduct of *m*CPBA participates as a nucleophile.[18] Generally, organic electrochemistry necessitates selection of highly polar organic solvents and inclusion of supporting electrolytes to engender conductivity. These parameters can present a hindrance to development of electrochemical variants of many organic reactions, especially enantioselective reactions. However, the high concentrations of HF-pyridine required for many of our group's catalytic fluorination reactions suggested that this chemistry may be particularly well suited to an electrochemical approach.

Drawing on the conditions employed by Hara, Yoneda, and coworkers for electrochemical generation of *p*-iodotoluene difluoride *in situ*, we began by subjecting a solution of 1.0 equiv of *p*-iodotoluene (**1a**) and alkene **2** and to electrolysis at 2.1 V in triethylamine trihydrofluoride (Scheme 3.5).[19] After 3 h, an aliquot of the reaction mixture was quenched and analyzed by ^{1}H NMR, which revealed that the desired 1,2-difluoride **3** had formed in 24% yield. The background reaction in the absence of the aryl iodide does not proceed, indicating that *p*-iodotoluene difluoride forms *in situ* and mediates the alkene fluorination reaction.

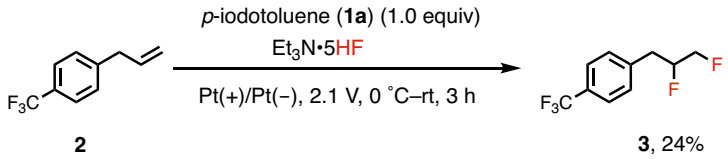

2 **3**, 24%

Scheme 3.5 Electrochemical difluorination of **2** with stoichiometric **1a** in Et_3N•5HF.

[18] Banik, S. M.; Medley, J. W.; Jacobsen, E. N. *J. Am. Chem. Soc.* **2016**, *138*, 5000–5003.

[19] See ref. 10.

While this result provided proof-of-concept for electrochemical alkene difluorination, attempts to improve the yield of this transformation and to difluorinate other alkene substrates were unsuccessful. Compounding this problem, the use of neat triethylamine pentahydrofluoride as the reaction solvent rendered reaction setup and workup hazardous. With the aim of developing milder and safer reaction conditions that would be more broadly applicable, we decided to explore other solvent systems and fluoride sources.

Fluoroalcohols such as HFIP have been widely used as solvents for electrochemical reactions.[20] In particular, fluoroalcohols have proved effective as solvents for the anodic generation of iodine(III) compounds: fluoroalcohols serve as ligands to iodine(III), exhibit a large electrochemical window and high conductivity, stabilize cationic and radical cationic species, and enable facile proton reduction as the cathodic half-reaction.[21,22] Based on previously described studies showing that stoichiometric iodoarene difluorides difluorinate alkenes in HFIP under HF-free conditions, we attempted to develop an electrocatalytic protocol using HFIP as the solvent and a fluoride salt as the fluoride source.[23]

Using cyclic voltammetry, we assessed the oxidation potentials of several aryl iodides in HFIP (see Experimental Information for details). Because of their structural simplicity and ease of oxidation, we selected *p*-iodoanisole (**1b**) and iodobenzene (**1c**) for our initial studies. We found that electrolysis of alkene **2** and **1b** in HFIP with fluoride salts failed to afford any

[20] (a) Colomer, I.; Chamberlain, A. E. R.; Haughey, M. B.; Donohoe, T. J. *Nat. Rev. Chem.* **2017**, *1*, 0088. (b) Schulz, L.; Waldvogel, S. R. *Synlett* **2019**, *30*, 275–286.

[21] Francke, R.; Broese, T.; Roesel, A. F. Electrochemistry of Hypervalent Iodine Compounds. In *PATAI'S Chemistry of Functional Groups*, John Wiley & Sons, Ltd. **2018**.

[22] For a recently reported example of hypervalent iodine electrocatalysis in HFIP, see: Maity, A.; Frey, B. L.; Hoskinson, N. D.; Powers, D. C. *J. Am. Chem. Soc.* **2020**, *142*, 4990–4995.

[23] See Chapter 2 of this thesis.

difluorinated products (Table 3.1, entries 1–2). Using **1c** instead and including $TBAPF_6$ as an additional supporting electrolyte did not initiate reactivity (entries 3–6).

Table 3.1 Evaluation of fluoride sources and electrolytes for the electrochemical, HF-free difluorination of **2**.

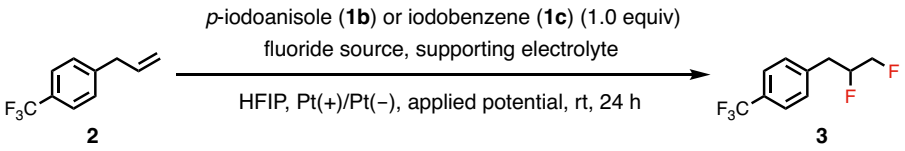

2 **3**

entry	aryl iodide	fluoride source/ electrolyte	applied potential (V)	yield of **3** (%)
1	**1b**	CsF	1.6	0
2	**1b**	TBAF	1.6	0
3	**1c**	CsF	2.0	0
4	**1c**	CsF + $TBAPF_6$	2.0	0
5	**1c**	TMAF + $TBAPF_6$	2.0	0
6	**1c**	$TBAPF_6$	2.0	0

A number of possible explanations could account for the lack of reactivity observed under these conditions. A high concentration of fluoride could inhibit alkene fluoroiodination if this process involves the dissociation of a fluoride ligand from the iodoarene difluoride. Additionally, iodoarene difluorides may not form under the reaction conditions, or they may not be the only aryl iodide oxidation products formed. Previous reports have indicated that electrolysis of aryl iodides in HFIP can produce bis(hexafluoroisopropoxy)iodoarenes.[24] If formed in the electrochemical oxidation of an aryl iodide **I**, we envisioned that ligand exchange with fluoride could convert intermediates such as **II** to iodoarene difluorides **III**, which should promote the alkene difluorination reaction (Scheme 3.6). However, halide ions, including fluoride, have been shown to promote the decomposition of iodine(III) adducts such as **II**

[24] Broese, T.; Francke, R. *Org. Lett.* **2016**, *18*, 5896–5899.

through a reductive elimination pathway that regenerates the aryl iodide and forms an equivalent of hexafluoroacetone.[25]

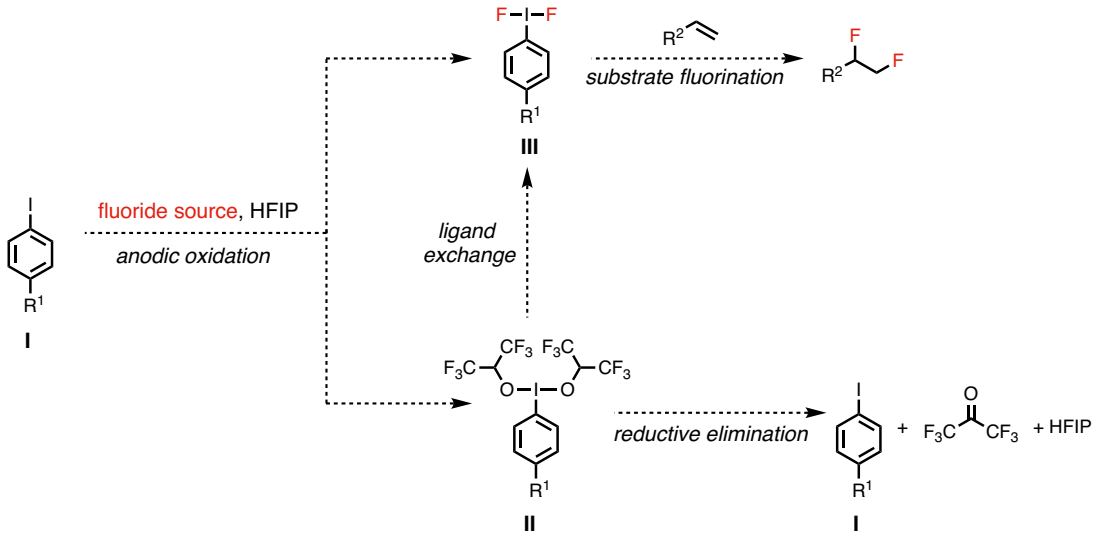

Scheme 3.6 Plausible pathways and reaction outcomes for the anodic oxidation of an aryl iodide and a fluoride source in HFIP.

Synthesis of bis(hexafluoroisopropoxy)iodobenzene (**4**) by electrolysis of aryl iodides in HFIP has been reported, and the ligand exchange reactions of this compound to form reagents such as PIDA and Koser's reagent have been demonstrated to be facile.[26] To assess the feasibility of ligand exchange with fluoride, we prepared a solution of **4** in HFIP by following the reported method and treated this solution with a variety of fluoride sources (Table 3.4).[27] We then added alkene substrate **2** to each reaction mixture and determined whether 1,2-difluoride product **3** formed. In contrast to the results obtained in the in-cell reactions described above, fluoride salts CsF and TMAF afforded the 1,2-difluoride, albeit in very low yields (entries 1–2).

[25] Koleda, O.; Broese, T.; Noetzel, J.; Roemelt, M.; Suna, E.; Francke, R. *J. Org. Chem.* **2017**, *82,* 11669–11681.

[26] Elsherbini, M.; Winterson, B.; Alharbi, H.; Folgueiras-Amador, A. A.; Génot, C.; Wirth, T. *Angew. Chem. Int. Ed.* **2019**, *58*, 9811–9815.

[27] Using the same method, we attempted to prepare the bis(perfluoro-*tert*-butoxy) analog of **4**, which should not be able to access the putative deleterious reductive elimination pathway; however, preparation of the compound was unsuccessful.

Substantially higher yields were observed when HF-amine complexes were employed as fluoride sources (entries 3–4). Notably, we observed difluorination products even in the absence of an added fluoride source (entry 5). We attributed this result to the presence of $TBAPF_6$, which served as a supporting electrolyte in the electrochemical oxidation step; under acidic conditions and without rigorous drying of the solvent, $TBAPF_6$ could potentially generate HF, allowing the difluorination reaction to proceed.[28] When we attempted to run the difluorination reaction in an in-cell manner with $TBAPF_6$ as the sole fluoride source, however, no product formed, suggesting that any hexafluorophosphate hydrolysis that may take place requires a long time period to generate an appreciable concentration of HF (Table 3.1, entry 6). A similar explanation may account for the reactivity of CsF and TMAF under the ex-cell conditions but not under the in-cell conditions previously described.

Table 3.2 Evaluation of fluoride sources for the ex-cell difluorination of **2** with stoichiometric bis(hexafluoroisopropoxy)iodobenzene **4**.

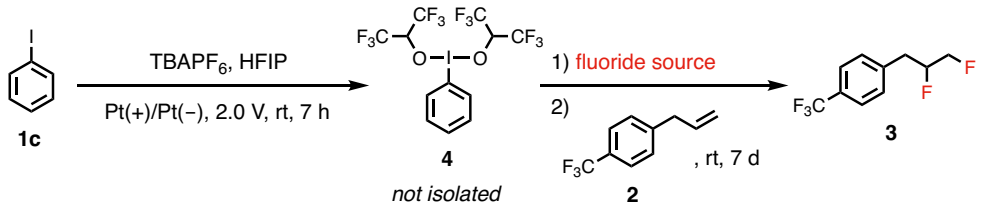

entry	fluoride source	yield of **3** (%)
1	CsF	12
2	TMAF	13
3	$Et_3N{\cdot}3HF$	58
4	pyr·9HF	46
5	—	28

[28] Hydrolysis of hexafluorophosphate salts to form HF is precedented. See: (a) Gebala, A. E.; Jones, M. M. *J. Inorg. Nucl. Chem.* **1969**, *31*, 771–776. (b) Barlow, C. G. *Electrochem. Solid-State Lett.* **1999**, *2*, 362–364. (c) Lux, S. F.; Chevalier, J.; Lucas, I. T.; Kostecki, R. *ECS Electrochem. Lett.* **2013**, *2*, A121–A123.

These results suggested that HF is required for generation of an iodoarene difluoride under electrochemical conditions. However, experiments with stoichiometric iodoarene difluorides in HFIP have indicated that HF is not a necessary component for activating these compounds to promote alkene fluorination.[29] As a result, we hypothesized that electrochemical fluorination in HFIP may not demand the extremely high HF loadings required in catalytic reactions employing *m*CPBA as the oxidant. Indeed, electrochemical fluorination of alkene **2** proceeded with only 8.0 equiv HF (Scheme 3.7).[30]

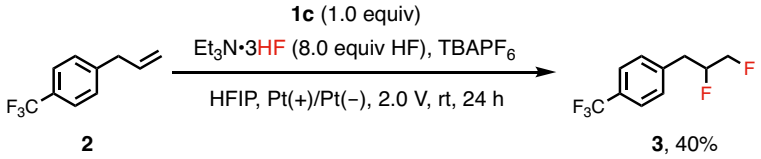

Scheme 3.7 Electrochemical difluorination of **2** with stoichiometric **1c** and $Et_3N•3HF$ in HFIP.

Next, we investigated whether the electrochemical reaction could be rendered catalytic in aryl iodide. We found that electrolysis of terminal alkene **2** and catalytic **1a** in HFIP with triethylamine trihydrofluoride as the fluoride source afforded the desired 1,2-difluoride **3** (Scheme 3.8). The yield (43%) exceeded the catalyst loading (20 mol %), indicating that catalyst turns over in this transformation.

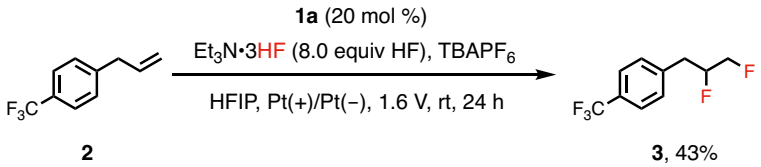

Scheme 3.8 Electrochemical difluorination of **2** with catalytic **1a** and $Et_3N•3HF$ in HFIP.

[29] See Chapter 2 of this thesis.

[30] In contrast, the difluorination of **2** using the catalytic conditions with *m*CPBA employed 100 equiv HF; see ref. 18.

Additional optimization would be required to improve the yield and assess the scope of this electrocatalytic transformation.[31] In particular, however, we were interested in determining if enantioselectivity could be achieved in an electrocatalytic fluorination reaction. We found that when chiral catalyst **1d** was used, no product formed (Figure 3.4). To gain insight into potential reasons for this loss of reactivity, we tested two truncated catalysts. Catalyst **1e**, which lacks the chiral center methine and the benzyl groups of catalyst **1d**, also failed to promote the reaction. However, catalyst **1f**, which lacks the sidearm esters, gave product in 25% yield. In combination, this data suggests that these proximal esters suppress reactivity. This effect could potentially result from coordination of the esters to the iodine center following oxidation.

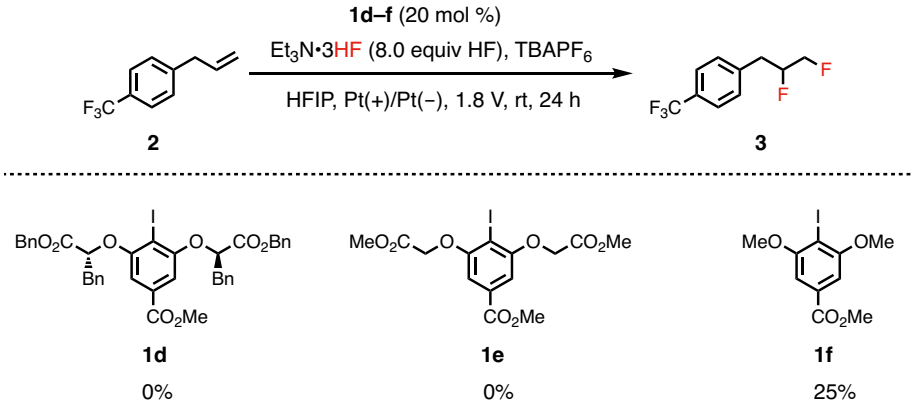

Figure 3.4 Evaluation of resorcinol-derived catalysts in the electrochemical difluorination of **2**.

3.4 Conclusions and Outlook

We have investigated the *in situ* electrochemical generation of iodoarene difluorides for alkene difluorination reactions. Using *p*-iodotoluene as the catalyst and triethylamine

[31] Attempts to apply this methodology to the cinnamamide substrates described in Chapters 1–2 of this thesis were unsuccessful, resulting in substrate decomposition. We attribute this result to direct anodic oxidation of cinnamamides at the potentials required to achieve catalyst oxidation (see Experimental Information for relevant CV data). Development of more electron-rich and thus more readily oxidized catalysts could potentially enable electrochemical difluorination of cinnamamides and other oxidation-sensitive substrates.

trihydrofluoride at low concentrations as the fluoride source, we achieved an electrocatalytic difluorination of a terminal alkene in HFIP. Through studies of a small selection of catalysts, we identified catalyst features that modulate oxidation potential and affect reactivity. Insights gained through these efforts could be leveraged to design chiral catalysts for application to development of an enantioselective electrocatalytic transformation.

3.5 Experimental Information

3.5.1 General Experimental Procedures and Note of Caution

General Experimental Procedures

All electrochemical experiments were performed using a CH Instruments 760D bipotentiostat or a DC power supply. A platinum wire working electrode and a platinum mesh counter-electrode were used for all electrochemical experiments. A Warner Instruments leak-free reference electrode with a 3.0 M KCl filling electrolyte was used for electrochemical experiments performed with a potentiostat. A Teflon undivided cell was used as the reaction vessel. Reported concentrations refer to solution volumes at room temperature. Concentration of organic solutions under reduced pressure was performed using house vacuum (ca. 40 mm Hg) at 30 ºC.

Note of Caution

Pyridine•9HF, triethylamine•5HF, and triethylamine•5HF are corrosive and toxic substances. Pyridine•9HF and triethylamine•5HF will corrode glassware. Safe handling can be conducted with plastic syringes and metal needles, with $NaHCO_3$ (aq.) or NaOH (aq.) employed to quench excess HF. Though reactions should not be conducted in glassware when employing these reagents, glassware may be used to quench reactions provided sufficient quantities of base are present. Always handle these and other HF reagents while wearing gloves and in a fume hood. As a precautionary measure, have calcium gluconate gel nearby and apply immediately and liberally on skin exposed to any HF reagent.

3.5.2 Materials and Instrumentation

Materials

Reagents were purchased in reagent grade from commercial suppliers and used as received, unless otherwise described. Hexafluoroisopropanol was dried over molecular sieves or distilled over CaH_2 prior to use.

Instrumentation

Proton nuclear magnetic resonance (^{1}H NMR) spectra were recorded on an Inova-500 spectrometer, are reported in parts per million downfield from tetramethylsilane, and are referenced to the residual protium resonances of the NMR solvent ($CDCl_3$: 7.26 [$CHCl_3$], acetone-d6: 2.05 [acetone-d5], DMSO-d6: 2.50 [DMSO-d5]). Chemical shifts for fluorine-19 nuclear magnetic resonance (19F NMR) were recorded on an Inova-500 spectrometer, are reported in parts per million downfield from chlorotrifluoromethane, and are referenced to the fluorine resonance of chlorotrifluoromethane ($\delta = 0$). Data are represented as follows: chemical shift, multiplicity (br = broad, s = singlet, d = doublet, t = triplet, q = quartet, quin = quintet, sept = septet, m = multiplet), coupling constants in Hertz (Hz), integration.

3.5.3 Cyclic Voltammetry of Aryl Iodides and Substrates

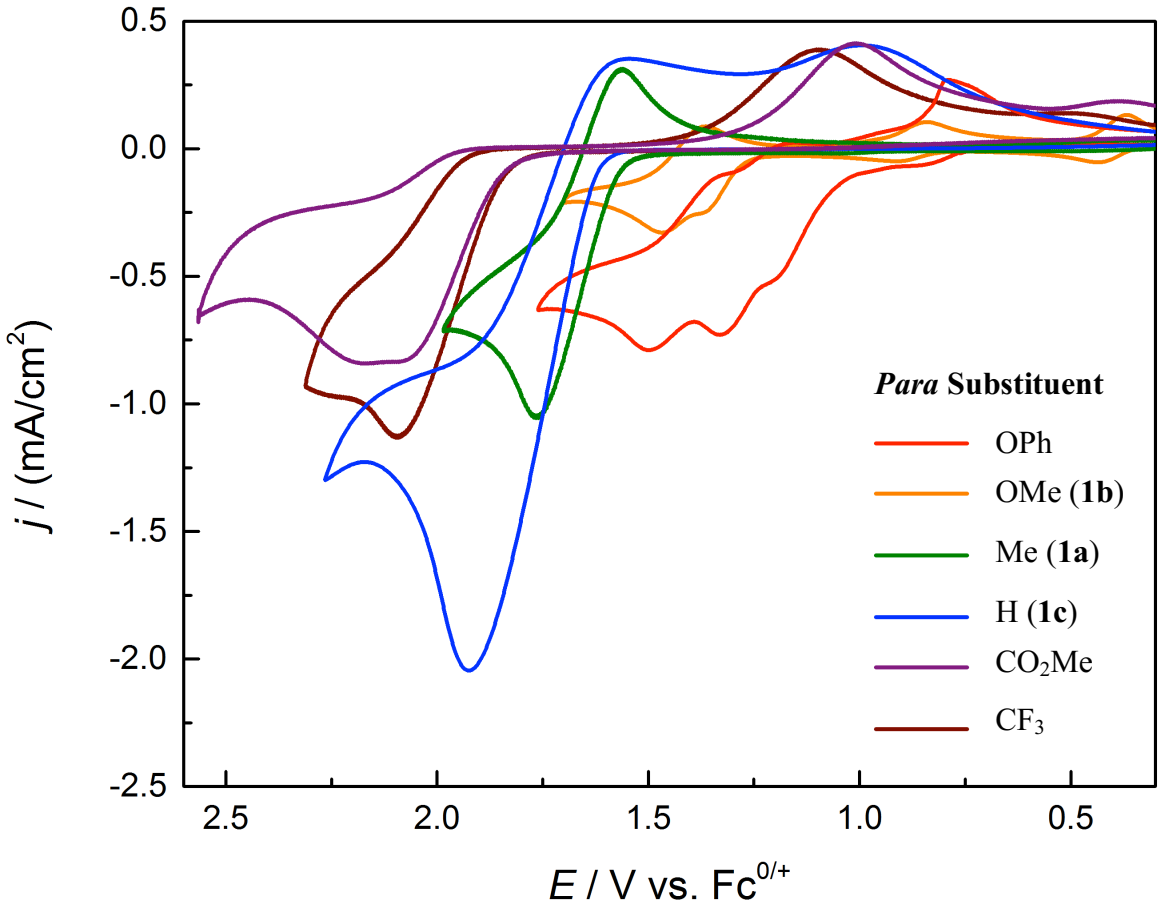

Figure 3.5 CVs of para-substituted iodobenzenes.

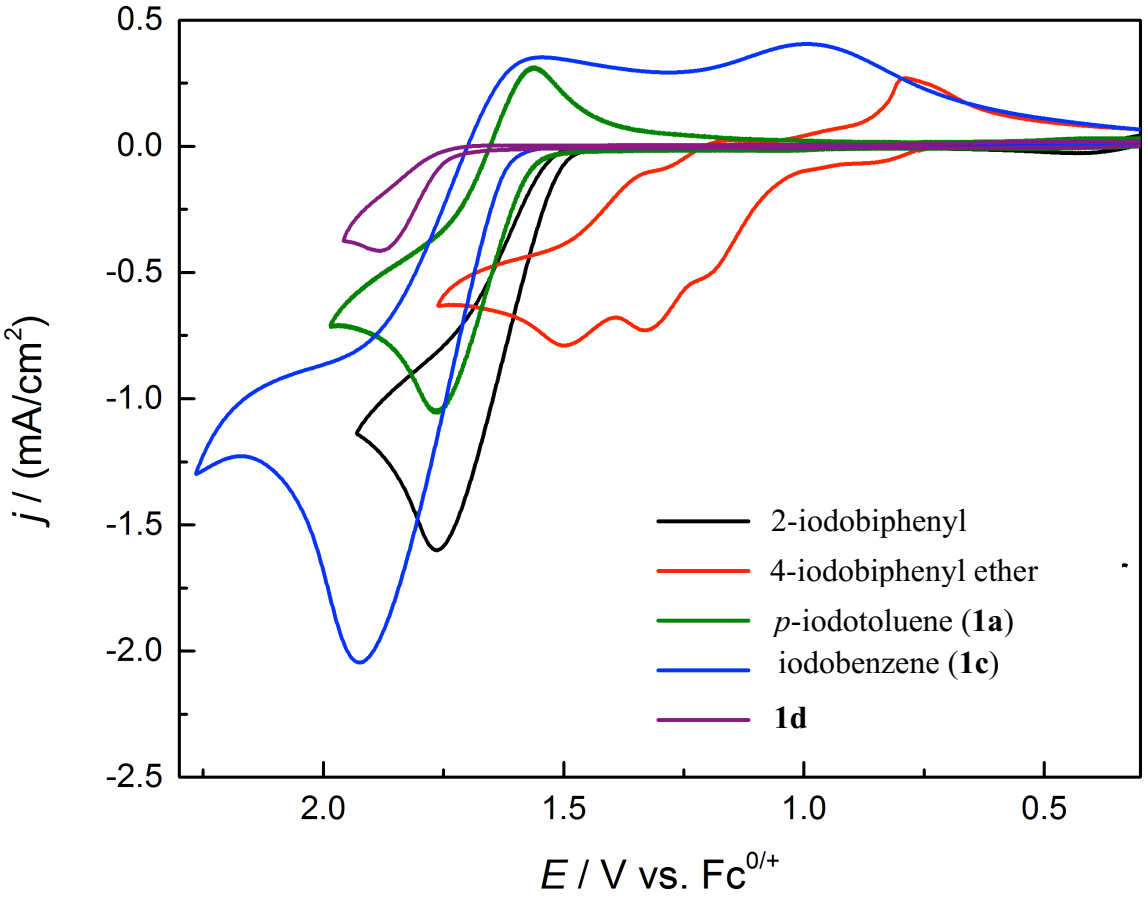

Figure 3.6 CVs of resorcinol-derived aryl iodides and other 2– and 4–substituted iodoarenes.

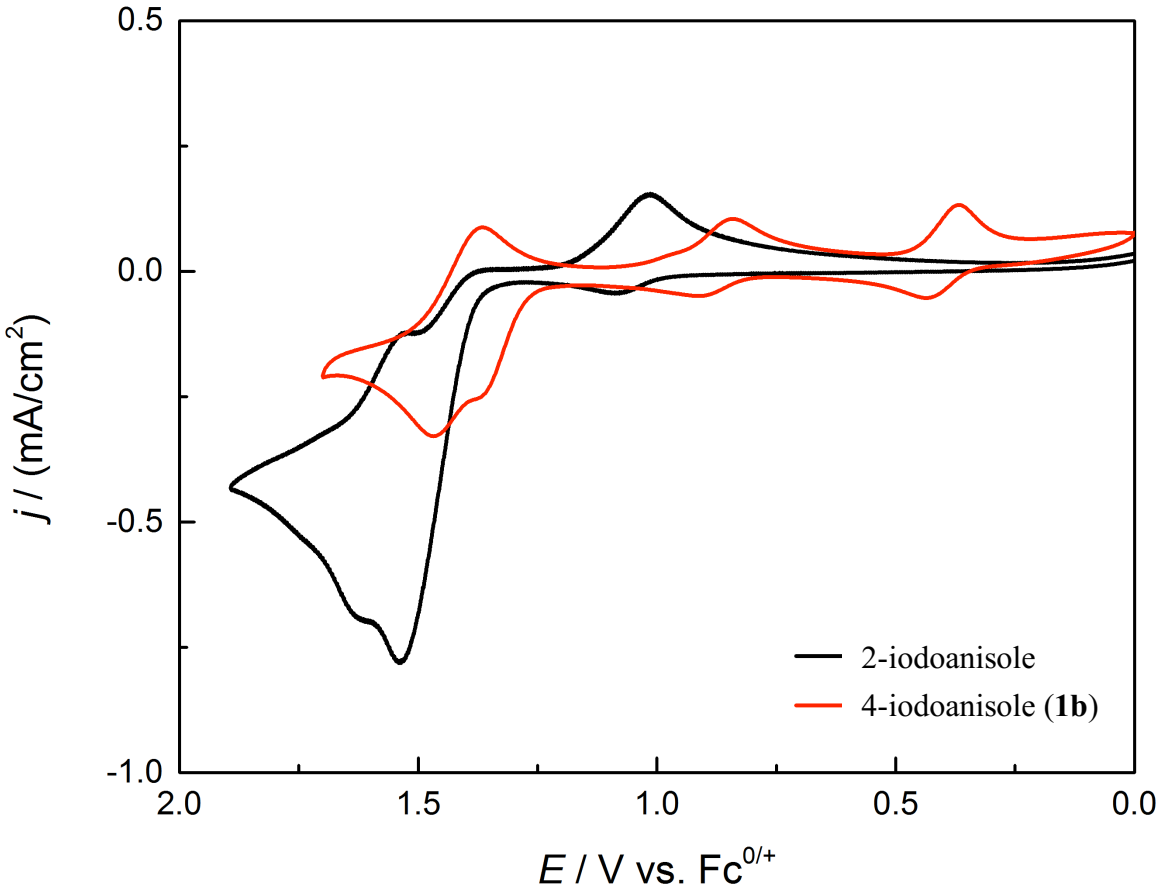

Figure 3.7 CVs of 2-iodoanisole and 4-iodoanisole.

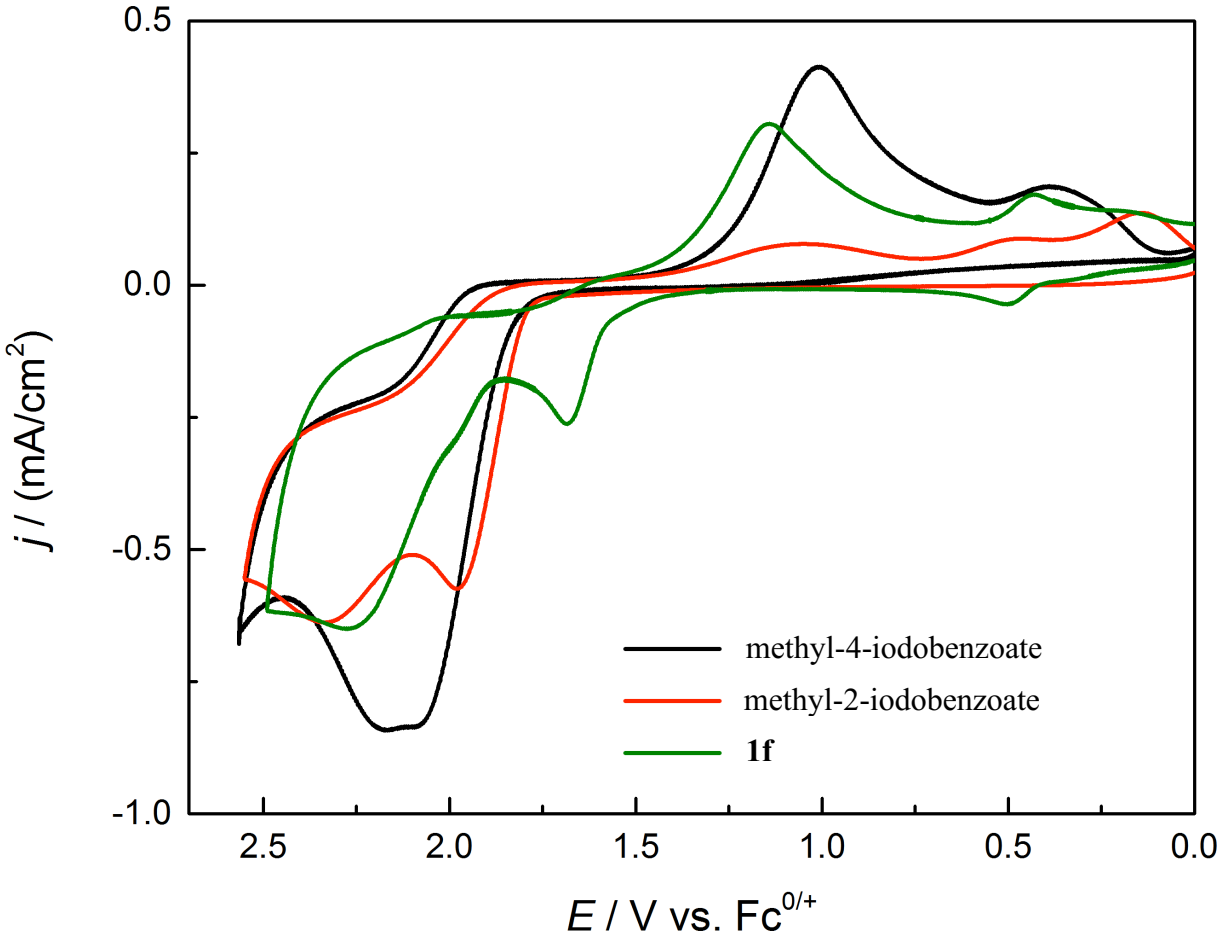

Figure 3.8 CVs of resorcinol-derived aryl iodides and other 2– and 4–substituted iodoarenes.

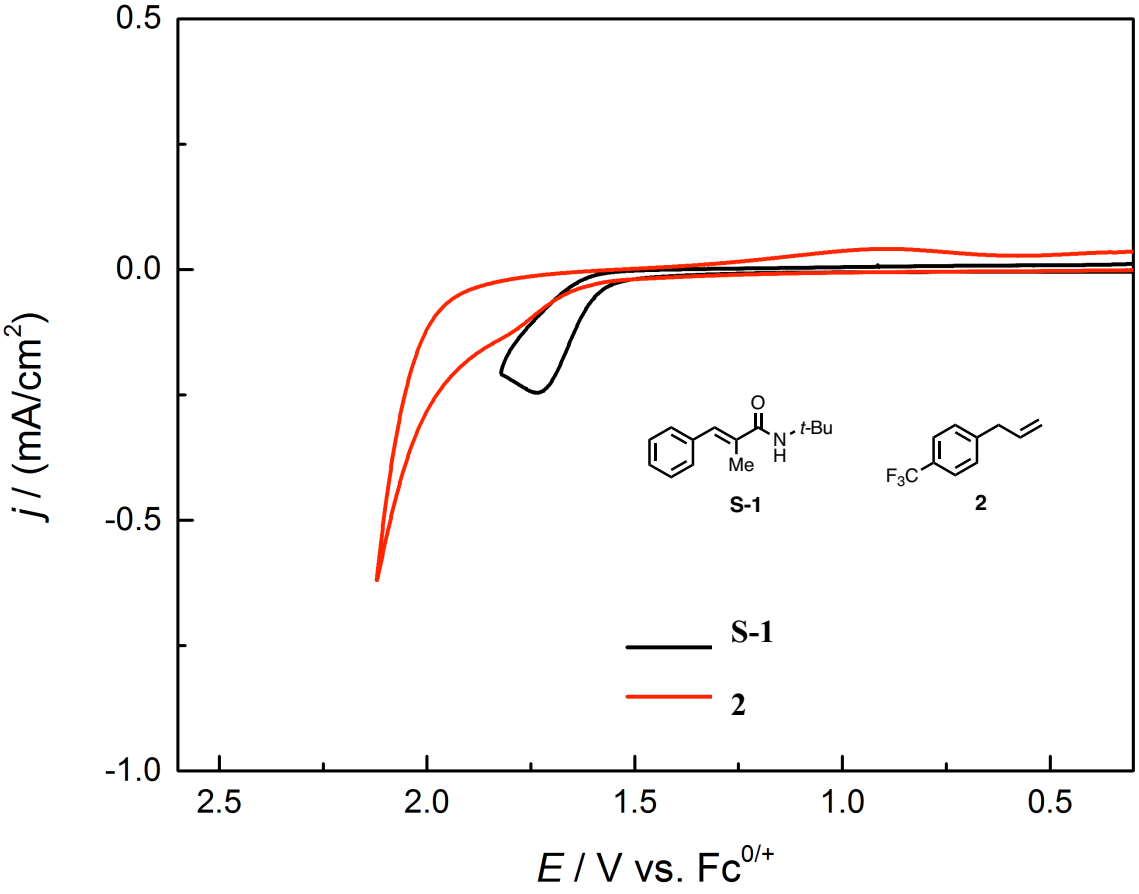

Figure 3.9 CVs of alkene substrates.

3.5.4 Electrochemical Reactions

Electrochemical Difluorination in Et_3N•5HF

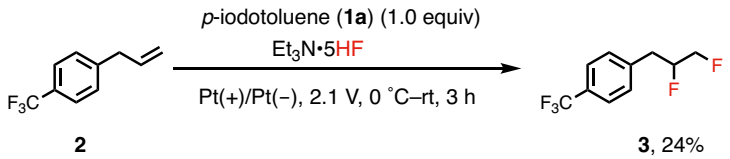

To a stirred solution of **2** (99 mg, 0.53 mmol) in triethylamine pentahydrofluoride (4.00 mL) was added *p*-iodotoluene (**1a**) (116 mg, 0.53 mmol). The solution was cooled to 0 ˚C, and electrolysis was initiated at 2.1 V using a DC power supply, resulting in an initial current of 21 mA. The reaction was allowed to come to room temperature, and the electrolysis was stopped after 3 h when the current had fallen to 6 mA. The spectral data for **3** were in accordance with the literature.[32]

Anodic Oxidation of Iodobenzene in HFIP

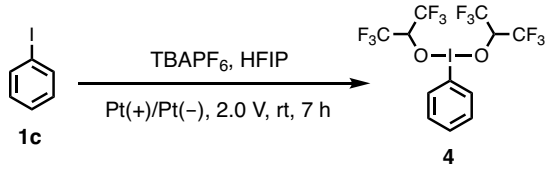

To a stirred solution of iodobenzene (**1c**) (56 µL, 0.50 mmol) in HFIP (5.00 mL) was added tetrabutylammonium hexafluorophosphate (194 mg, 0.50 mmol). Using a potentiostat, electrolysis was initiated at 2.0 V at room temperature. After 7 h, the electrolysis was stopped. The resulting solution of **4** was used immediately and without workup or purification. To

[32] See ref. 18.

characterize the product, an aliquot of the solution was dissolved in $CDCl_3$. The spectral data for **4** were in accordance with the literature.[33]

^{1}H NMR (500 MHz, $CDCl_3$) δ 8.08 (d, J = 8.2 Hz, 2H), 7.72 – 7.67 (m, 1H), 7.63–7.56 (m, 2H) (protons resulting from incorporation of HFIP into the product are indistinguishable due to the presence of HFIP solvent in the sample); ^{19}F NMR (470.4 MHz, $CDCl_3$) δ -75.1 (br s, 6F).

Ex-Cell Ligand Exchange Fluorination Experiments

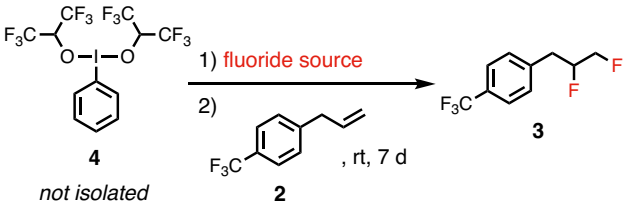

To a freshly prepared solution of **4** in HFIP (500 µL, 0.10 M) was added a fluoride source (10 µL of amine•xHF or 0.20 mmol fluoride salt). The solution was stirred, and **2** (8 µL, 0.05 mmol) was added at room temperature. After 7 d, an aliquot of the solution was analyzed by ^{1}H and ^{19}F NMR. The spectral data for **3** were in accordance with the literature. Yields were determined by ^{19}F NMR using 1-fluorooctane as an internal standard.

[33] See ref. 26.

General Procedure for Electrochemical Reactions in HFIP with $Et_3N•3HF$

To a stirred solution of aryl iodide (0.10–0.50 mmol, 0.20–1.00 equiv) and alkene (0.50 mmol, 1.00 equiv) in HFIP (4.80 mL) was added tetrabutylammonium hexafluorophosphate (194 mg, 0.50 mmol, 1.00 equiv) and triethylamine trihydrofluoride (200 μL, 8.00 equiv HF). Using a potentiostat, electrolysis was initiated at 1.6–2.0 V at room temperature. After 24 h, the electrolysis was stopped. Yields were determined by solvent-suppressed ^{19}F NMR analysis of the crude reaction mixture using 1-fluorooctane as an internal standard.